

University of Windsor

Scholarship at UWindor

Electronic Theses and Dissertations

Theses, Dissertations, and Major Papers

2003

The role of crustal contamination and volatiles in the genesis of the Marathon PGE-copper deposit, Ontario: Constraints from micometre scale LA-ICP-MS lead isotope systematics and PGE distribution

Sean Andrew Crowe
University of Windsor

Follow this and additional works at: <https://scholar.uwindsor.ca/etd>

Recommended Citation

Crowe, Sean Andrew, "The role of crustal contamination and volatiles in the genesis of the Marathon PGE-copper deposit, Ontario: Constraints from micometre scale LA-ICP-MS lead isotope systematics and PGE distribution" (2003). *Electronic Theses and Dissertations*. 4237.
<https://scholar.uwindsor.ca/etd/4237>

This online database contains the full-text of PhD dissertations and Masters' theses of University of Windsor students from 1954 forward. These documents are made available for personal study and research purposes only, in accordance with the Canadian Copyright Act and the Creative Commons license—CC BY-NC-ND (Attribution, Non-Commercial, No Derivative Works). Under this license, works must always be attributed to the copyright holder (original author), cannot be used for any commercial purposes, and may not be altered. Any other use would require the permission of the copyright holder. Students may inquire about withdrawing their dissertation and/or thesis from this database. For additional inquiries, please contact the repository administrator via email (scholarship@uwindsor.ca) or by telephone at 519-253-3000ext. 3208.

NOTE TO USERS

This reproduction is the best copy available.

UMI[®]

**THE ROLE OF CRUSTAL CONTAMINATION AND VOLATILES IN THE
GENESIS OF THE MARATHON PGE-CU DEPOSIT, ONTARIO: CONSTRAINTS
FROM MICROMETRE SCALE LA-ICP-MS Pb ISOTOPE SYSTEMATICS AND PGE
DISTRIBUTION**

By
Sean Andrew Crowe

A Thesis Submitted to the
Faculty of Graduate Studies and Research
Through the Department of Earth Sciences
In Partial Fulfillment of the Requirements for
The Degree of Master of Science at the
University of Windsor

Windsor, Ontario, Canada

2003

© 2003 Sean Andrew Crowe, All rights reserved



National Library
of Canada

Bibliothèque nationale
du Canada

Acquisitions and
Bibliographic Services

Acquisitions et
services bibliographiques

395 Wellington Street
Ottawa ON K1A 0N4
Canada

395, rue Wellington
Ottawa ON K1A 0N4
Canada

Your file *Votre référence*
ISBN: 0-612-86702-1
Our file *Notre référence*
ISBN: 0-612-86702-1

The author has granted a non-exclusive licence allowing the National Library of Canada to reproduce, loan, distribute or sell copies of this thesis in microform, paper or electronic formats.

L'auteur a accordé une licence non exclusive permettant à la Bibliothèque nationale du Canada de reproduire, prêter, distribuer ou vendre des copies de cette thèse sous la forme de microfiche/film, de reproduction sur papier ou sur format électronique.

The author retains ownership of the copyright in this thesis. Neither the thesis nor substantial extracts from it may be printed or otherwise reproduced without the author's permission.

L'auteur conserve la propriété du droit d'auteur qui protège cette thèse. Ni la thèse ni des extraits substantiels de celle-ci ne doivent être imprimés ou autrement reproduits sans son autorisation.

In compliance with the Canadian Privacy Act some supporting forms may have been removed from this dissertation.

Conformément à la loi canadienne sur la protection de la vie privée, quelques formulaires secondaires ont été enlevés de ce manuscrit.

While these forms may be included in the document page count, their removal does not represent any loss of content from the dissertation.

Bien que ces formulaires aient inclus dans la pagination, il n'y aura aucun contenu manquant.

Canada

ABSTRACT

The Marathon deposit is a platinum group element (PGE)-Cu deposit hosted by the Coldwell intrusive complex, located on the north shore of Lake Superior, Ontario. Contradictory models have been proposed for the genesis of the deposit. This paper investigates the relative importance of different ore forming processes responsible for the PGE and Cu enrichment in the deposit and tests these contradictory models.

A method has been developed for the precise determination of Pb isotope ratios in solid materials using quadrupole LA-ICP-MS. The advantages of this method are several, including; micrometer-scale spatial resolution, rapid analysis time, and low risk of contamination during sample preparation. Importantly, in samples with low Pb concentrations (~2 ppm), quadrupole LA-ICP-MS, with N₂ added to the nebulizer gas, can yield Pb isotope ratio measurements with a precision (0.2% RSE) that is comparable to LA-MC-ICP-MS.

Pb isotope ratios were measured in minerals from the Marathon deposit by LA-ICP-MS. The Pb isotope ratios in plagioclase are different than in chalcopyrite in PGE- and Cu-rich gabbroic rocks. This suggests an external Pb component in the chalcopyrite. Textural relationships were found to be most consistent with chalcopyrite mineralization and Cu enrichment under sub-solidus conditions. The presence of external Pb (likely from an Archean upper crustal source) in chalcopyrite, in conjunction with textural constraints, suggests that chalcopyrite precipitated from hydrothermal fluids that have been derived from, or have interacted with, Archean country rocks. Thus, for Cu enrichment (i.e. chalcopyrite mineralization), the work presented in this thesis is consistent with a hydrothermal model. However, as the PGE distribution maybe controlled by processes other than chalcopyrite mineralization, the origin of the PGE enrichment remains uncertain. It is reasonable to suspect that PGE enrichment is related to chalcopyrite mineralization as there is a strong association between PGMs and chalcopyrite, and also, good correlation between Cu, Pt, and Pd concentrations. This is the subject of continuing research that is investigating the distribution and fractionation of the PGE within the Marathon deposit and is also studying the relationship of the PGE to other trace elements.

ACKNOWLEDGEMENTS

My supervisors, Dr. Iain Samson and Dr. Brian Fryer are sincerely thanked for their scientific direction, supervision, considerable patience, encouragement, guidance, financial support, and their seemingly infinite wisdom. I am exceedingly grateful to Mr. Joel Gagnon who very kindly provided much of his time and his considerable expertise in the use of the LA-ICP-MS instrumentation and in the interpretation of the LA-ICP-MS data.

I sincerely thank Dr. John Greenough for his support, patience, direction, encouragement, inspiration and many invaluable suggestions. I acknowledge Dr. Henry Longerich for providing numerous insightful comments and suggestions. I thank Dr. Bruce Perry for his encouragement and inspiration. I also thank Dr. Robert Letcher, Dr. Ali Polat and Dr. Bob Linnen for their valuable comments and suggestions.

I am grateful to Dr. Tucker Barrie and Mr. Phil Walford for their direction and guidance during the initial fieldwork and to Dr. Tucker Barrie for his continued support throughout the project. I acknowledge Geomaque Explorations Ltd. for providing financial and logistical support for most of the fieldwork and I also acknowledge NSERC and the University of Windsor for financial and logistical support.

I am thankful to Lachlan MacLean for his many unique suggestions, enduring support, and good friendship. Similarly, I would like to thank Elisabeth Sabo, Johari Pannalal, Erin Bennet, Dr. Shaunquan Zhang, Tom Collins, Scott Song, Magda Scarlat, Arne Sturm, Hans Davina and Kamal Raikhy for their friendship and support. I also thank Dr. David Fowle, Dr. Mike Harris, J.C. Barrette, Dr. Phil Graneiro and Dr. Phil McCausland for their many helpful suggestions.

Finally, I would like thank my family, especially my parents, Dennis and Terry Crowe for their seemingly infinite patience and encouragement, financial assistance, and guidance and direction. I would also like to thank my daughter Tenille for her understanding and patience, and Erin, Paul and Catherine for their friendship and encouragement. Meghan Wise is thanked for her friendship and patience.

For my parents Dennis and Terry Crowe and my daughter Tenille Crowe

With Love

TABLE OF CONTENTS

ABSTRACT	III
ACKNOWLEDGEMENTS	IV
DEDICATION	V
LIST OF ABBREVIATIONS	VIII
INTRODUCTION	1
1.1 OVERVIEW	1
1.2 BACKGROUND	2
1.2.1 <i>Classical Magmatic PGE enrichment</i>	3
1.2.2 <i>Hydrothermally Controlled PGE enrichment</i>	4
1.3 PREVIOUS WORK	5
1.3.1 <i>Marathon as a hydrothermal deposit</i>	5
1.3.2 <i>Marathon as a magmatic deposit</i>	6
1.3.3 <i>Marathon as a hybrid-contact type deposit</i>	7
1.4 RESEARCH METHODOLOGY	8
1.4.1 <i>Pb Isotopes</i>	8
1.4.2 <i>Metal Distribution</i>	11
1.5 ANALYTICAL STRATEGY	14
1.6 SUMMARY	15
1.7 ACKNOWLEDGEMENTS	16
1.8 REFERENCES	17
PRECISE ISOTOPE RATIO DETERMINATION OF COMMON PB USING QUADRUPOLE LA-ICP-MS WITH OPTIMIZED LASER SAMPLING CONDITIONS AND A ROBUST MIXED-GAS PLASMA	21
2.1 INTRODUCTION	21
2.2 EXPERIMENTAL	22
2.2.1 <i>Sample Preparation</i>	22
2.2.2 <i>Imaging and Stage Control</i>	23
2.2.3 <i>Micro-sampling</i>	23
2.2.4 <i>Laser</i>	24
2.2.5 <i>ICP-MS and Data Acquisition</i>	25
2.2.6 <i>Data Reduction and Analysis</i>	25
2.2.7 <i>Statistics and Measures of Precision</i>	26
2.3 RESULTS	27
2.3.1 <i>Focal Position</i>	27
2.3.2 <i>Beam Restriction</i>	27
2.3.3 <i>Raster Rate</i>	28
2.3.4 <i>Combined and Interactive effects</i>	28
2.3.5 <i>Mass Bias Correction by External vs. Internal Methods</i>	28
2.3.6 <i>Analytical Merits of Measurements made under OSC</i>	30
2.4 DISCUSSION	30
2.4.1 <i>Poisson Counting Statistics</i>	31
2.4.2 <i>Mass Bias</i>	32
2.5 APPLICATION TO ISOTOPE TRACER STUDIES	32
2.5.1 <i>Results</i>	33
2.5.2 <i>Discussion</i>	33
2.6 CONCLUSIONS	34
2.7 ACKNOWLEDGEMENTS	35

2.8 REFERENCES	36
2.9 TABLES	39
2.10 FIGURES	45
MICROMETRE SCALE PB ISOTOPE COMPOSITION OF MAJOR MAGMATIC PHASES AND ALTERATION PRODUCTS FROM THE MARATHON PGE-CU DEPOSIT: CONSTRAINTS ON MAGMATIC HYDROTHERMAL EVOLUTION	53
3.1 INTRODUCTION	53
3.2 BACKGROUND	54
3.2.1 Regional Geological Setting.....	54
3.2.2 Deposit Petrology and Mineralization	55
3.2.3 Relevant Previous Isotope Studies.....	56
3.3 EXPERIMENTAL.....	57
3.3.1 Sampling.....	57
3.3.2 Pb Isotope Ratio Determination	58
3.4 RESULTS	59
3.4.1 Petrography.....	59
3.4.2 Pb Isotopes	61
3.5 DISCUSSION	63
3.5.1 Textural Relationships.....	63
3.5.2 Pb Isotope Systematics	64
3.5.4 Constraints on Models.....	70
3.6 SUMMARY.....	73
3.7 REFERENCES	75
3.8 TABLES	79
3.9 FIGURES	81
PRELIMINARY INVESTIGATION OF PLATINUM-GROUP ELEMENT AND TRACE ELEMENT DISTRIBUTION AND FRACTIONATION IN THE MARATHON PGE-CU DEPOSIT:	- 90 -
4.1 INTRODUCTION	- 90 -
4.2 GEOLOGICAL SETTING	- 92 -
4.3 DEPOSIT PETROLOGY AND MINERALIZATION	- 93 -
4.4 EXPERIMENTAL.....	- 94 -
4.4.1 Sampling.....	- 94 -
4.4.2 Whole Rock PGE determination.....	- 94 -
4.4.3 Mineral Pb Chemistry	- 95 -
4.5 RESULTS	- 96 -
4.5.1 Evaluation of the Ion exchange method.....	- 96 -
4.5.2 Precious Metals content of Marathon Samples	- 97 -
4.5.3 Pb distribution in Marathon Sulphides.....	- 97 -
4.6 DISCUSSION	- 98 -
4.6.1 DETERMINATION OF THE PGE USING THE NiS FA, CATION EXCHANGE ICP-MS TECHNIQUE	- 98 -
4.6.2 Precious metals content of Marathon Deposit.....	- 98 -
4.7 SUMMARY.....	- 100 -
4.8 REFERENCES	- 102 -
4.9 TABLES	- 104 -
4.10 FIGURES	- 108 -
SUMMARY.....	- 112 -
5.1 SUMMARY AND WORK PROGRESS	- 112 -
5.2 REFERENCE	- 113 -
VITA AUCTORIS.....	- 114 -

LIST OF ABBREVIATIONS

ANOVA	analysis of variance
AR	<i>aqua regia</i>
D	distribution coefficient
<i>f</i>	fugacity
FA	fire assay
Ga	giga anna
ICP-MS	Inductively coupled plasma-mass spectrometer
iss	intermediate solid solution
κ	present-day $^{232}\text{Th}/^{238}\text{U}$
LA	laser ablation
MC	multi-collector
mg	milligram
ml	milliliter
μ	present-day $^{238}\text{U}/^{204}\text{Pb}$
μg	micrometer
μm	micrometer
Ma	mega anna
MORB	mid-ocean ridge basalt
mss	monosulphide solid solution
NiS	nickel sulphide
PGE	platinum-group elements
PGM	platinum-group minerals
ppb	parts per-billion
ppm	parts per-million
SEM	scanning electron microscope
SHRIMP	sensitive high-resolution ion-microprobe
SIMS	secondary ion mass spectrometry
SN	solution nebulization
SSC	standard sampling conditions
RF	response factor
TDL	Two Duck Lake
TIMS	thermal ionization mass spectrometry

CHAPTER 1

Introduction

1.1 Overview

The Marathon Deposit is a platinum group element (PGE)-Cu prospect hosted by the Coldwell intrusive complex, located on the North Shore of Lake Superior. The following thesis project investigates the relative importance of various ore forming processes responsible for the PGE and Cu enrichment of the deposit. Sulphide-hosted PGE deposits in mafic to ultramafic intrusions have traditionally been associated with dominantly orthomagmatic ore forming processes. However, many researchers have implicated volatile-rich late-stage magmatic (deuteric) and post-magmatic hydrothermal fluids in the mobilization and redistribution of the PGE to form deposits. Both primary magmatic and hydrothermal processes have been proposed as mechanisms for the enrichment of the PGE and Cu in the Marathon deposit. This thesis project evaluates these proposed mechanisms and, using geochemical studies of both mineralized and non-mineralized rocks, tests both the magmatic and hydrothermal models. This work focuses on the role of crustal contamination as a source for sulphur and metals, and the role of both late-stage magmatic and post-magmatic hydrothermal fluids in the formation of the PGE-enriched lithologies. A LA-ICP-MS method has been developed to conduct mineral-scale Pb isotope ratio measurements at low concentrations. A Pb isotope study has been conducted to address the issue of crustal contamination. The Pb isotope work is followed by noble metal and trace element studies to examine that examine the distribution of the PGE and trace elements from the mineral to deposit scale.

Platinum group elements (PGE) are economically important metals and are indispensable for many applications in the communications, catalyst, and pharmaceutical industries (Basset 2001, Christian 2001). With the known existence of only three major deposits, namely; the Noril'sk-Talnakh deposits (Russia), the Stillwater Igneous Complex (SIC) (Montana, USA), and the Bushveld Igneous Complex (BIC) (South Africa), and less than twelve other significant deposits globally there exists considerable need to develop a more diversified supply of these metals. A more complete understanding of the geochemical behavior of the PGE and the relative roles of PGE ore-forming processes would be

invaluable to the pursuit of new deposits and the development of these resources in Canada, and worldwide (Sutcliffe and Peck 2001). A study of the Marathon deposit provides an opportunity to evaluate the relative roles of ore forming processes, most importantly the extent and mechanism by which volatile components and crustal contamination contribute to PGE enrichment.

1.2 Background

The generation of a classical magmatic PGE deposit has been outlined as involving: 1) the formation of a magma due to the partial melting of mantle material; 2) the emplacement and crystallization of this magma; 3) the segregation of an immiscible sulphide phase, partitioning of PGE into the sulphide liquid, and concentration of the PGE-enriched sulphide liquid by gravitational settling; and 4) the possible redistribution of metals by post crystallization processes (Naldrett et al. 1989). However, some researchers would contest this model and suggest that a magmatic volatile phase forms in a cumulate pile and migrates upward due to density and concentration gradients. As this fluid front migrates, the volatiles collect the PGE (as volatile complexes) from the crystal mush and concentrate them in the fluid phase. The PGE are subsequently deposited at the mush–melt interface when volatiles re-dissolve in the melt or as a result of changing intensive properties (Boudreau et al. 1986, Boudreau and Meurer 1999, Willmore et al. 2000).

The average PGE content of the mantle is well documented (although poorly constrained) and has been determined based on chemical analyses of mantle xenoliths, alpine peridotites, and ultramafic rocks from ophiolite sequences (Barnes et al. 1985). However, the heterogeneity of the mantle with respect to PGE distribution is not well understood and the importance of PGE-enriched mantle sources for generating magmas that form PGE deposits is not known. Nevertheless, the requirement of anomalous PGE concentrations in initial magmas that form PGE ore deposits is unlikely. The fact that there is little difference between the PGE contents of the primary magmas associated with the non-economic Skaergard, and economic Bushveld and Stillwater intrusions indicates that high PGE concentrations in primary melts are not a dominant factor in the formation of these deposits. This necessitates the operation of processes that concentrate PGE from source magmas to form enriched zones (Crocket 1979). The average Pt content of mafic to ultramafic magmas

is approximately 10 ppb, with a range from 0.1 ppb to 500 ppb, whereas the average concentration of PGE in ore deposits is 5-10 ppm. This requires enrichment factors of approximately one thousand (MacDonald 1987). Current thinking on mechanisms responsible for PGE enrichment favor either dominantly magmatic or dominantly hydrothermal processes and thus proponents of these models can be divided into two camps, the hydrothermal camp, and the magmatic camp.

1.2.1 Classical Magmatic PGE enrichment

It has been said that in excess of 99 % of the world's supply of PGE originates from sulphides of magmatic origin (Naldrett 1989). The world's largest PGE deposits (hosted by the Bushveld and the Stillwater Complexes) are characterized by reef-type stratiform zones of PGE mineralization in mafic and ultramafic rocks. These deposits were originally thought to have been generated by magmatic processes. The definitive characteristics of these and other "magmatic" PGE deposits have been described as being hosted by cumulate, layered, locally pegmatitic, rock units in medium to large, mafic to ultramafic intrusions and possessing an association with minor sulphide or significant oxide components. In addition, the local presence of minor hydrous phases and evidence for the occurrence of multiple magma influxes and the mingling of these distinct magmas are common features of these deposits (Naldrett, 1989).

The dominant mechanism responsible for the formation of PGE deposits by magmatic processes is the segregation of an immiscible sulphide liquid from a silicate melt and collection of chalcophile elements by the sulphide liquid from the remaining silicate fraction. This process alone would result in disseminated sulphides with little change to the PGE content of the whole rock. In order to form an ore deposit, the metal-enriched sulphide liquid must accumulate near the base of an intrusion or in oxide reefs. This generally occurs by gravity settling due to the greater density of the sulphide liquid than the silicate melt. Sulphide saturation in magmas results from either the addition of exotic S to a melt or by changes in factors controlling sulphur solubility in the melt (e.g. FeO content, f_{O_2} , f_{S_2} and SiO₂ content). These changes can result from fractional crystallization, magma mixing, or contamination processes (Naldrett, 1989)

The effective concentration of PGE in the immiscible sulphide liquid is due to high

partition coefficients (D) of the PGE, where D is defined as:

$$D = \frac{[M]_{\text{sulphide}}}{[M]_{\text{silicate}}}$$

and [M] represents the concentration of the metal (i.e. Pd, Pt, Rh, Ru, Os, and Ir) in the sulphide and silicate phases. Values of D for PGE range from approximately 10^3 to 10^7 under typical magmatic conditions (Naldrett 1989, Barnes et al. 1997, Fleet et al. 1999, Andrews and Brenan 2002). The extent of PGE enrichment is critically dependent on mechanisms that allow for mixing of the sulphide phase with a significant volume of silicate magma (Campbell et al. 1983, Campbell and Barnes 1984, Naldrett 1989). The strongest arguments against magmatic origins for PGE deposits are the fact that the PGE are often fractionated within deposits and that the PGE concentrations in sulphides are higher than those allowed by experimentally determined distribution coefficients (D values).

1.2.2 Hydrothermally Controlled PGE enrichment

The high solubility of PGE in hot chlorine gas and aqua regia led some early researchers to hypothesize that PGE would also be similarly soluble in volatile-rich geological fluids (Cousins and Vermaak 1976). Thermodynamic calculations have shown that PGE may be complexed by Cl^- and OH^- ions under acidic and oxidizing or neutral conditions respectively, at various temperatures (Mountain and Wood 1988, Sassani and Shock 1998). In addition, experiments have shown that the degree of chloride complex formation generally shows a positive correlation with f_{O_2} , f_{HCl} , and temperature and a negative correlation with $f_{\text{H}_2\text{O}}$ and f_{S_2} (Fleet and Wu 1995, Pan and Wood 1994). Experimental studies have also shown that both sulphur and metals, including PGE, can be mobilized by the same fluid at high temperatures, and that the partitioning of metals between the vapor and melt is proportional to the chlorine content of the vapor (Groves and Keays 1979). It can be reasoned that a relationship would exist that could describe the PGE content of sulphides and silicates that interacted with chlorine-bearing solutions based on the relative solubility of the various PGE in these fluids (Boudreau et al. 1986, Greenough and Fryer 1995). The general model presented for the genesis of hydrothermal PGE deposits suggests that PGE can form hydroxide, chloride and sulphide complexes in geological fluids are transported in this fluid phase and are precipitated around sulphide melt droplets with

changing intensive properties (ie. P, T, $f_{\text{H}_2\text{O}}$, f_{S_2} , f_{O_2}) resulting in the enrichment of these sulphides (Ripley et al. 1993, Ballaus and Stumpfl 1986). Thus, it seems that the anomalously high and fractionated PGE tenors of ore bearing sulphides can be explained by the interaction of these phases with volatile fluids. Extensive empirical evidence including pegmatitic textures, association of PGE bearing sulphides with hydrous mineral phases, high halogen contents in volatile-bearing minerals, and anomalous PGE distribution patterns supports the role of hydrothermal processes in the formation of PGE deposits (Prichard et al. 2001, Harris and Chaumba 2001, Boudreau and Muerer 1999, Pasteris et al, 1995).

1.3 Previous Work

The regional geology and mineral deposits of the Coldwell complex have been well documented. Given that there are two distinct schools of thought with respect to the formation of PGE deposits in general, it is not surprising that both of these schools are represented in the literature pertaining to the genesis of the Marathon deposit. Proponents of the hydrothermal school, (Ohnenstetter et al.1991, Watkinson and Ohnenstetter, 1992), present a model that attributes PGE enrichment to the interaction of primary magmatic minerals with volatile-bearing hydrothermal fluids. Conversely, proponents of the magmatic school, (Wilkinson 1983, Good, 1993, Good and Crocket 1994) have described a model whereby the PGE were collected by an immiscible sulphide liquid which in turn crystallized PGE-bearing magmatic sulphides. Recently, a model that involves the collection of PGE in magmatic sulphides followed by redistribution (on the scale of 10s of meters) as a result of fluid fluxing and zone refining has been proposed (Barrie et al. 2002).

1.3.1 Marathon as a hydrothermal deposit

Based on initial observations of chemically zoned rhodium arsenosulphides, and the presence of platinum group minerals in fluid inclusions, Watkinson and Ohnenstetter (1992) have proposed a hydrothermal origin for PGE-Cu mineralization in the Eastern Gabbro. The occurrence of PGE enrichment in coarse-grained to pegmatitic gabbroic rocks, rich in halogens, and proximal to partially digested country rock xenoliths, was attributed to the interaction of magmatic mineral assemblages with deuteric fluids, and fluids derived from partial melting and assimilation of country rock xenoliths. Mineral assemblages associated

with PGE enrichment were described as epidote + actinolite + chlorite + sericite + calcite in otherwise unaltered gabbro. It was hypothesized that the hydrothermal fluid transported metals in the form of chloride complexes which were precipitated with increasing f_{S_2} and/or decreasing f_{O_2} as a result of interaction with magmatic pyrrhotite, magnetite, and silicates (Watkinson and Ohnenstetter 1992).

1.3.2 Marathon as a magmatic deposit

Several features of the Marathon deposit support enrichment as a result of primary magmatic processes. The well-developed semi-massive and net texture in the Basal Zone sulphides is strong evidence that deposition occurred as a result of crystal settling processes (Wilkinson 1983, Good 1993). Good and Crocket (1994) have indicated that the strong correlation between chalcophile elements, the coherent behavior of Ni and Ir, and preservation of primary minerals precludes the interaction of the rock with a significantly large volume of fluid. They have noted that, based on the calculations of Mountain and Wood (1988) that show low PGE solubility in fluids at low temperature under reducing conditions, a high fluid/rock ratio would be required for the transport of appreciable amounts of PGE. According to Good and Crocket, this high ratio would result in extensive alteration of primary minerals which has not been observed at Marathon. The model Proposed by Good and Crocket (1994) involves the development of a compositionally stratified magma chamber caused by density differences from fractional crystallization and intermittent replenishment with non-fractionated magma. They suggest that the assimilation of siliceous country rocks presents a possible mechanism to induce sulphur saturation by sulphur addition. The textures and distribution of the mineralized horizons are attributed to the emplacement of a crystal mush and aggregation of sulphide droplets, gravity settling of crystals, sulphide liquid, and silicate melt, and the migration of volatile-rich interstitial melt to form pegmatitic zones. Subsolvus reactions between cumulate minerals and volatile-bearing fluids caused local migration of elements and the formation of hydrous silicates, and would account for the replacement of pyrrhotite by chalcopyrite and deposition of PGM in association with hydrous silicates (Good 1993, Good and Crocket 1994).

1.3.3 Marathon as a hybrid-contact type deposit

Barrie et al. have indicated that a model involving the addition of sulphur by volatile fluxing and zone refining processes can account for the spatial distribution of chalcophile elements and sulphur, including their association with coarse-grained to pegmatite textures. Furthermore, the spatial association of the deposit with felsic metavolcanic country rocks can be explained by the fact that the low temperature melting points and relatively high volatile element and sulphur contents of these rocks are more conducive to deposit formation by volatile fluxing and zone refining than the granitic and mafic country rocks adjacent to non-mineralized gabbros (Barrie et al. 2002).

Although the fluid fluxing and zone refining mechanism is not described in detail by Barrie et al., a similar mechanism has been proposed by Brüggmann et al. to explain the PGE distribution in the Lac des Iles deposit (Brüggmann et al. 1989). In their model, partial melting occurs when water comes into contact with hot cumulates. The movement of water upward through the cumulate pile produces a migrating zone of partial melting, which leaves behind a zone of refractory minerals and minerals crystallized from the secondary melt. Incompatible elements become concentrated in the upward migrating volatile-rich melt in a process that is analogous to metallurgical zone-refining. If the melt is undersaturated in sulphide, any sulphide in the original cumulate will be dissolved in the melt, and, as a result, chalcophile elements including PGE will be added to this migrating melt. Once the melt is saturated in sulphur, sulphide minerals precipitate forming a sulphide bearing zone enriched in chalcophile elements.

Petrographically, rocks that represent the residuum, or restite (refractory minerals and re-crystallized partial melt) are varitextured and would be equivalent to the Basal Zone rocks in Marathon deposit, as described by Barrie et al. (2002). Rocks that crystallize from, or in the presence of, the evolved melt would have a pegmatitic texture, due to enhanced diffusivity, caused by the elevated volatile contents of the melt. Furthermore, these rocks could have an increase in the modal abundance of hydrous minerals depending on the H₂O activity at the time of crystallization (Brüggmann et al. 1989). The zone refining and volatile-induced melting processes have been described in detail by McBirney (1987) and Kerr (1994), however, a more detailed discussion is beyond the scope of this proposal. These

processes are similar to those proposed by Boudreau et al. (1986), Boudreau and Meurer (1999) and Willmore et al. (2000) for the genesis of the Bushveld and Stillwater deposits.

1.4 Research Methodology

The three models presented for the genesis of the Marathon deposit can be evaluated by testing mechanisms responsible for the transport of trace elements and those responsible for precipitation of ore-bearing sulphide minerals. The model of Barrie et al. (2002) necessitates precipitation of sulphides from a hydrothermal fluid or volatile-enriched melt. This fluid/melt may have a component derived in-situ from the metavolcanic country rocks. As an alternative, Barrie et al. have also suggested that the fluids may have been derived from late-stage interstitial melt. Similarly, the model of Watkinson et al. requires that sulphides be precipitated from a hydrothermal fluid. They too have suggested that the fluid may have been derived from magmatic or country rock sources. Good and Crocket have indicated that the assimilation of country rock may have contributed to the precipitation of magmatic sulphides. All previous authors have suggested that crustal contamination, by various mechanisms, may have been important for the genesis of the PGE bearing sulphides. By addressing this issue, constraints can be placed on mechanisms responsible for sulphide saturation and on potential sources of hydrothermal fluids.

1.4.1 Pb Isotopes

Pb isotope systematics can be very useful indicators of geological history and can yield important constraints on numerous geological processes, including crustal contamination. With respect to this study, the Pb isotopic composition of minerals can be used to infer information about the source of base and precious metals in ore deposits (Tosdal et al. 1999). This is based on the fact that magmas can have isotope signatures that are distinct from the country rocks into which they intrude. Minerals derived from magmas in the absence of crustal contamination will have initial Pb isotopic ratios corresponding to the mantle/crustal source reservoir from which they were derived. However, minerals that have a component of lead derived from the country rocks resulting from crustal contamination will give hybrid initial isotopic ratios reflecting the degree of contamination from the country rock. Lead isotopes are an ideal tracer system for the investigation of crustal contamination at

the Marathon deposit. The large age difference between the Archean country rocks (ca. 2.7 Ga) (Corfu and Muir 1989) and the Proterozoic (1.108 Ga) (Heaman and Machado 1992) intrusion has allowed sufficient time for the evolution of distinct isotopic compositions. Thus, the isotope ratios of sulphides in the complex should be quite sensitive to small amounts of contamination. The Pb isotopic composition of different phases will provide information on the timing of introduction of exotic Pb (not initial magma) and the identity and origin of these phases may provide information on the mechanisms by which the exotic lead was introduced.

The use of lead isotopes to model geological processes is dependent on the fact that because of ionic charge and radius differences between U, Th and Pb, certain minerals, including feldspars and many sulphides, exclude uranium and thorium from their crystal structure while including lead to a much greater degree. The association and textural relationships of Pb-rich minerals with other ore minerals allows for the interpretation of their origin in relation to that of the Pb-rich minerals.

Lead isotopes have been used to characterize the extent and mechanism of crustal contamination in the Stillwater igneous complex in Montana (SIC) (Wooden et al. 1991). Sulphides in the SIC have been observed not to be in isotopic equilibrium with pristine plagioclase, meaning that the differences between Pb isotope ratios of the two minerals were greater than could be accounted for by fractionation, based on crystal chemical effects, during equilibrium crystallization (McCallum et al. 1999). The observed isotopic discrepancies have been attributed to the remobilization of sulphides and incorporation of exotic lead derived from hydrothermal fluids. As a result of a high degree of scatter in the isotopic ratios the authors were unable to attribute the disequilibrium to simple mixing between magmatic lead and lead derived from the adjacent country rock. Therefore, exotic lead was attributed to multiple source regions scavenged by hydrothermal fluids generated during an episode of regional metamorphism.

Pb isotope studies of the Duluth Complex, Minnesota indicate that as much as 50% of the Pb in sulphides hosted by the complex was derived from external sources (Ripley et al. 1999). This contamination has been attributed to the assimilation of country rock during residence in crustal magma chambers, magma ascent, or in situ as a result of volatile fluxing and partial melting. Based on similarities in mineral textures, abundances, and composition,

it has been implied that the Marathon deposit formed by processes analogous to those that formed the deposits in the Duluth Complex (Good and Crocket 1994). This confirms that a lead isotope study of the Marathon deposit is an appropriate method for addressing the issue of crustal contamination.

In the case of the Marathon deposit, the lead isotope systematics would be different for the three proposed models. The model presented by Barrie et al. (2002) indicates that the volatile fluids required for fluid fluxing may have been derived from the country rocks. This situation would produce PGE-bearing sulphides in Pb isotope disequilibrium with primary magmatic sulphides and pristine magmatic silicates. The isotope ratios could show a moderate degree of variability, which is characteristic of minerals precipitated by hydrothermal fluids. Alternatively, ore-bearing sulphides that would be produced by the mechanisms proposed by Good and Crocket (1994) would yield isotope ratios identical to those of unaltered silicates regardless of local crustal contamination. This can be explained by the fact that Good and Crocket have proposed that crustal contamination occurred in a deep magma chamber prior to emplacement. However, it is possible that some of the plagioclase and olivine would have crystallized prior to contamination and sulphides could yield Pb isotope ratios different from these early-crystallizing silicates. If the assimilation of country rock, by partial melting, occurred *in situ* and sulphur saturation was induced as a result of this in-situ contamination, early crystallizing minerals would be in disequilibrium with sulphides as the silicates would have crystallized prior to intrusion and therefore prior to contamination. In this case, zoned plagioclase may show isotopic variations between zones, where late plagioclase rims may have equilibrated with contaminated interstitial melt/fluid. Isotope ratio variations produced by a magmatic system, such as the one proposed by Good and Crocket, should show relatively low degrees of scatter between minerals from the same source. However, the hydrothermal model of Watkinson et al. (1992) would show a considerable degree of scatter and ore bearing sulphides could be in disequilibrium with magmatic minerals. If the ore-bearing sulphides are in equilibrium with magmatic minerals then crustal xenoliths or country rock would be an unlikely source for fluids as proposed by Watkinson et al.. If sulphides crystallized from a hydrothermal fluid that was either derived from the intrusion, or contained insignificant amounts of exotic lead, the Pb isotope ratios would appear to be the same as primary silicates.

Isotope ratio determinations of country rock samples should accompany interpretations of isotopic variations in igneous rocks associated with the deposit as the country rocks may be isotopically heterogeneous and this could be reflected in rocks subject to contamination. This is especially important if the rocks were subjected to hydrothermal activity (Ripley et al. 1999). Although all three models are capable of producing rocks with isotope ratios influenced by crustal components, the lead isotope study could yield important constraints with respect to the magmatic model of Good and Crocket (1994) and the models that involve hydrothermal systems. These constraints can be used to provide a framework within which to interpret further petrological and geochemical data. It is important to note that the interpretation of the isotope data will be strongly dependent on textural observations. As a result, it will be important to classify sulphide and silicate minerals and their associations and relationships.

Although a lead isotope study can be very informative with respect to the relationship of crustal contamination to deposit formation, the mechanism of hydrothermal enrichment (i.e. magmatic zone-refining or subsolidus hydrothermal) would be only loosely defined by the degree of scatter observed in the data. As a result there would still be very little constraint on the relative appropriateness of the models proposed by Barrie et al. (2002) and Watkinson and Ohnenstetter (1992).

1.4.2 Metal Distribution

To develop models that explain PGE enrichment processes it is necessary to obtain information regarding how the PGE are distributed in the PGE-enriched and poor phases (Ballhaus and Sylvester 2000, Barnes and Maier 1999). It is likely that the most distinguishable differences between each of the proposed models would be their distinct PGE, Cu, and Ni distribution patterns. For example the model of Barrie et al. (2002) suggests that, during zone refining, the PGE were collected from the stratigraphically low rocks of the Basal Zone by upward migrating volatiles or volatile rich melt. As a result, rocks stratigraphically below the ore zone should be depleted in PGE relative to the initial magma and the rock above the mineralized zone should retain the initial magmatic PGE content (Brüggmann et al. 1989). Alternatively, the model of Watkinson and Ohnenstetter (1992) requires that the PGE have been scavenged by fluids from the surrounding rock. This

requires that the PGE be depleted where the fluids have interacted with the rock. The magmatic model of Good and Crocket (1994) suggests that the PGE have been partitioned into an immiscible sulphide liquid. As a result, rocks that crystallized from silicate liquid in equilibrium with immiscible sulphide would be depleted in PGE relative to those that crystallized from a melt that had not reached sulphide saturation.

In addition to the distribution of PGE in rocks, the PGE tenors of sulphides may also be used to evaluate enrichment processes. For example, if the PGE distribution in the deposit is the result of magmatic mixing than the PGE tenors in the sulphides should conform to the following equation:

$$C_{\text{sulph.}}^{\text{PGE}} = C_{\text{silicate}}^{\text{PGE}} \cdot D \cdot (R+1)/(R+D)$$

where C is the concentration of metal, D is the sulphide/silicate distribution coefficient and R is the ratio of silicate liquid to equilibrate with the sulphide liquid. The only inter-element noble metal fractionation would occur as a result of varying distribution coefficients between metals. This effect is accentuated at high R values where large differences in D can moderately affect the relative PGE abundances in sulphides. It has been suggested, however, that because of the similar D values between PGE that simple sulphide segregation and magma mixing cannot cause inter-element PGE fractionation (Peach et al. 1996). In contrast, sulphides deposited by hydrothermal fluids would possess noble metal tenors that reflect the relative solubility of the metals in the hydrothermal fluids.

Mantle-normalized precious metal, Cu, and Ni patterns can be very useful in distinguishing various petrological and hydrothermal processes (Barnes et al. 1997a,b) The PGE concentrations of the initial unfractionated magma in deposits can be obtained from samples that represent chilled margins and a plot of this pattern can yield information about the magma source and the degree of partial melting. As a result of the much higher partition coefficients of the PGE than Cu and Ni into magmatic sulphide, the separation and settling of a sulphide liquid will produce a cumulate that is enriched in the noble metals relative to Cu and Ni and will leave the remaining magma depleted in these elements. A mantle-normalized plot of the cumulate, sulphide bearing rocks will express an arch shaped pattern with the noble metals enriched relative Cu and Ni. The same plot of any rock that subsequently

crystallizes from this fractionated magma will show a trough shaped pattern. Similarly, the crystallization of silicate and oxide phases into which Os, Ir, and Ru are compatible leave residual magmas that show steeper positive slopes than the initial melt. However, there is considerable debate as to the compatibility of PGE into silicate phases, especially with respect to Rh, Pt and Ru (Sattari et al. 2002).

Further complications arise when trying to model geological processes based on mantle-normalized PGE patterns. The most significant of these is the fact that mantle PGE concentrations are poorly constrained (Ballhaus 1995). In addition, the presence of small amounts of sulphides in nonmineralized samples can dramatically affect the noble metal patterns due to the “nugget” effect and there is considerable difficulty associated with analyzing PGE at trace concentrations (Barnes et al. 1988, Barefoot and Van Loon 1999). These issues, however, can be partly circumvented by using element ratios and by recalculating to 100% sulphide. Both procedures serve to eliminate the dilution effects of silicate material, and compensate for heterogeneous sulphide distribution.

Plots of PGE, Cu and Ni ratios (e.g. Ni/Pd, Pd/Ir, Cu/Ir) and mantle-normalized plots can be used to characterize hydrothermal events. Unlike magmatic processes, hydrothermal events produce rocks that yield highly variable, irregular, mantle-normalized PGE patterns, and ratios (Farrow and Watkinson, 1996). Hydrothermal fluids are capable of producing fractionated PGE patterns based on the variable solubility of the metals in fluids of a given composition. In addition to generating extremely fractionated Pd-Pt-Rh vs. Os-Ir-Ru, patterns, hydrothermal fluids can also fractionate Pt from Pd due to the greater mobility of Pd as a chloride complex at high pH values (Mountain and Wood 1988, Pan and Wood 1994, Sassani and Shock 1998).

. Although the distribution patterns of the noble metals may be quite diagnostic of the processes responsible for mineralization, they may be difficult to accurately access due to analytical complications (see Analytical Strategy below). This is especially true for rocks in which the PGE abundances approach the detection limits of the most sensitive analytical techniques.

1.5 Analytical Strategy

The success of this analytically intensive project is critically dependent on the selection and development of the appropriate analytical methodology. Laser ablation inductively coupled plasma mass spectrometry (LA-ICP-MS) and solution nebulization ICP-MS are used for the majority of analyses. The use of the LAM in conjunction with ICP-MS for the determination of many elements over a broad range of concentrations is well established (Fryer et al. 1995).

As mentioned above, the correct interpretation of the isotope data with respect to deposit formation depends on how this data relates to PGE distribution in both mineralized and non-mineralized rocks. The determination of the PGE at low concentrations, such as those present in non-mineralized rocks, is an analytically difficult task (Barefoot and Van Loon 1999). The decomposition of geological matrices for PGE analyses is complicated by the fact that the platinum group elements are resistant to attack from all but the strongest acids and high temperature fusion processes. Factors to consider in the decomposition of a sample include the contribution of matrix components to both additive and deductive interference in instrumental measurements and the presence of contaminant PGE in reagents (reported to be up to 1ppb) as a result of their use in purification processes (Jackson et al. 1990).

High temperature fusion processes, including fire assay (FA) using Pb, NiS, and Sn collectors and various alkaline digestions, are often employed to pre-concentrate and separate the noble metals from geological matrices. Of the fire assay procedures, collection by nickel sulfide is well-suited to the determination of all six of the PGE. However, accurate, precise determinations of Au are difficult to achieve with the nickel sulfide technique (Chen et al. 1996). The nickel sulfide technique offers several advantages over that of the classical Pb technique including: a smaller flux to sample ratio, lower fusion temperature, and applicability to the determination of all six PGE. With the exception of chromite-rich ores, the performance of the NiS fire assay is not affected by the sample matrix composition, and samples with a large variance in felsic and mafic composition can be analyzed without an adjustment to the flux mixture. Disadvantages, compared to lead collection, include the fact that the NiS technique is considerably more time consuming and recoveries of gold are 10-20% lower than those of a lead collection FA.

An inherent problem of fire assay techniques is that an effective recovery of the noble metals is dependent on their initial concentration in samples. At exceedingly low concentrations, significant biases may occur in determinations of PGE due to the fact that the partition coefficient decreases non-linearly with concentration (Frimpong et al. 1995). This is not the case for analyses of samples, such as mineralized rocks, where the PGE are present at concentrations above low ppb.

The use of ICP-MS in conjunction with NiS fire assay and Te co-precipitation for the determination of PGE is well established (Jackson et al. 1990, Oguri et al. 1999). Methods to deal with interferences, such as those that result from high iron, copper, or nickel concentrations have been described, with most of these techniques use ion exchange columns or solvent extractions with the NiS preconcentration technique (e.g. Chen et al. 1996).

In this study, Pb Isotope ratios have been determined using LA-ICP-MS. The use of ICP-MS for the determination of lead isotopes is generally accomplished with solution nebulization (Longerich et al. 1987), however, recently, LA-ICP-MS has been applied to U-Pb geochronology using multi-collector instruments (Fryer et al. 1993, Horn et al. 2000). The use of LA-ICP-MS for determining isotopes in feldspars and sulphides has not been previously documented, however, the laser ablation technique has several advantages over conventional methods. For example, previous studies have typically analyzed lead isotopes in mineral separates using thermal ionization mass spectrometry (TIMS). An advantage of the LA technique is that it avoids the time consuming procedure of preparing mineral separates. In addition, although the single collector instrument used in this study does not have the high precision of TIMS, it has the advantage of increased spatial resolution. In this way some of the precision lacking in the instrumentation can be compensated for with the ability to avoid impurities, such as inclusions that would cause imprecision in mineral separate data. Furthermore, isotopic variation in zoned minerals can be studied without the use of stepped leach processes.

1.6 Summary

This thesis tests the various models proposed for the genesis of the Marathon deposit. The following studies yield constraints with respect to the relative role of fluids in the generation of the deposit and evaluate crustal contamination as a source for sulphur and/or

metals. Information gleaned from this study is useful for future exploration at the Coldwell complex and development of the Marathon deposit. In addition, this study provides some insights into processes operating in the formation of other, similar deposits and contributes to the overall understanding of the geochemical behavior of the platinum group elements.

1.7 Acknowledgements

The conceptualization of this project is the result of combined thoughts from Iain Samson, Brian Fryer, Robert Linnen, Tucker Barrie, and Phillip Walford. Initial field work has been supported by Geomaque Explorations Ltd.. Sample collection and mapping efforts in the summer of 2001 were achieved with considerable help from Phillip Walford, Richard Middaugh, Robert Chatteway, Tucker Barrie, Richard Whalford, and David Patterson. Lachlan Maclean contributed to revisions and is thanked for helpful comments. The author is indebted to John Greenough for inspiration and many insightful thoughts and comments. The author is also indebted to Bruce Perry for similar contributions.

1.8 References

- Andrews, D., and Brenan, J.M. (2002) The solubility of ruthenium in sulfide liquid: implications for platinum group mineral stability and sulfide melt-silicate melt partitioning. *Chemical Geology*, **192**, 163-191
- Ballhaus, C.G., and Stumpfl, F.F. (1986) Sulfide and Platinum mineralization in the Merensky reef; evidence from hydrous silicates and fluid inclusions. *Contributions to Mineralogy and Petrology*, **94**, 193-204
- Ballhaus C.G. (1995) Is the upper mantle metal-saturated? *Earth and Planetary Science Letters*, **132**, 75-86
- Ballhaus, C., Sylvester, P. (2000) Noble metal enrichment processes in the Merensky Reef, Bushveld Complex. *Journal of Petrology*, **41**, 545-561
- Barefoot, R.R., Van Loon, J.C. (1999) Recent advances in the determination of the platinum group elements and gold. *Talanta*, **49**, 1-14
- Barnes S-J, Naldrett, A.J., Gorton, M.P. (1985) The origin of the fractionation of platinum-group elements in terrestrial magmas. *Chemical Geology*, **53**, 303-323
- Barnes, S.J., Campbell, I.H. (1988) The role of late magmatic fluids in Merensky-type platinum deposits-discussion. *Geology*, **16**, 488-491
- Barnes, S-J, Makovicky, E., Makovicky, M., Rose-Hansen, J., and Karup-Moller, S. (1997a) Partition coefficients for Ni, Cu, Pd, Pt, Rh, and Ir between monosulfide solid solution and sulfide liquid and the formation of compositionally zoned Ni-Cu sulfide bodies by fractional crystallization of sulfide liquid. *Canadian Journal of Earth Sciences*, **34**, 366-374
- Barnes, S.J., Zientek, M.L., and Severson, M.J. (1997b) Ni, Cu, Au, and platinum-group element contents of sulphides associated with intraplate magmatism: a synthesis. *Canadian Journal of Earth Sciences*, **34**, 337-351
- Barrie, C.T., MacTavish, A.D., Walford, P.C., Chataway, R., and Middaugh, R. (2002) Contact-type and Magnetite Reef-type Pd-Cu Mineralization in Ferroan Olivine Gabbros of the Coldwell Complex, Ontario. In *The Geology, Geochemistry, Mineralogy and Mineral Beneficiation of Platinum-Groups* (ed. L.J. Cabri), pp. 321-337. Canadian Institute of Mining, Metallurgy and Petroleum.
- Basset, G.H. (2001) Platinum group metals, supply and demand review. *Cordilleran Roundup Abstracts*, p. 45
- Boudreau, A.E., Mathez, E.A. and McCallum, I.S. (1986) The halogen geochemistry of the Stillwater and Bushveld Complexes: Evidence for the transport of the platinum-group elements by Cl-rich fluids. *Journal of Petrology*, **27**, 967-986
- Boudreau, A.E., and Meurer, W.P. (1999) Chromatographic separation of the platinum-group elements, gold, base metals and sulfur during degassing of a compacting and solidifying igneous crystal pile. *Contributions to Mineralogy and Petrology*, **134**, 174-185
- Brüggemann, G.E., Naldrett, A.J., MacDonald, A.J. (1989) Magma mixing and constitutional zone refining in the Lac des Iles Complex, Ontario: Genesis of platinum-group element mineralization. *Economic Geology*, **84**, 1557-1573
- Campbell, I.H., Naldrett, A.J., and Barnes S.J. (1983) A model for the origin of the platinum-rich sulfide horizons in the Bushveld and Stillwater complexes. *Journal of Petrology*, **24**, 133-165
- Campbell, I.H., and Barnes, S.J. (1984) A model for the geochemistry of the platinum-group elements in magmatic sulfide deposits, *Canadian Mineralogist*, **22**, 151-160

- Chen, Z., Fryer, B.J., Longerich, H.P., and Jackson, S.E. (1996) Determination of Precious Metals in Milligram Samples of Sulfides and Oxides Using Inductively coupled Plasma Mass Spectrometry After Ion Exchange Preconcentration. *Journal of Analytical Atomic Spectrometry*, **11**, 805-809
- Corfu, F. and Muir, T.L. (1989) The Hemlo-Heron Bay greenstone belt and Hemlo Au-Mo deposit, Superior Province, Ontario, Canada. A sequence of igneous activity determined by zircon U-Pb geochronology. *Chemical Geology*, **79**, 183-200
- Cousins, C.A., and Vermaak, C.F. (1976) The contribution of South Africa ore deposits to the geochemistry of the platinum group metals. *Economic Geology*, **71**, 287-305
- Christian, J.M. (2001) Platinum, palladium and silver markets and outlook. *PDAC Abstracts*, p. 1
- Crocket, J.H. (1979) Platinum-group elements in mafic and ultramafic rocks: a survey. *The Canadian Mineralogist*, **17**, 391-402
- Farrow, C.E.G., Watkinson, D.H. (1996) Geochemical Evolution of the Epidote Zone, Fraser Mine, Sudbury, Ontario: Ni-Cu-PGE remobilization by saline fluids. *Exploration and Mining Geology*, **5**, 17-31
- Fleet, M.E., and Wu, T-W. (1995) Volatile transport of precious metals at 1000°C: speciation, fractionation, and the effect of base metal sulfide. *Geochimica et Cosmochimica Acta*, **59**, 487-495
- Fleet, M.E., Crocket, J.H., Liu, M., and Stone, W.E. (1999) Laboratory Partitioning of platinum-group elements (PGE) and gold with application to magmatic sulfide-PGE deposits. *Lithos*, **47**, 127-142
- Frimpong, A., Fryer, B.J., Longerich, H.P., Chen, Z., and Jackson, S.E. (1995) Recovery of precious metals using nickel sulfide fire assay collection – problems at nanogram per gram concentrations. *Analyst*, **120**, 1675-1680
- Fryer, B.J., Jackson, S.E., and Longerich, H.P. (1993) The application of laser ablation microprobe – inductively coupled plasma–mass spectrometry (LAM-ICP-MS) to in-situ (U)-Pb geochronology. *Chemical Geology*, **109**, 1-8
- Fryer, B.J., Jackson, S.E., and Longerich, H.P. (1995) The design, operation and role of the laser-ablation microprobe coupled with an inductively coupled plasma-mass spectrometer (LAM-ICP-MS) in earth sciences. *Canadian Mineralogist*, 303-312
- Good, D.J. (1993) Genesis of Copper-Precious Metal Sulfide Deposits in the Port Coldwell Alkalic Complex, Ontario Geological Survey, Open File Report 5839, 231p
- Good D.J., and Crocket J.H. (1994) Genesis of the Marathon Cu-platinum-group element deposit, Port Coldwell Alkalic Complex, Ontario: A Midcontinent Rift-related magmatic sulfide deposit. *Economic Geology*, **89**, 131-149
- Greenough, J.D., and Fryer, B.J. (1995) Behavior of the platinum-group elements during differentiation of the North-Mountain basalt, Nova-Scotia. *Canadian Mineralogist*, **33**, 153-163
- Groves, D.I., and Keays, R.R. (1979) Mobilization of ore-forming elements during alteration of dunites Mt. Keith-Betheno, Western Australia. *Canadian Mineralogist*, **17**, 373-390
- Harris, C., and Chaumba, J.B. (2001) Crustal Contamination and Fluid-Rock Interaction during the Formation of the Platreef, Northern Limb of the Bushveld Complex, South Africa. *Journal of Petrology*, **42**, 1321-1347
- Heaman, L.M., Machado, N (1992) Timing and origin of mid-continent rift alkaline magmatism, North America: evidence from the Coldwell Complex. *Contributions to Mineralogy and Petrology*, **110**, 289-303

- Horn, I., Rudnick, R.L., McDonough, W.F. (2000) Precise elemental and isotope ratio determination by Simultaneous solution nebulization and laser ablation-ICP-MS: Application to U-Pb geochronology. *Chemical Geology*, **164**, 281-301
- Longerich, H.P., Fryer, B.J., and Strong, D.F. (1987) Determination of lead isotope ratios by inductively coupled plasma mass spectrometry (ICP-MS). *Spectrochimica Acta, Part B*, **42**, 39-48
- Jackson, S.E., Fryer, B.J., Gosse, W., Healey, D.C., Longerich, H.P., and Strong, D.F. (1995) Determination of precious metals in geological materials by inductively coupled plasma-mass spectrometry (ICP-MS) with nickel sulphide fire-assay collection and tellurium coprecipitation. *Chemical Geology*, **83**, 119-132
- Kerr, R.C. (1994) Dissolving driven by vigorous compositional convection. *Journal of Fluid Mechanics*, **280**, 287-302
- MacDonald, A.J. (1987) The Platinum Group Element Deposits: Classification and Genesis. In *Ore deposit models* (eds. Roberts, R.G., and Sheahan, PA), pp. 117-131. Geological Association of Canada
- McBirney, A.R., Russell, W.J. (1987) Constitutional zone refining of magmatic intrusions. *Nato ISI Series, Series E, Applied Sciences*, **125**, 349-365
- Maier, W.D., Barnes, S-J, (1999) Platinum-group elements in silicate rocks of the Lower Critical and Main Zones at Union section, Bushveld Complex. *Journal of Petrology*, **40**, 1647-1671
- McCallum, I.S., Thurber, M.W., O'Brien, H.E., and Nelson, B.K. (1999) Lead isotopes in sulfides from the Stillwater Complex, Montana: evidence for subsolidus remobilization. *Contributions to Mineralogy and Petrology*, **137**, 206-219
- Mountain, B.W., and Wood, S.A. (1988) Chemical Controls on the Solubility, Transport, and Deposition of Platinum and Palladium in Hydrothermal Solutions: A Thermodynamic Approach. *Economic Geology*, **83**, 492-510
- Naldrett, A.J. (1989) Magmatic Sulfide Deposits. Oxford Monographs on Geology and Geophysics No 14. Clarendon Press, New York, 186 pp.
- Ohnenstetter, D., Watkinson, D.H., and Dahl, D. (1991) Zoned hollingworthite from the Two Duck Lake Intrusion, Coldwell complex, Ontario. *American Mineralogist*, **76**, 1694-1700
- Pan, P., and Wood, S.A. (1994) Solubility of Pt and Pd sulfides and Au metal in aqueous bisulfide solutions .2. results at 200-degrees-C to 350-degrees-C and saturated vapor-pressure. *Mineralium Deposita*, **29**, 373-390
- Sattari, P., Brenan, J.M., Horn, I., McDonough, W.F. (2002) Experimental constraints on the sulfide-chromite-silicate melt partitioning behavior of rhenium and platinum-group elements. *Economic Geology*, **97**, 385-398
- Oguri, K., Shimoda, G., Tatsumi Y. (1999) Quantitative determination of gold and the platinum group elements in geological samples using improved NiS fire-assay and tellurium coprecipitation with inductively coupled plasma mass spectrometry (ICP-MS). *Chemical Geology*, **157**, 189-197
- Pasteris, J.D., Harris, T.N., and Sassani, D.C. (1995). Interactions of mixed volatile-brine fluids in rocks of the southwestern footwall of the Duluth Complex, Minnesota:evidence from fluid inclusions. *American Journal of Science*, **295**, 125-172
- Peach, C.L., and Mathez, E.M. (1996) Constraints on the formation of platinum-group element deposits in igneous rocks. *Economic Geology*, **91**, 439-450

- Peck, D.C. (2001) PGE exploration in Canada: Recent successes and future opportunities. *PDAC Abstracts*, p.16
- Prichard, H.M., Sa J.H.S., and Fisher, P.C. (2001) Platinum-group mineral assemblages and chromite composition in the altered and deformed Bucuri complex, Amapa, northeastern Brazil. *The Canadian Mineralogist*, **39**, 377-396
- Ripley, E.M., Butler, B.K., Taib, N.I., and Lee, I. (1993) Hydrothermal alteration in the Babbit Cu-Ni deposit, Duluth Complex-mineralogy and hydrogen isotope systematics. *Economic Geology*, **88**, 679-696
- Ripley, E.M., Lambert, D.D., Frick, L.R. (1999) Re-Os, Sm-Nd, and Pb isotopic constraints on mantle and Crustal contributions to magmatic sulfide mineralization in the Duluth Complex. *Geochimica et Cosmochimica Acta*, **62**, 3349-3365
- Sassani, D.C., and Shock, E.L. (1998) Solubility and transport of the platinum-group elements in supercritical fluids: Summary and estimates of thermodynamic properties for ruthenium, rhodium, palladium, and platinum solids, aqueous ions, and complexes to 1000 degrees C and 5 kbar. *Geochimica et Cosmochimica Acta* ,**62**, 2643-2671
- Tosdal, R.M., Wooden, J.L., and Bouse R.M. (1999) Pb Isotopes, Ore Deposits, and Metallogenic Terranes. In Application of Radiogenic Isotopes to Ore Deposit Research and Exploration (Ed. Lambert, D.L., and Ruiz, R.). Society of Economic Geologists Inc.,Boulder, CO, USA, pp. 1-25
- Watkinson, D.H., and Ohnenstetter, D. (1992) Hydrothermal Origin of platinum-group mineralization in theTwo DuckLake Intrusion, Coldwell Complex, northwestern Ontario. *Canadian Mineralogist*, **30**, 121-136
- Wilkinson, S.J. (1983) Geology and sulfide mineralization of the marginal phases of the Coldwell Complex, Northwestern Ontario. M.Sc. thesis, Carleton University, Ottawa, 129p.
- Willmore, C.C., Boudreau, A.E., Kruger, F.J. (2000) The Halogen Geochemistry of the Bushveld Complex, Republic of South Africa: Implications for Chalcophile Element Distribution in the Lower and Critical Zones. *Journal of Petrology*, **41**, 1517-1539
- Wooden, J.L., Czmannske, G.K., Zientek, M.N. (1991) A lead isotope study of the Stillwater Complex, Montana: constraints on crustal contamination and source regions. *Contributions to Mineralogy and Petrology*, **107**, 80-93

CHAPTER 2

Precise Isotope Ratio Determination of Common Pb Using Quadrupole LA-ICP-MS with Optimized Laser Sampling Conditions and a Robust Mixed-Gas Plasma

2.1 Introduction

Lead isotopes can be a useful tool in many geologic, environmental, and biologic investigations. In the U-Th-Pb system, the decay of two long-lived radioactive isotopes of U (^{238}U and ^{235}U) and the radioactive isotope of Th (^{232}Th) yields three radiogenic isotopes of lead (^{206}Pb , ^{207}Pb , and ^{208}Pb , respectively). As a result, Pb-bearing material has a time-dependent Pb isotopic composition that reflects the relative abundances and decay schemes of the three parent isotopes. Due to its relatively high atomic mass, Pb isotopes are not easily fractionated by natural chemical or physical processes and are therefore, primarily changed by radioactive decay or mixing. Therefore, many materials have distinct Pb isotope signatures that reflect their origin and geologic history. As a result, Pb isotope signatures can be used to delineate the sources of metals in a variety of systems. The efficacy of the Pb isotope system in these applications is limited by the degree to which small differences in ratios can be resolved and by the spatial-scale at which the material can be sampled. Therefore, improvements in both the spatial resolution of sampling techniques and in analytical precision would enhance the application of the Pb isotope system to many problems.

Conventional methods for the determination of Pb isotope ratios involve measurement using either thermal ionization mass spectrometry (TIMS) (Krogh 1983, Tera and Wasserburg 1975, Krogh 1983, Kober 1986) or solution nebulization ICP-MS (SN-ICP-MS) (Longerich et al. 1987, Hinnert et al. 1987, Encinar et al. 2001, Ehrlich et al. 2001). The TIMS technique has been more widely used due to its higher precision. However, SN-ICP-MS methods offer a cost effective and relatively rapid technique for initial screening analyses and can produce moderately precise isotope ratios in samples with high Pb concentrations. As a result, considerable effort has been focused on improving the precision of isotope ratio measurements made by ICP-MS techniques (Encinar et al. 2001, Ehrlich et al. 2001, Halicz et al. 1996, Monna et al. 1998, Belshaw et al. 1998).

However, solution based methods suffer from time consuming dissolution procedures that are especially sensitive to Pb contamination from the laboratory environment and

reagents (Thirlwall 2000), which severely limits precision and accuracy. Additionally, valuable micro-scale information is lost with the dissolution of relatively large quantities of sample material. The use of LA-ICP-MS for micrometre-scale, Pb isotope ratio determinations was first proposed by Fryer et al. (1993) and Feng et al. (1993). Both groups described a method capable of producing moderately precise (1-2% RSD) U-Pb age dates based on high spatial resolution ($\geq 30\mu\text{m}$) analyses of Archean zircons (Fryer et al. 1993, Feng et al. 1993) and pitchblende (Fryer et al. 1993). Recently, laser ablation coupled with multiple-collector ICP-MS instrumentation (LA-MC-ICP-MS) has been used to conduct *in situ* Pb-Pb dating of apatite, monazite and sphene with a precision of better than 1% (Willigers et al. 2002). However, MC-ICP-MS instrumentation is expensive and must be dedicated to a limited range of isotopes. Furthermore, although ion counting detectors are available for some new instruments (e.g. Nu-Plasma, Isoprobe and Neptune) the use of Faraday detectors (which require large ion beams) in most MC-ICP-MS instruments limits the application of LA-MC-ICP-MS to materials with high Pb concentrations. These limitations present the possibility for useful applications of single-detector, quadrupole instruments.

This paper examines the use of quadrupole LA-ICP-MS for common Pb isotope ratio measurements at low ppm concentrations. Experiments were conducted which study the effect of laser sampling conditions and mixed gas plasmas on the precision and accuracy of Pb isotope ratio measurements. This paper also presents an example application to the determination of Pb isotope ratios in minerals.

2.2 Experimental

2.2.1 Sample Preparation

NIST 610 series synthetic glass reference material was analysed in the form of polished wafers. The glass wafers were polished for 5 minutes using 1000 grit silicon carbide powder and for 1 minute with 0.05 μm high purity gamma alumina powder (Buehler). The polished wafers were then sonicated for 15 minutes in ethyl alcohol and for 15 minutes in ultra-pure milli-Q distilled water. Mineral samples were analysed in the form of polished, 100 μm thick, thin-sections. Surfaces were re-polished for 1 minute with high purity gamma

alumina powder. The polished sections were then sonicated for 15 minutes in ethyl alcohol and for 15 minutes in ultra-pure (UP) milli-Q water.

2.2.2 *Imaging and Stage Control*

Observation during laser ablation was accomplished with a Sony analog camera interfaced to a PC with a video capture cord. Image Pro Plus[®] image analysis software was used for real-time imaging, photography, and making spatial measurements. A Prior Scientific[®] motorized microscope stage, controlled by a Stage Pro[®] module in the Image Pro Plus[®] software, was used for stage translation (x-y-z). Stage movement was controlled both manually (using a joystick) and by macros written in Visual Basic[®] within the Image Pro Plus[®]/Stage Pro[®] software. The computer-controlled motorized stage has a horizontal (x,y) accuracy of $\pm 1.0 (3\sigma) \mu\text{m}$ and can be moved in $2.0 \mu\text{m}$ steps. Vertical (z) motion was accomplished with a Prior Scientific[®] focus drive, also controlled in the Image Pro Plus[®]/Stage Pro[®] software. The focus drive is capable of a resolution of $0.2 \mu\text{m}$.

2.2.3 *Micro-sampling*

Measurements were made as a single 2-minute long signal acquisition with the laser turned on, which followed 30 seconds of data collection on the combined instrument and gas background with the laser beam turned off (Christensen et al. 1997, Li et al. 2001). The number of measurements used for a single ratio determination was selected based on the concentration of Pb in the sample and the desired precision. As a result, the number of traverses on different minerals varied with Pb content. At low concentrations (~ 2 ppm), 20, 2-minute traverses were used for a single analysis. This resulted in a total acquisition time of approximately 70 minutes including measurements of reference materials. Measurements of NIST 612 glass bracketed the mineral samples and were conducted in the 1st, 2nd, 3rd, 14th, 15th, 26th, 27th and 28th positions of the analysis sequence. Traverses had a spacing of greater than or equal to $150 \mu\text{m}$ to avoid any possible effects of elemental migration due to heating (Jeffries et al. 1996). Standard sampling conditions (SSC), similar to those typically used for trace element analysis in our lab are; a raster rate of $3.6 \mu\text{m s}^{-1}$, the laser focused $150 \mu\text{m}$ above the sample surface, and no beam restriction. Traverses on the NIST glass under SSC were $430 \mu\text{m}$ in length, had a width of $38 \mu\text{m}$, and a depth of $11 \mu\text{m}$ (sampling $1.8 \times 10^5 \mu\text{m}^3$

(0.005 μg) of glass). Traverses on plagioclase feldspar ($\text{Ca,Na}[\text{Al}_{1-2}\text{Si}_{2-3}\text{O}_8]$) grains under SSC were 430 μm in length, had a width of 45 μm , a depth of 21 μm , and sampled $4.0 \times 10^5 \mu\text{m}^3$ (0.01 μg) of feldspar. Sulphide minerals sampled under SSC had traverse widths of 38 μm , lengths of 430 μm , depths of 14 μm , and yielded sample masses of 1.0 μg . The dimensions of the craters were determined using image analysis. Traverse locations on mineral grains were selected using optical microscopy to avoid visibly recognizable alteration products, inclusions, and fractures.

2.2.4 Laser

This work was conducted using a non-homogenized, high power (approximately 1.0 mJ pulse^{-1}), frequency quadrupled (266nm) Continuum[®] (Santa Clara, CA) Surelite[®] I Nd-YAG laser. The laser was operated in the Q-switched mode at a pulse rate of 17 to 20Hz with a pulse width of 4-6 ns and a beam diameter of approximately 5mm. The use of a non-homogenized beam profile preserves the Gaussian energy distribution within the laser beam. The laser optics system was designed by BJF and the Metals Research Laboratory of the Great Lakes Institute for Environmental Research (GLIER), and the Department of Earth Sciences at the University of Windsor and is presented in schematic form in Fig. 1. The beam was directed through one of a series of removable, precision-machined, aluminium disks (beam constrictors) with apertures ranging from 1-4 mm in diameter. The beam constrictors were employed to systematically remove the outer, lower-energy portion of the laser beam. The incident power of the beam changed systematically with the diameter of the constrictor (Table 2). The power of the incident beam was measured after the beam constrictor mount using a Melles Griot[®] (Carlsbad, CA) broadband power/energy meter equipped with a large area thermopile, high-density graphite sensor disc. The beam was directed, using two 90° solid aluminium (coated for 266 nm) mirrors, into the laser port of an Olympus[®] (Markham, ON) BX-51 petrographic microscope. The beam was then reflected by a Melles Griot[®] 266 nm coated mirror and focused using an Optics For Research[®] (OFR[®]) (Caldwell, NJ) 266 nm 5x objective lens. The optics of the system has been set up to allow versatility for a wide range of applications. The sample cell was custom-designed and consisted of a Lexan cylinder with a screw-top removable lid and a fused silica window. The sample cell has a volume of approximately 100ml (when samples are in the form of thin sections).

The ablated sample material was delivered from the sample cell to the ICP-MS via 4 mm inside diameter plastic tubing and was introduced directly to the ICP torch (a standard 1.5 mm i.d. Thermo Elemental[®] torch). The transport gas consisted of a mixture of ultra-pure nebulizer Ar gas (BOC[®], Windsor) diverted from the ICP-MS and ultra-pure N₂ gas (BOC[®], Windsor). The N₂ gas was introduced to the Ar nebulizer gas prior to the sample cell using an Aridus[®] micro-concentric desolvating nebulizer. The ratio of nebulizer Ar to N₂ (generally 50:1) was precisely controlled and was determined by adjusting the Ar and N₂ flow rates to obtain maximum sensitivity.

2.2.5 ICP-MS and Data Acquisition

The ICP-MS analyses were conducted using a high-sensitivity (450 million cps ppm⁻¹ on U using solution nebulization) Thermo Elemental[®] (Mississauga, ON) X-7 quadrupole instrument. The X-7 instrument, operated with ultra-high purity gases, has very low backgrounds of 15 cps for ²⁰⁸Pb and less than 1 cps for ²³⁸U and ²³²Th. The instrument was operated in rapid peak jumping mode and data was acquired for the 206, 207, 208, 232 and 238 masses using a dwell time of 10 ms and an average settling time of 0.8 ms. The detailed operating conditions are presented in Table 1.

2.2.6 Data Reduction and Analysis

Data reduction was conducted using commercially-available spreadsheets with macros written in Visual Basic[®]. Short-term instrumental drift was corrected based on systematic differences between the NIST glass measurements. During preliminary work, a number of data reduction schemes, using different integration intervals, were investigated. However, although each scheme resulted in different values, no one scheme investigated proved superior to another for this data set. This is currently the subject of continuing research. For consistency, we have used the following procedure for all work reported here. First, 10 sweep means were calculated for individual isotopes from the raw data produced from the instrument software. This provided a smoothed signal and allowed the separation of the time-dependent variation in the signal from the noise. Integration regions were selected visually, based on the stability of the count rate, from plots of the 10 sweep means for a single measurement. The mean count rate of the 10 sweep means was then calculated for

individual isotopes from the selected integration region. Measurement ratios were calculated by dividing the means of the relevant isotopes, in essence, isotope ratios were calculated as the ratio of the mean integrated signal intensities. To quantify signal noise (reported as % RSD, equation 1), ratios were also calculated from the 10 sweep means however; these ratios are not reported.

2.2.7 Statistics and Measures of Precision

Several measures of precision are reported in this work. Although these measures are commonly used, there is some discrepancy as to how they are used in the literature pertaining to Pb isotope measurements. A brief discussion is included here to avoid confusion and allow easy comparison with other work. Repeatability is defined in this study as the precision of ratios calculated from the 10 sweep averages, and is used as a measure of signal noise. It will be reported as relative standard deviation (RSD) or % RSD and is the standard deviation of the ratios obtained from 10 sweep averages ($n \sim 130$) divided by the mean ratio of the 10 sweep averages.

$$\%RSD = \frac{\sqrt{\frac{\sum (x_i - \bar{x})^2}{n(n-1)}}}{\bar{x}} \cdot 100 \quad [1]$$

Reproducibility is defined as the precision of N measurements made for a single sample, where N is the number of measurements. This will be given as relative standard error (RSE) or % RSE. RSE is calculated as RSD divided by the square root of N , where RSD is calculated by dividing the standard deviation of N measurements by the mean of N measurements.

$$\%RSE = \frac{\sqrt{\frac{\sum (x_i - \bar{x})^2}{n(n-1)}}}{\bar{x}} \div \sqrt{N} \cdot 100 \quad [2]$$

Poisson counting statistics are calculated by dividing the square root of the number of counts by the number of counts. For instruments with significantly high backgrounds, the background corrected counting statistics error (RSD_{BCS}) is calculated as:

$$RSD_{BCS} = \frac{\sqrt{n_x + n_b}}{n_x - n_b} \quad [3]$$

where n_x is the total number of counts in the integrated laser ablation signal and n_b is the total counts on the background for the same time period. However, as the backgrounds in this work are much lower than the signal intensity the approximation:

$$\text{RSD}_{\text{CS}} = \frac{\sqrt{n_x}}{n_x} = \frac{1}{\sqrt{n_x}} \quad [4]$$

was used. The background corrected counting statistics error for isotope ratios (RSD_{BCSR}) is calculated by taking the square root of the counting statistics error of the numerator squared plus the denominator squared. This is calculated as:

$$\text{RSD}_{\text{BCSR}} = \sqrt{\left(\frac{\sqrt{n_{(n)x} + n_{(n)b}}}{n_{(n)x} - n_{(n)b}}\right)^2 + \left(\frac{\sqrt{n_{(d)x} + n_{(d)b}}}{n_{(d)x} - n_{(d)b}}\right)^2} \quad [5]$$

which, for insignificant backgrounds, can be reduced to:

$$\text{RSD}_{\text{CSR}} = \sqrt{\frac{1}{n_n} + \frac{1}{n_d}} \quad [6]$$

2.3 Results

2.3.1 Focal Position

To investigate the effects of laser focal position relative to the sample surface, experiments were conducted in which the microscope stage was lowered, at 50 μm intervals, from an initial focal position at the sample surface, to a final focal position 500 μm above the sample surface (Fig. 2). Increasing the focal position from 0 to 500 μm above the sample surface resulted in no significant change in the measured $^{208}\text{Pb}/^{206}\text{Pb}$ isotope ratios (Fig. 2a). The best precision for $^{208}\text{Pb}/^{206}\text{Pb}$ ratios (4 % RSD) was obtained at a focal position 250 μm above the sample surface which corresponds approximately to the maximum count rate (Fig. 2c). The measured $^{208}\text{Pb}/^{206}\text{Pb}$ ratios are within 3 % of the literature value (calculated from Pearce et al. 1997, and Woodhead and Hergt 2001)(Fig. 2a).

2.3.2 Beam Restriction

A series of beam constrictors, with diameters ranging from 1.0 to 4.0 mm, were placed in the beam path (Fig. 3). Beam restriction had no significant effect on the $^{208}\text{Pb}/^{206}\text{Pb}$ ratios which ranged from 2.140 to 2.232 (Fig. 3a). The best precision was obtained using a constrictor with a diameter of 3 mm (Fig. 3b) which yielded the maximum count rate

obtained for Pb in this experiment (Fig. 3c). Measured $^{208}\text{Pb}/^{206}\text{Pb}$ ratios were within 3% of the nominal value (Fig. 3c).

2.3.3 Raster Rate

The stage velocity was varied from 1.8 to 9 $\mu\text{m s}^{-1}$ at 1.8 $\mu\text{m s}^{-1}$ intervals (Fig. 4). Measured $^{208}\text{Pb}/^{206}\text{Pb}$ isotope ratios remained unchanged with varying raster rate (Fig. 4a). The best precision on the $^{208}\text{Pb}/^{206}\text{Pb}$ ratio was obtained with a raster rate of 2 $\mu\text{m s}^{-1}$ (Fig. 4b), which does not correspond to the maximum count rate for any of the measured isotopes (Figs. 4b and 4c). The measured $^{208}\text{Pb}/^{206}\text{Pb}$ ratios were within 2 % of the literature value for all raster rates (Fig. 4a).

2.3.4 Combined and Interactive effects

A 2^k factorial design was used to identify possible interactive effects between focal position, raster rate, and beam restriction. The parameter levels selected for the experiment are given in table 3. The optimum precision on $^{208}\text{Pb}/^{206}\text{Pb}$ measurements resulted from a combination of a focal position of 300 μm above the sample surface, a raster rate of 5.4 $\mu\text{m s}^{-1}$, and a beam constrictor diameter of 3.5 mm. The short-term reproducibility of $^{208}\text{Pb}/^{206}\text{Pb}$ ratios made under the range of conditions in this experiment is 0.579 (% RSD).

To estimate the significance (95% confidence level) of the different factors and combinations of factors on repeatability, an analysis of variance (ANOVA) was conducted on the results of the factorial design experiments (Table 4). The only parameter that significantly affected the precision of $^{208}\text{Pb}/^{206}\text{Pb}$ ratio measurements at the levels tested was beam restriction.

2.3.5 Mass Bias Correction by External vs. Internal Methods

An experiment was conducted to determine the accuracy of different schemes for the correction of mass bias. Several models (Monna et al. 1998) were investigated using Tl isotope ratios to monitor instrumental mass bias. These included:

a linear internal model:

$$\left(\frac{A}{B}\right)_{\text{corr}} = \left(\frac{A}{B}\right)_{\text{meas}} \cdot (1 + \delta m \cdot \alpha)$$

a power internal model:

$$\left(\frac{A}{B}\right)_{\text{corr}} = \left(\frac{A}{B}\right)_{\text{meas}} \cdot (1 + \alpha)^{\delta m}$$

an exponential internal model:

$$\left(\frac{A}{B}\right)_{\text{corr}} = \left(\frac{A}{B}\right)_{\text{meas}}^{(\delta m + \alpha)}$$

and an external model:

$$\frac{\left(\frac{A}{B}\right)_{\text{lit.}}}{\left(\frac{A}{B}\right)_{\text{meas}}} = \alpha$$

where $\left(\frac{A}{B}\right)_{\text{meas}}$ and $\left(\frac{A}{B}\right)_{\text{corr}}$ are the measured and mass bias corrected isotope ratios, respectively,

and δm is the difference in mass between the two isotopes (amu) and α is a correction factor.

The correction factor for the internal models is obtained from the measured proxy isotope ratio by substituting the accepted value for the corrected value in the appropriate model. For

the external model, a correction factor (α) was obtained by dividing the literature value, $\left(\frac{A}{B}\right)_{\text{lit.}}$, of a reference material (in this case NIST 612 glass) by the measured ratio.

Corrections were then made by multiplying the measured ratios of the unknowns by the correction factor.

A series of 8 measurements of NIST 612, corrected using a linear model and the $^{205}\text{Tl}/^{203}\text{Tl}$ ratio, yielded mean $^{206}\text{Pb}/^{207}\text{Pb}$ and $^{208}\text{Pb}/^{207}\text{Pb}$ ratios of 1.111 ± 0.002 (RSE) and 2.388 ± 0.002 (RSE) respectively. Use of the exponential and power models both resulted in mass bias corrected $^{206}\text{Pb}/^{207}\text{Pb}$ ratios of 1.106 ± 0.002 (RSE) and resulted in corrected $^{208}\text{Pb}/^{207}\text{Pb}$ values of 2.380 ± 0.002 (RSE) and 2.388 ± 0.002 (RSE) respectively. The same 8 measurements yielded mean $^{206}\text{Pb}/^{207}\text{Pb}$ and $^{208}\text{Pb}/^{207}\text{Pb}$ ratios of 1.102 ± 0.002 (RSE) and 2.382 ± 0.002 (RSE) when corrected externally with NIST 612. Using an external correction followed by an internal correction using an exponential law resulted in mass bias-corrected ratios of 1.102 ± 0.002 and 2.391 ± 0.002 for $^{206}\text{Pb}/^{207}\text{Pb}$ and $^{208}\text{Pb}/^{207}\text{Pb}$, respectively. Use of the linear and power models, with the external model, in place of the exponential law did not significantly improve these values.

2.3.6 Analytical Merits of Measurements made under OSC

To estimate the best possible precision and accuracy for Pb isotope ratio measurements made at low concentrations under OSC using external calibration, an experiment was conducted using NIST 614 glass ($(\text{Pb}) = 2.07 \pm 0.09$ ppm) (Kurosawa et al. 2002). Measurements were conducted using a raster rate of $5.4 \mu\text{m s}^{-1}$, a 3.5 mm diameter beam constrictor, and a focal position 300 μm above the sample surface (Fig. 6).

Mean $^{206}\text{Pb}/^{207}\text{Pb}$ and $^{208}\text{Pb}/^{207}\text{Pb}$ ratios of 1.155 ± 0.002 (RSE) and 2.416 ± 0.001 (RSE) respectively, were obtained from 20 measurements of NIST 614 glass corrected for mass bias by external calibration with NIST 612 (Fig. 6a and b). Externally corrected $^{232}\text{Th}/^{207}\text{Pb}$ and $^{238}\text{U}/^{207}\text{Pb}$ ratios were measured at 1.142 ± 0.009 (RSE) and 1.518 ± 0.005 (RSE) respectively. These measurements are accurate (compared to literature values calculated from Kurosawa et al. (2002) and Woodhead and Hergt²⁰ 2001) within 0.7 %, 0.15 %, 23 %, and 15 % for $^{206}\text{Pb}/^{207}\text{Pb}$, $^{208}\text{Pb}/^{207}\text{Pb}$, $^{232}\text{Th}/^{207}\text{Pb}$ and $^{238}\text{U}/^{207}\text{Pb}$ ratios respectively.

2.4 Discussion

Previous studies have shown that the precision and accuracy of quadrupole LA-ICP-MS isotopic measurements are limited primarily by counting statistics and instrumental mass bias (Fryer et al. 1993, Willigers et al. 2002, Fryer et al. 1995, Longerich et al. 1996a, Longerich et al. 1996b, Scott and Gauthier 1996). In this work, efforts to optimize the external precision (reproducibility) of Pb isotope ratio measurements, at low concentrations, are based on maximizing the count rate and the within-run repeatability (i.e. minimizing signal noise) for the desired ratios, and stabilizing mass bias. From the existing literature (Fryer et al. 1993, Feng et al. 1993, Li et al. 2001, Outridge et al. 1996, Borisov et al. 2000, Liu et al. 2000, Motelica-Heino et al. 2001, Aries et al. 2001, Guillong and Günther 2002, Machado and Simonetti 2002) and preliminary investigations (Crowe et al. 2002) we identified three conditions, namely; laser focus position, raster rate, and beam restriction, as having the largest effect on count rate at equivalent incident power, repetition rate and wavelength.

2.4.1 Poisson Counting Statistics

Fryer et al. (1993) showed that LA-ICP-MS isotope ratio precision was dominantly a function of Poisson counting statistics and suggested that using a more sensitive ICP-MS should yield better isotope ratio precision. Adding N₂ to the nebulizer gas flow significantly increases (by a factor of up to 2 to 3 times) sensitivity in the low mass region and results in ²³⁸U sensitivity of up to 1 billion cps ppm⁻¹ in solution mode using a micro-concentric desolvating nebulizer. In addition to the ICP-MS sensitivity, we have found that laser conditions significantly influence the count rate in laser ablation analyses.

The precision of Pb/Pb ratios varies considerably with changes in focal position, beam restriction, and raster rate. Although the maximum repeatability was generally obtained under the conditions that yielded the highest count rate, some exceptions were observed. Focal positions of 250 and 300 μm above the sample surface yielded Pb isotope ratios with a repeatability of 4 %. Although focal positions at a greater distance from the sample surface resulted in an increase in count rate, the repeatability decreased, with RSDs becoming greater than 5 % at focal positions greater than 450 μm above the sample surface. Beam constrictors with diameters of greater than 3.0 mm yielded the best Pb isotope ratio precision at 4 % RSD. In our investigation of the use of constrictors, the maximum precision was obtained using the constrictor that yielded the highest count rate for Pb. In contrast to the effects of focal position and beam restriction, the best Pb/Pb precision was obtained at a raster rate of 2 μm s⁻¹, which, interestingly, corresponds to the lowest count rate for Pb. Based on these experiments, the OSC for obtaining precise Pb/Pb ratios, with no consideration for U/Pb or Th/Pb ratios, were a focal position of 250-300 μm above the sample surface, beam restriction with a 3.0 mm constrictor and a raster rate of 2 μm/s. An investigation of the combined effects showed that interactive effects between conditions were negligible with respect to precision.

Under OSC the external reproducibility of uncorrected measurements closely approximates that of counting statistics. Twenty measurements of the ²⁰⁶Pb/²⁰⁷Pb and ²⁰⁸Pb/²⁰⁷Pb ratios of NIST 614 glass have σ ratios (Fryer et al. 1993), defined as:

$$\sigma \text{ ratio} = \frac{[\text{RSD of N measurements}]}{\text{RSD}_{\text{CSR}}}$$

where RSD_{CSR} is the counting statistics error (Eqn. 6) of 1.4 and 1.2, respectively, which is marginally better than the value of 1.5 obtained by Fryer et al. (1993). The σ ratio values of $^{232}\text{Th}/^{207}\text{Pb}$ and $^{238}\text{U}/^{207}\text{Pb}$ are 68 and 46 respectively, indicating that additional factors affect precision.

2.4.2 Mass Bias

Several studies (Longerich et al. 1987, Christensen et al. 1997, Horn et al. 2000) have described the mass discrimination, or mass bias, effects in ICP-MS that result from non-equivalent sensitivities for different masses, according to models (i.e. linear, exponential, and power) that were originally proposed for sector field TIMS mass spectrometers and include mass fractionation. However, several other studies have shown that mass discrimination in plasma-based instruments is not accurately described by such models (Hinnert et al. 1987, Monna et al. 1998, Aries et al. 2001). An external correction scheme was proposed (Aries et al. 2001) in which a correction factor was calculated from the difference of SRM values, measured before and after the unknowns, and known ratios. The use of both correction schemes has been investigated and it was found that the external model was more accurate. However, the internal models may be more robust and as a result may produce more reproducible results in the long term. This possibility needs to be investigated. The ability to use the external calibration scheme in this work is enhanced by the relatively flat response of the X7 instrument over a large range of masses with the introduction of N_2 to the nebulizer gas. For example, the mass bias correction in this work is only 0.2 % per amu in comparison to the 1.5 % per amu observed in the study of Horn et al. (2000) using a PQ II +, or the 0.9 % per amu observed by Belshaw et al. (Belshaw et al. 1998) using a Nu-plasma MC-ICP-MS. The magnitude of the mass bias correction (0.2 % amu^{-1}) obtained using the Ar- N_2 plasma approaches that of TIMS instruments (0.1 % amu^{-1}) (Thirlwall et al. 2000). In addition, mass bias drift within runs and between runs was insignificant compared to counting statistics error.

2.5 Application to Isotope Tracer Studies

As a test of the applicability and utility of the quadrupole, single detector LA-ICP-MS instrument for the determination of Pb isotope ratios in geological materials, a selection of

minerals from the Marathon PGE-Cu deposit was analysed. The Marathon deposit is hosted by a gabbroic unit of the 1.108 Ga (Heaman and Machado 1992) Coldwell Intrusive Complex on the North Shore of Lake Superior, Ontario, Canada.

2.5.1 Results

The concentrations of Pb, Th, and U in stoichiometric plagioclase $(\text{Ca},\text{Na})[\text{Al}_{1-2}\text{Si}_{2-3}\text{O}_8]$ and hornblende $\text{Ca}_2(\text{Mg},\text{Fe})_4\text{Al}[\text{Si}_7\text{AlO}_{22}](\text{OH})_2$ has been determined by LA-ICP-MS (Table 5). Pb concentrations in plagioclase are approximately 2 ppm with Th and U concentrations of 0.02 ppm and less than 0.001 ppm respectively. Hornblende has much higher Pb concentrations of 13.6 ppm, and Th and U concentrations of 0.22 and 0.5 ppm, respectively.

The isotope ratios measured for these minerals are presented in Fig. 7 along with the isotope ratios obtained using TIMS³⁸ from the same rocks. The mean $^{206}\text{Pb}/^{207}\text{Pb}$ and $^{208}\text{Pb}/^{207}\text{Pb}$ ratios obtained from 20 measurements of plagioclase corrected for the *in situ* decay of U and Th, to 1.108 Ga, are 1.075 ± 0.003 (RSE) and 2.369 ± 0.006 (RSE) respectively. The mean $^{206}\text{Pb}/^{207}\text{Pb}$ and $^{208}\text{Pb}/^{207}\text{Pb}$ ratios obtained from 5 measurements of hornblende and corrected for the *in situ* decay of U and Th are 1.059 ± 0.002 (RSE) and 2.345 ± 0.006 (RSE) respectively. Measured chalcopyrite (CuFeS_2) ratios have means of 1.052 ± 0.003 (RSE) and 2.354 ± 0.007 (RSE) for $^{206}\text{Pb}/^{207}\text{Pb}$ and $^{208}\text{Pb}/^{207}\text{Pb}$, respectively, for 10 traverses and have not been corrected for U and Th decay. Pyrrhotite (Fe_{1-x}S) yielded mean ratios from 20 measurements of 1.050 ± 0.004 (RSE) and 2.356 ± 0.008 (RSE) for $^{206}\text{Pb}/^{207}\text{Pb}$ and $^{208}\text{Pb}/^{207}\text{Pb}$, respectively.

2.5.2 Discussion

LA-ICP-MS measurements of the Pb isotope composition of plagioclase from the Marathon deposit are in good agreement with the ratios obtained using TIMS (Heaman and Machado 1992) for plagioclase separates from the same rocks. Obtaining the same ratio by LA-ICP-MS gives confidence in the accuracy of the external mass bias correction scheme used. In addition, the external reproducibility (RSE), 0.003 and 0.006 for $^{206}\text{Pb}/^{207}\text{Pb}$ and $^{208}\text{Pb}/^{207}\text{Pb}$, respectively, of the measurements made on plagioclase is equivalent to that obtained for the same number of measurements made on NIST 614 glass. Thus, the OSC

designed to obtain high precision measurements using NIST glass are applicable to minerals with similar Pb and major element compositions. Furthermore, the measurements made by LA-ICP-MS under OSC have comparable precision (0.3 % RSE) to those made by TIMS (0.4 %)(Heaman and Machado, 1992) despite the much smaller sampling volume.

The precision of Pb isotope ratio measurements made by LA-ICP-MS under OSC has proven to be sufficient to discern differences in the Pb isotope composition between different minerals in the same rocks. At Marathon, this could have important implications in studies regarding different models proposed for the genesis of the PGE-Cu mineralization in these rocks (Barrie et al. 2002).

2.6 Conclusions

Quadrupole LA-ICP-MS is capable of producing precise (0.2 % RSE on NIST 614 glass) and accurate ($\pm 0.7\%$ on NIST 614 glass) Pb isotope ratio measurements of silicate and sulphide minerals at low ~ 2.0 ppm Pb concentrations. This capability is particularly useful for isotope tracer studies using common Pb, where elemental fractionation between U, Th and Pb is not critical. We have established that, as shown by Fryer et al.¹³, isotope ratio precision is primarily a function of counting statistics, and that the count rate can be maximized by optimizing laser sampling conditions and using an Ar-N₂ plasma. The degree of variability between traverses on the same matrix is related to signal noise which is significantly affected by the focus and raster rate. Thus, to maximize precision between samples, it is necessary to be able to accurately reproduce the raster rate and focal position. Furthermore, we have found that the application of the classical mass bias laws does not work well at the high count rates, and the low (0.2%) degree of instrumental mass bias, of measurements made in this study. As a result, it is best to use an external calibration scheme which brackets unknown samples with SRMs.

Under OSC, Pb isotope ratio measurements of common Pb using LA-ICP-MS are much better than those reported for high resolution SIMS (Belshaw et al. 1994). The SIMS method described by Belshaw et al. (1994) yielded a precision of 1 % (RSE) for measurements of $^{206}\text{Pb}/^{207}\text{Pb}$ in NIST 610 (422 ppm Pb), whereas we have been able to obtain a precision of 0.2 % (RSE) for $^{206}\text{Pb}/^{207}\text{Pb}$ in NIST 614 (~ 2 ppm Pb). This is largely a function of enhanced sensitivity and hence better counting statistics when using LA-ICP-MS.

Similarly, Compston et al. (1991) obtained a precision of 1.3 % (RSE) for measurements of $^{206}\text{Pb}/^{207}\text{Pb}$ ratios in plagioclase feldspars (approximately 3 ppm Pb) using SHRIMP. We have obtained better precision (0.3 % RSE) for $^{206}\text{Pb}/^{207}\text{Pb}$ Pb isotope ratios of plagioclase with similar (2 ppm) Pb concentrations.

Measurements of Pb isotope ratios in NIST 611 (422 ppm Pb) by LA-MC-ICP-MS yielded $^{206}\text{Pb}/^{207}\text{Pb}$ ratios with a precision of 0.02 % (RSE) (Christensen et al. 1997)¹⁶. In comparison, Pb isotope ratios of NIST 610 by LA-ICP-MS under OSC would yield a precision of approximately 0.04 % (RSD_{CS}) based on a σ ratio of 1.4. Thus, under optimized laser sampling conditions, using mixed gas (Ar-N₂) plasma, LA-ICP-MS is a cost effective alternative to TIMS, SHRIMP, or MC-ICP-MS for making precise Pb isotope ratio measurements at low concentrations. A detailed comparison of measurements made over a range of concentrations using laser ablation coupled to different MC-ICP-MS instruments equipped with ion-counting detectors and quadrupole ICP-MS instruments would be useful. The effect of adding N₂ to the nebulizer gas on isotope ratio precision should also be investigated using MC-ICP-MS.

2.7 Acknowledgements

This work was supported by NSERC CRD and CFI/OIT grants to IMS and BJB and NSERC discovery grants to IMS and BJB. Dr. Henry Longerich is thanked for an insightful review. Dr. John Greenough, Lachlan MacLean, Dr. David Fowle, J-C Barrette, Dr. Shaunquan Zhang, and Dr. Mike Harris are thanked for helpful suggestions. Johari Pannalal and Scott Song, are acknowledged for comments and suggestions. John Robinson is thanked for help with SEM imaging.

2.8 References

- Aries, S., Motelica-Heino, M., Fredier, R., Grezes, T., and Polvé, M. (2001) Direct determination of lead isotope ratios by laser ablation-inductively coupled plasma-quadrupole mass spectrometry in lake sediment samples *Geostandards Newsletter*, **25**, 387-398
- Barrie, C.T., MacTavish, A.D., Walford, P.C., Chataway, R., and Middaugh, R. (2002) Contact-type and Magnetite Reef-type Pd-Cu Mineralization in Ferroan Olivine Gabbros of the Coldwell Complex, Ontario. In *The Geology, Geochemistry, Mineralogy and Mineral Beneficiation of Platinum-Groups* (ed. L.J. Cabri), pp. 321-337. Canadian Institute of Mining, Metallurgy and Petroleum.
- Belshaw, N.S., O'Nions, R.K., Martel, D.J., and Burton, K.W. (1994) High-resolution SIMS Analysis of common lead. *Chemical Geology*, **112**, 57
- Belshaw, N.S., Freedman, P.A., O'Nions, R.K., Frank, M., and Guo, Y. (1998) A new variable dispersion double-focusing plasma mass spectrometer with performance illustrated for Pb isotopes. *International Journal of Mass Spectrometry*, **181**, 51
- Borisov, O.V., Mao, X., and Russo, R.E. (2000) Effects of crater development on fractionation and signal intensity during laser ablation inductively coupled plasma mass spectrometry *Spectrochimica Acta, Part B*, **55**, 1693
- Christensen, J.N., Halliday, A.N., Godfrey, L.V., Hein, J.R., and Rea, D.K. (1997) Climate and ocean dynamics and the lead isotopic records in pacific ferromanganese crusts. *Science*, **277**, 913-918
- Compston, W., Williams, I.S. and Meyer, C. (1991) Initial Pb isotopic compositions of lunar granites as determined by ion microprobe. In *Stable Isotope Geochemistry: A tribute to Samuel Epstein*, ed. H.P. Taylor Jr., J.R. O'Neil and I.R. Kaplan. Geochemical Society, Special Publication No. 3, 1991
- Crowe, S.A., Fryer, B.J., Samson, I.M., Barrie, C.T., and Walford, P.C. (2002) Crustal contamination and the role of volatile fluxing in the genesis of the Marathon Pd-Cu Deposit: Preliminary results from a Pb isotope study of sulphides and feldspars by LAM-ICP-MS. GAC-MAC Abstracts and Program, 2002, **27**, 24
- Ehrlich, S., Karpas, Z. Ben-Dor L., and Halicz, L. (2001) High precision lead isotope ratio measurements by multi-collector-ICP-MS in variable matrices. *Journal of Analytical Atomic Spectrometry*, **16**, 975-977
- Encinar J.R., Alonso, J.I.G., Sanz-Medel, A., Main, S. and Turner, P.J. (2001) A comparison between quadrupole, double focusing and multicollector ICP-MS instruments. Part I. Evaluation of total combined uncertainty for lead isotope ratio measurements. *Journal of Analytical Atomic Spectrometry*, **16**, 315-321
- Feng, R., Machado, N., and Ludden, J. (1993) Lead geochronology of zircon by Laserprobe-Inductively Coupled Plasma-Mass Spectrometry (LP-ICPMS). *Geochimica et Cosmochimica Acta*, **57**, 3479-3486
- Fryer, B.J., Jackson, S.E., and Longerich, H.P. (1993) The application of Laser Ablation Microprobe Inductively Coupled Plasma-Mass Spectrometry (LAM-ICP-MS) to in-situ (U)-Pb geochronology. *Chemical Geology*, **109**, 1-8
- Fryer, B.J., Jackson, S.E., and Longerich, H.P. (1995) The design, operation and role of the laser-ablation microprobe coupled with an inductively coupled plasma-mass spectrometer (LAM-ICP-MS) in earth sciences. *Canadian Mineralogist*, 303-312
- Guillong M., and Günther, D. (2002) Effect of particle size distribution on ICP-induced elemental fractionation in laser ablation-inductively couple plasma-mass spectrometry. *Journal of Analytical Atomic Spectrometry*, **17**, 831

- Halicz, L., Erel, Y., and Veron, A. (1996) Lead isotope ratio measurements by ICP-MS: Accuracy, precision, and long-term drift. *Atomic Spectroscopy*, **17**, 186-189
- Heaman, L.M., Machado, N (1992) Timing and origin of mid-continent rift alkaline magmatism, North America: evidence from the Coldwell Complex. *Contributions to Mineralogy and Petrology*, **110**, 289-303
- Hinners, T.A., Heithmar, E.M., Spittler, T.M., and Henshaw, J.M. (1987) Inductively coupled plasma-mass spectrometric determination of lead isotopes. *Analytical Chemistry*, **59**, 2658-2662
- Horn, I., Rudnick, R.L. McDonough, W.F. (2000) Precise elemental and isotope ratio determination by Simultaneous solution nebulization and laser ablation-ICP-MS: Application to U-Pb geochronology. *Chemical Geology*, **164**, 281-301
- Jeffries, T.E., Pearce, N.J.G., Perkins, W.T., and Raith, A. (1996) Chemical fractionation during infrared and ultraviolet laser ablation inductively coupled plasma mass spectrometry - Implications for mineral microanalysis *Analytical Communications*, **33**, 35-39
- Kober, B. (1986) Whole grain evaporation for $^{207}\text{Pb}/^{206}\text{Pb}$ age investigations on single zircons using a double filament thermal ion-source. *Contributions to Mineralogy and Petrology*, **93**, 482-490
- Krogh, T.E. (1973) A low contamination method for hydrothermal decomposition of zircon and extraction of U and Pb for isotopic age determinations. *Geochimica et Cosmochimica Acta*, **37**, 485-494
- Krogh, T.E. (1982) Improved accuracy of U-Pb zircon ages by the creation of more concordant systems using an air ablation technique. *Geochimica et Cosmochimica Acta*, **46**, 637
- Kurosawa, M., Jackson, S.E., and Sueno, S. (2002) Trace element analysis of NIST SRM 614 and 616 glass reference materials by laser ablation microprobe-inductively coupled plasma-mass spectrometry. *Geostandards Newsletter*, **26**, 75-84
- Li, X-H, Liang, X.R., Sun, M., Guan H., and Malpas, J.G. (2001) Precise $^{206}\text{Pb}/^{238}\text{U}$ age determination on zircons by laser ablation microprobe-inductively coupled plasma-mass spectrometry using continuous linear ablation. *Chemical Geology*, **175**, 209-219
- Liu, H., Borisov, O.V., Mao, X., Shuttleworth, S., and Russo, R.E. (2000) Pb/U fractionation during Nd : YAG 213 nm and 266 nm laser ablation sampling with inductively coupled plasma mass spectrometry *Applied Spectroscopy*, **54**, 1435-1442
- Longerich, H.P., Fryer, B.J., and Strong, D.F. (1987) Determination of lead isotope ratios by inductively coupled plasma mass spectrometry (ICP-MS). *Spectrochimica Acta, Part B.*, **42**, 39-48
- Longerich, H.P., Günther, D., and Jackson, S.E. (1996a) Elemental fractionation in laser ablation inductively coupled plasma mass spectrometry. *Fresenius Journal of Analytical Chemistry*, **355**, 538-542
- Longerich, H.P., Jackson, S.E., and Günther, D. (1996b) Laser ablation inductively coupled plasma mass spectrometric transient signal data acquisition and analyte concentration calculation. *Journal of Analytical Atomic Spectrometry*, **11**, 899-904
- Machado N., and Simonetti, A. (2002) U-Pb dating of zircon by excimer laser ablation MC-ICP-MS: A multi-parameter problem solved...almost. GAC-MAC Abstracts and Program, 2002, **27**, 70
- Monna, F., Loizeau, J-L, Thomas, B.A., Guéguen, C., and Favarger, P-Y. (1998) Pb and Sr isotope measurements by inductively coupled plasma-mass spectrometer: efficient time management for precision improvement. *Spectrochimica Acta, Part B*, **53**, 1317

- Motelica-Heino, M., Le Coustumer P., and Donard, O.F.X. (2001) Micro- and Macro-scale investigation of fractionation and matrix effects in LA-ICP-MS at 1064 nm and 266 nm on glassy materials. *Journal of Analytical Atomic Spectrometry*, **16**, 542-550
- Outridge, P.M., Doherty, W. and Gregoire, D.C. (1996) The formation of trace element-enriched particulates during laser ablation of refractory materials. *Spectrochimica Acta, Part B*, **51**, 1451
- Pearce, N.J.G., Perkins, W.T., Westgate, J.A., Gorton, M.P., Jackson, S.E., Neal, C.R., Chenery, S.P. (1997) A compilation of new and published major and trace element data for NIST SRM 610 and NIST SRM 612 glass reference materials. *Geostandards Newsletter*, **21**, 115-144
- Scott, D.J., Gautier, G. (1996) Comparison of TIMS (U-Pb) and laser ablation microprobe ICP-MS (Pb) techniques for age determination of detrital zircons from Paleoproterozoic metasedimentary rocks from northeastern Laurentia, Canada, with tectonic implications. *Chemical Geology*, **131**, 127-142
- Tera, F., and Wasserburg G.J. (1975) Precise isotopic analysis of lead in picomole and sub picomole quantities. *Analytical Chemistry*, **47**, 2214-2220
- Thirlwall, M.F. (2000) Inter-laboratory and other errors in Pb isotope analyses investigated using a ^{207}Pb - ^{204}Pb double spike. *Chemical Geology*, **163**, 299-322
- Willigers, B.J.A., Baker, J.A., Krogstad E.J., and Peate, D.W. (2002) *Geochimica et Cosmochimica Acta*, **66**, 1051-1066
- Woodhead, J.D., Hergt, J.M. (2001) Strontium, neodymium and lead isotope analyses of NIST glass certified reference materials: SRM 610, 612, 614. *Geostandards Newsletter*, **25**, 261-266

2.9 Tables

Table 1. LA-ICP-MS operating conditions

Table 2. The effect of beam restriction on laser power

Table 3. Parameter range for factorial design experiments

Table 4. ANOVA for factorial design experiment

Table 5. Pb, Th and U content of Marathon minerals

Table 1. LA-ICP-MS operating conditions

Laser-	
Model	Continuum Surelite I [®]
Wavelength	266nm
Mode	Q-switched
Energy per pulse	1.0 mJ
Repetition rate	17-20 Hz
Micro-Concentric Desolvating Nebulizer-	
Model	Cetac Aridus [®]
Temperature	70 °C
Sweep gas	4.27 l min ⁻¹
N ₂	38 ml min ⁻¹
ICP-MS-	
Model	ThermoElemental X7 [®]
<i>Plasma conditions:</i>	
RF power	1280 W
Auxiliary gas flow	0.70 l min ⁻¹
Nebulizer gas flow	0.75 l min ⁻¹
<i>Data acquisition:</i>	
Scanning mode	Rapid peak hop
Dwell time	10 ms
Points per peak	1
Settling time (average)	0.8 ms
M/Z	206, 207, 208, 232, 238

Table 2. The effect of beam restriction on incident power

Aperture diameter (mm)	Laser power (mJ)
-	18.0
4.0	14.5
3.5	13.5
3.0	10.5
2.5	9.0
2.0	6.0
1.5	2.8
1.0	1.1

Table 3. Selected condition range for the factorial design analysis.

	FP	TR	AD
E1	200	5.4	2.5
E2	300	5.4	2.5
E3	200	9	2.5
E4	300	9	2.5
E5	200	5.4	3.5
E6	300	5.4	3.5
E7	200	9	3.5
E8	300	9	3.5
E9	250	7.2	3.0
E10	250	7.2	3.0
E11	250	7.2	3.0
E12	250	7.2	3.0

FP=focal position (μm above sample surface)

TR=traverse rate ($\mu\text{m/s}$)

AD= aperture diameter (mm)

Table 4. ANOVA results. Levels of significance for the effects of parameters on the

Parameter	²⁰⁸ Pb/ ²⁰⁶ Pb	²³² Th/ ²⁰⁶ Pb	²³⁸ U/ ²⁰⁶ Pb
FP	0.71	1.57	2.03
RR	1.20	1.68	0.25
AD	9.89	9.14	10.89
FP x RR	0.09	0.00	0.01
FP x AD	0.00	0.55	0.01
RR x AD	0.85	0.40	0.98
FP x RR x AD	0.02	0.56	0.41

precision of ratio measurements. Significant factors are in bold and italicized

Table 5: Pb, Th and U content of Marathon Minerals

Sample	mineral	(n)	Pb (ppm)	Th (ppm)	U (ppm)
G-11-4	plagioclase	9	2.29	0.02	0.0003
G-10-2	hornblende	1	13.60	0.22	0.057
Detection Limit (3SD background)			0.0006	.00005	0.00001

2.10 Figures

Figure 1. Schematic of laser path optics

Figure 2. The effect of focal position on: (a) $^{208}\text{Pb}/^{206}\text{Pb}$ ratios, (b) $^{208}\text{Pb}/^{206}\text{Pb}$ RSD, and (c) ^{208}Pb count rate. Changing focal position has no significant effect on $^{208}\text{Pb}/^{206}\text{Pb}$ ratios. The best precision was obtained at a focal position between 250 and 300 μm above the sample surface. The literature $^{208}\text{Pb}/^{206}\text{Pb}$ ratio for NIST 612 is 2.1645²⁰

Figure 3. The effect of beam restriction on: (a) $^{208}\text{Pb}/^{206}\text{Pb}$ ratios, (b) $^{208}\text{Pb}/^{206}\text{Pb}$ RSD, and (c) ^{208}Pb count rate. Changing beam constrictor diameters has no significant effect on $^{208}\text{Pb}/^{206}\text{Pb}$ ratios and the best precision was obtained with diameter of 3 mm which also resulted in the maximum (non-systematic) count rate. Position 5 on the x-axis of the figures represents measurements made with no beam restriction. The literature $^{208}\text{Pb}/^{206}\text{Pb}$ ratio for NIST 612 is 2.1645²⁰

Figure 4. The effect of raster rate on: (a) $^{208}\text{Pb}/^{206}\text{Pb}$ ratios, (b) $^{208}\text{Pb}/^{206}\text{Pb}$ RSD, and (c) ^{208}Pb count rate. Changing raster rate has no significant effect on $^{208}\text{Pb}/^{206}\text{Pb}$ ratios. The best precision (which didn't change systematically) was obtained at a raster rate of 2 $\mu\text{m}/\text{s}$. The literature $^{208}\text{Pb}/^{206}\text{Pb}$ ratio for NIST 612 is 2.1645²⁰

Figure 5. RSD obtained for $^{208}\text{Pb}/^{206}\text{Pb}$ ratios obtained under the conditions presented in table 4.

Figure 6. Results from measurements of $^{206}\text{Pb}/^{207}\text{Pb}$ and $^{208}\text{Pb}/^{207}\text{Pb}$ ratios on NIST 614 glass. The nominal values are 1.1481 and 2.4124 respectively.²⁰ The Pb concentration is 2.07 ± 0.09 ppm.²¹

Figure 7. Results from measurements of $^{206}\text{Pb}/^{207}\text{Pb}$ and $^{208}\text{Pb}/^{207}\text{Pb}$ ratios on plagioclase (PLAG), chalcopyrite (CPY), Pyrrhotite (PO), and hornblende (HBLD) from the Marathon deposit. *HBLD_{ave} is the mean of the five plotted hornblende measurements. Hornblende has been corrected for in situ production of radiogenic Pb. LA-ICP-MS corrected (PLAG) has also been corrected for the in situ production of radiogenic Pb. Error bars are the standard deviation of n measurements. HBLD points represent single measurements and so error bars are not shown.

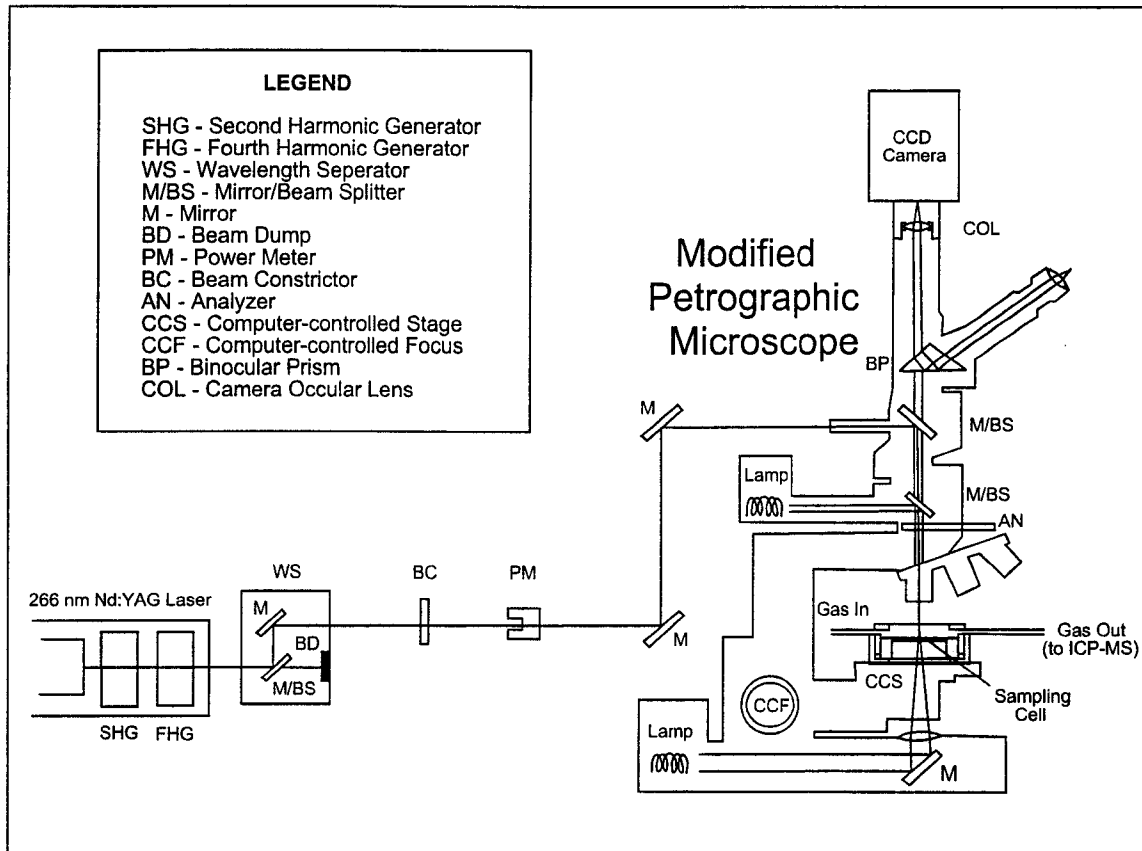


Figure 1.

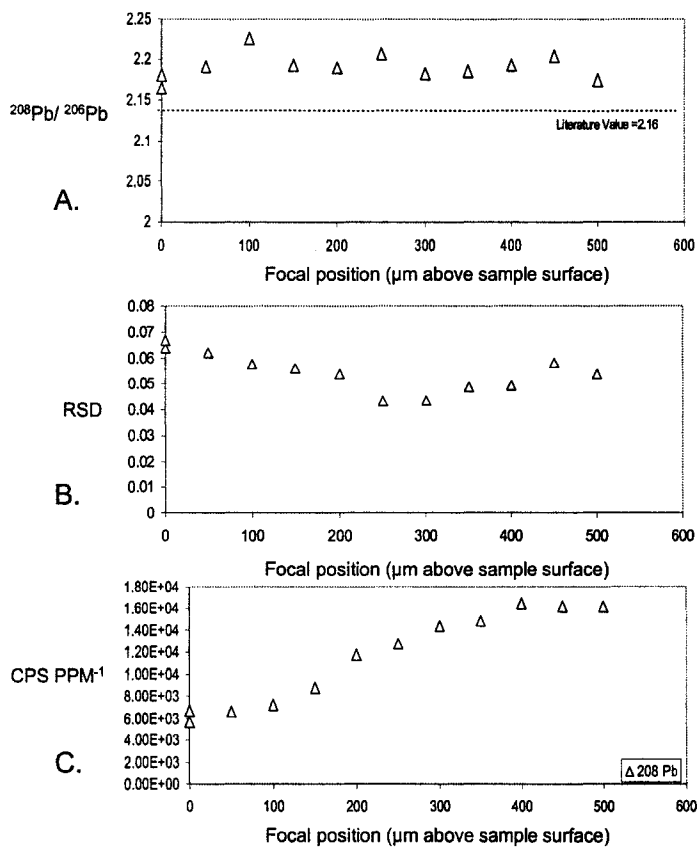


Figure 2.

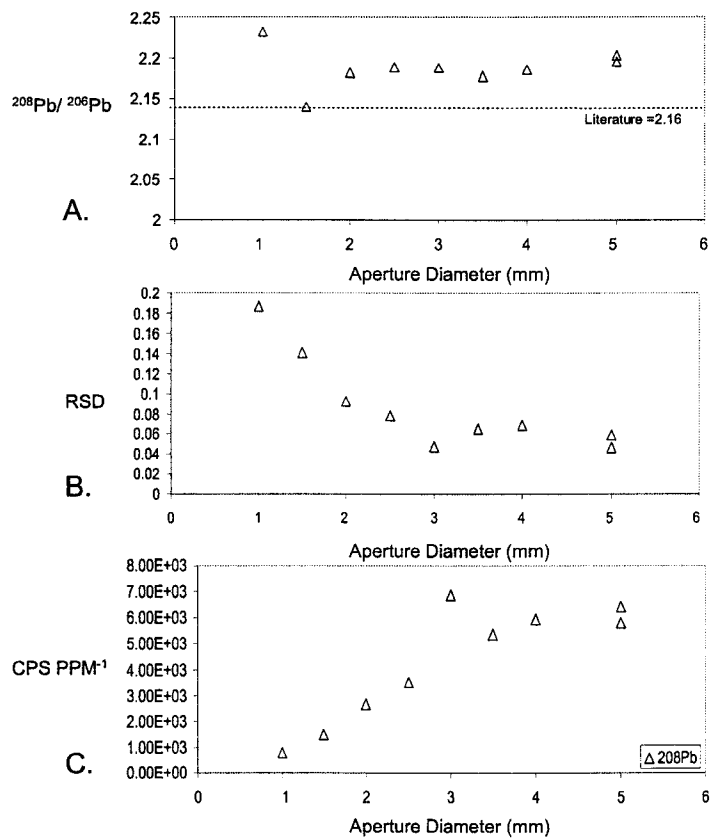


Figure 3.

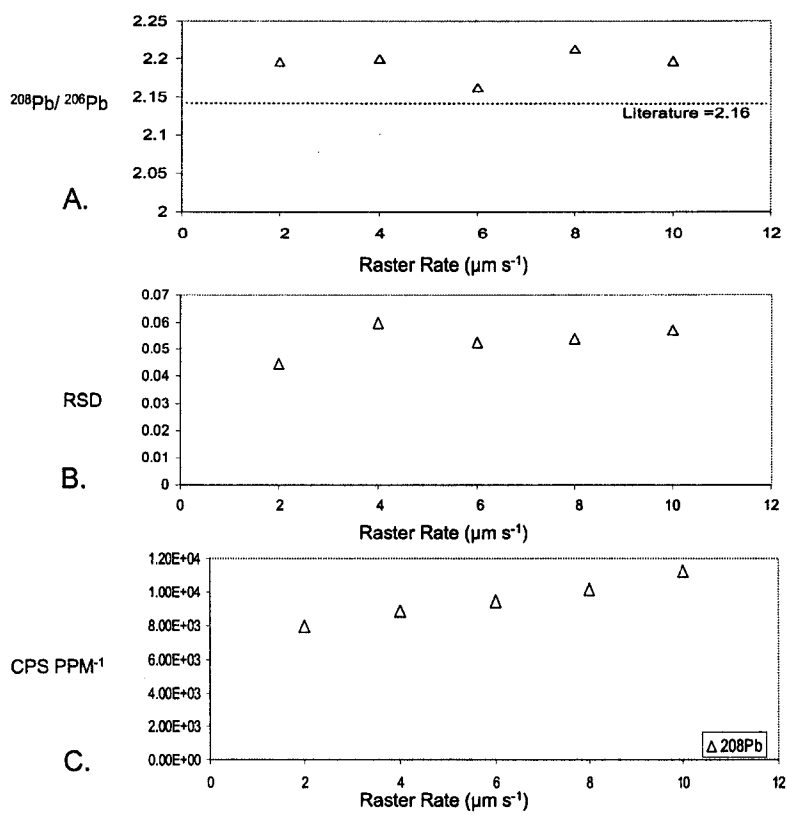


Figure 4.

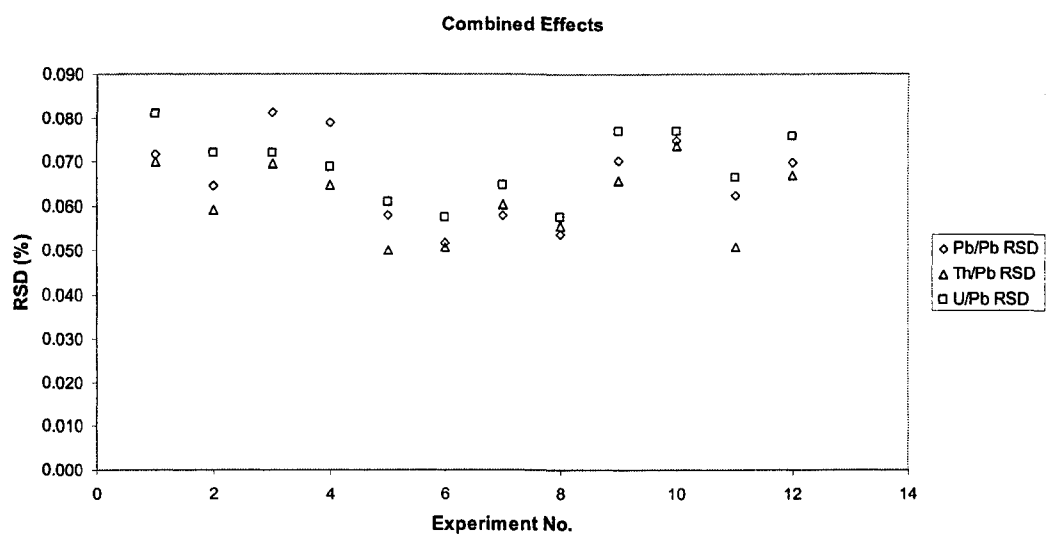


Figure 5.

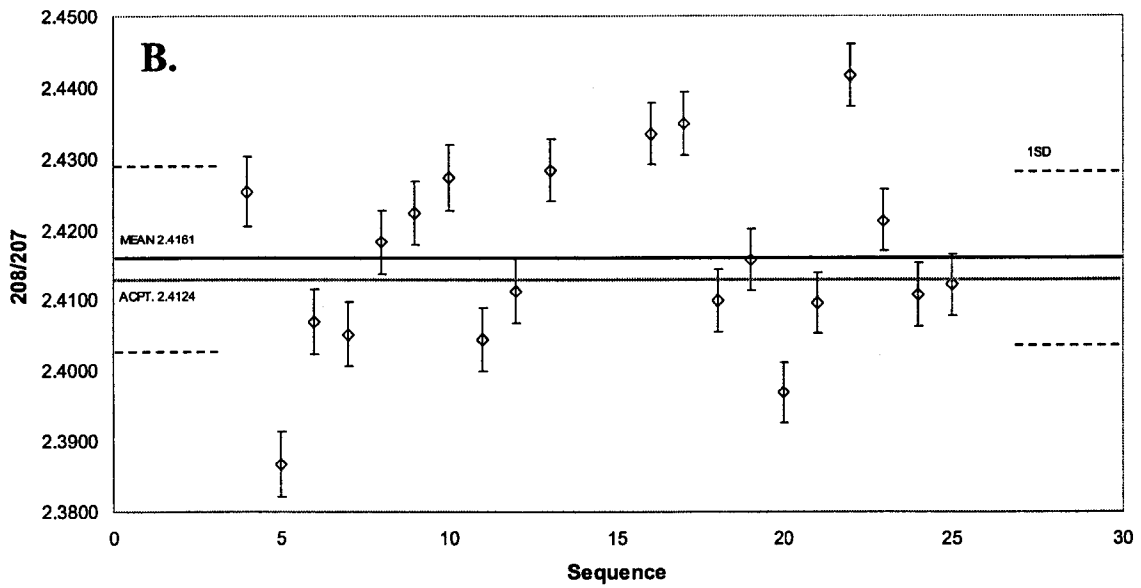
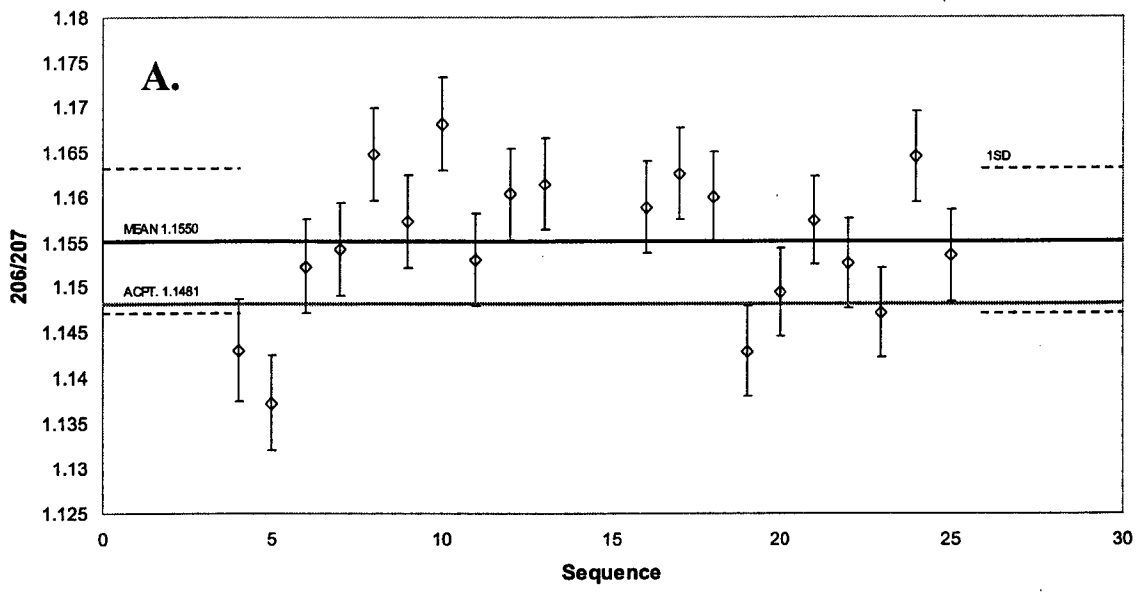


Figure 6.

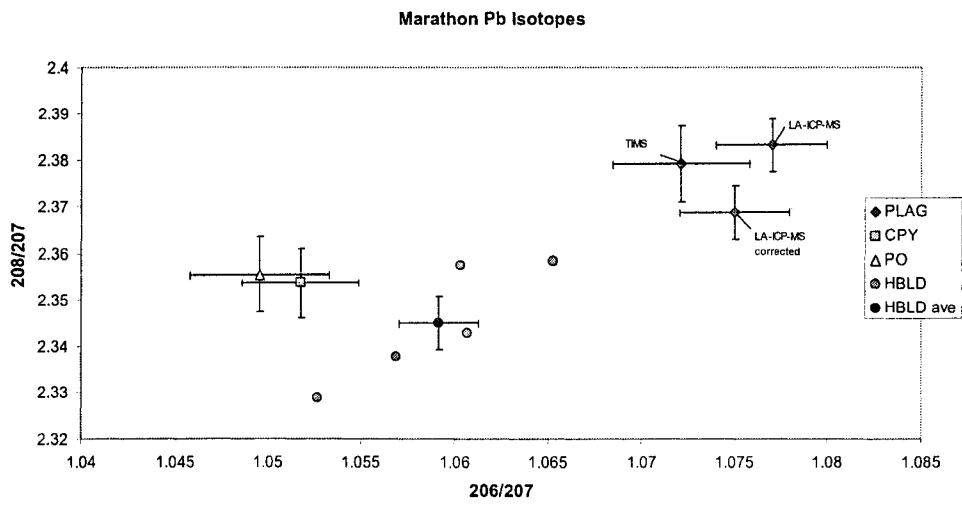


Figure 7.

CHAPTER 3

Micrometre scale Pb isotope composition of major magmatic phases and alteration products from the Marathon PGE-Cu deposit: Constraints on magmatic hydrothermal evolution

3.1 Introduction

The enrichment of the platinum group elements (PGE) in many mafic to ultramafic rocks has been attributed to a wide range of geological processes (MacDonald, A.J., 1990). Many empirical, experimental, and theoretical studies have provided good evidence to support the viability of these processes in many different geological environments (Campbell et al., 1983, Boudreau et al., 1986, Barnes et al. 1988, Mountain and Wood, 1988, Fryer and Greenough, 1992, Peach et al. 1994, Fleet and Wu, 1995, Greenough et al. 1995, Gammons, 1996, Crocket et al. 1997, Fleet et al. 1999, Boudreau and Meurer, 1999, Peck et al. 2001, Andrews and Brenan, 2002). However, the relative importance of these processes remains enigmatic. Notably, models invoking processes including; crustal contamination (Ripley and Al-Jassar, 1987, Watkinson and Ohnenstetter, 1992, Good and Crocket, 1994, Theiriault and Barnes, 1998, Harris and Chaumba, 2001, Barrie et al. 2002), magmatic volatile transport (Boudreau et al. 1986, Ballhaus and Stumpfl, 1986, Brüggmann et al. 1989, Boudreau and Meurer, 1999, Willmore et al. 2000, Barrie et al. 2002), and sub-solidus hydrothermal metal redistribution (McCallum et al., 1976, Nyman et al. 1990, Watkinson and Ohnenstetter, 1992, Farrow and Watkinson, 1992, Pasteris et al. 1995) are among the most contentious. As a result, many contradictory models have been proposed to describe the enrichment of PGE in ore deposits.

It is well documented that common Pb isotope systematics can provide valuable information on many petrogenetic processes (Mahnes et al., 1988, Wooden et al. 1991, Gariépy and Dupré, 1991, Tosdal et al. 1999, Ripley et al. 1999, McCallum et al. 1999). Importantly, Pb isotope ratios can be sensitive indicators of crustal-contamination in magmatic intrusions (Ripley et al. 1999, McCallum et al. 1999). This is especially true when there is a large age difference between the intrusive magmas and the host country rock, which allows the evolution of different Pb isotope ratios in the two components. The typically low (1-2 ppm) Pb concentration of mafic intrusions compared with the relatively high (10-30 ppm) Pb concentration of average crustal material makes the Pb isotope

signature of these intrusions relatively responsive to small amounts of external Pb of different isotopic composition (Tosdal et al. 1999). In addition to being used as an indicator of an external metal contribution, the distribution and heterogeneity of Pb isotope ratios in minerals from different stages of the paragenesis can be used to infer mechanisms of contamination.

The aim of this study was to determine the mineral-scale Pb isotope and trace-element composition of major magmatic phases (egs. plagioclase and pyrrhotite), accessory minerals (egs. biotite and apatite) and alteration products (egs. hornblende, chlorite and calcite). The mineral-scale common Pb systematics and mineral trace-element chemistry, within the context of textural relationships, have been used to determine when contamination occurred in the paragenetic sequence and test contradictory models that have been proposed for the genesis of the Marathon PGE-Cu deposit (Watkinson and Ohnenstetter, 1992, Good and Crocket, 1994, Barrie et al. 2002). The Pb isotope system was well suited for this study as there is greater than 1 billion years age difference between the Proterozoic Marathon deposit and the host Archean country rock. Thus, the Pb isotope ratios of the magmatic phases of the deposit should be relatively sensitive to country rock contamination.

Precise determination of Pb isotope ratios at the mineral-scale requires the use of techniques offering a high degree of spatial resolution. Furthermore, the typically low concentration of Pb in many genetically important minerals necessitates the use of high sensitivity mass spectrometry. For this study LA-ICP-MS has been used to conduct precise, mineral-scale Pb isotope ratio measurements at mineral concentrations as low as 2 ppm (Crowe et al. Chapter 2). As the scale of this isotope data is atypical, and the use of $^{206}\text{Pb}/^{207}\text{Pb}$ and $^{208}\text{Pb}/^{207}\text{Pb}$ ratios (as presented in this study) is unconventional, a discussion is given on micrometer Pb isotope systematics and their implications for petrogenetic studies.

3.2 Background

3.2.1 Regional Geological Setting

The Marathon deposit is hosted by the 1108 ± 1 Ma (U-Pb) (Heaman and Machdo, 1992) Coldwell Intrusive complex. The Coldwell Magmas were emplaced into the Archean rocks of the Abitibi and Wawa sub-provinces where continental-rifting events provided crustal dilation and the associated structural features. The structural geology of the region has

been described by Sage (1991) who determined that the emplacement of the mid-continent rift intrusive complexes occurred at inflections of major structural zones and sites of cross-faulting. The intrusion of the Coldwell magmas was contemporaneous with the extrusion of voluminous sections of tholeiitic, and transitional tholeiitic-alkaline basalt, also associated with Keweenawan rifting events (Sutcliffe, 1991). The Keweenawan intrusive rocks and their associated economic deposits were described by Smith et al. (1987). The Geology of the Coldwell complex was most recently described by Walker et al. (1993), who supported previous work and subdivided the complex into three intrusive centers (Figure 1.). Center 1, the earliest intrusion, is composed of a gabbroic unit, the Eastern Gabbro, and ferroaugite syenite. This was followed by the intrusion of the center 2 nepheline syenite magmas. Center 3, the youngest unit, is dominantly quartz-amphibole syenite.

3.2.2 Deposit Petrology and Mineralization

The Marathon deposit is hosted by the Two Duck Lake gabbro (TDL), a small intrusive phase of the Eastern Gabbro which has recently been described by Shaw (1997). The main intrusive phase of the Eastern Gabbro is a layered gabbro which constitutes 90% of the unit (Shaw, 1997). The layered gabbro is comprised of gabbro, olivine gabbro, troctolite, and anorthositic gabbro. The Eastern Gabbro contains two smaller units, the Two Duck Lake intrusion (TDL) and the Malpas Lake intrusion. The Malpas Lake unit intrudes the layered gabbro, constitutes 5% of the Eastern Gabbro, and is comprised of amphibole-bearing olivine gabbro (Shaw 1997). The TDL intrusion constitutes 3% of the Eastern Gabbro and intrudes the layered gabbro at the contact with the meta-volcanic and meta-sedimentary Archean country rocks. This contact trends north-northeast and dips moderately to the west. The TDL intrusion is comprised of gabbro, olivine gabbro, and leucogabbro (Shaw 1997). Although the existence of a distinct TDL intrusive unit has been contested by Barrie et al. (2002) there is field evidence (Dahl et al., 2001, and this study), including cross-cutting relationships and zones of igneous brecciation, that support a distinct intrusive phase.

The gabbroic rocks of the Marathon deposit have been subdivided into zones based on lithology and textural features (Good and Crocket 1994, Barrie et al. 2002). Although, the study of Barrie et al. has not considered the TDL unit as a separate intrusive phase the three-zone classification proposed in that work is most consistent with the observations of drill

core and field relationships made in this study. Thus, a slightly modified zonal classification is presented here. The Basal Zone is characterized by massive, fine-grained, altered gabbro hosting abundant meta-volcanic xenoliths and containing variable amounts of massive to net-textured sulphides. The Basal Zone also contains sporadic, irregular pods of granophyre that range in size from a few centimeters to several meters along the greatest dimension. The Lower Zone exhibits locally-developed cumulate layering defined by gradational changes in mineral abundance, irregular pegmatitic zones, and varies compositionally from biotite-hornblende gabbro to monzonite (Dahl et al. 2001). The Lower Zone is host to the bulk of the PGE and Cu mineralization, which occurs in variably-textured, commonly pegmatitic, hornblende gabbro that contains disseminated sulphide. The Lower Zone is broadly equivalent to the Lower zone of Good and Crocket (1994) and the heterogeneous gabbro of Wilkinson (1983). Mineralized zones are located several tens of meters stratigraphically above the Basal Zone sulphide-rich rocks and often occur near the transition to the Upper Zone. The Upper Zone consists of olivine gabbro with well-developed rhythmic layering defined by changes in mineral morphology, grain size and modal abundance. Although PGE mineralization is dominantly contained by the Lower Zone the Upper Zone is host to laterally continuous Pd-Cu-bearing reef-type magnetitite layers. A thin unit of leucogabbro has intruded between the contact of the TDL intrusion and the country rock (Good and Crocket 1994). The TDL and Eastern Gabbro are cut by vertically dipping quartz syenite dikes that are approximately parallel to the TDL intrusive contact. The TDL intrudes the Eastern Gabbro at the contact with country rocks which trends north to northeast and dips moderately to the west. The TDL varies compositionally from olivine gabbro to gabbroic anorthosite.

3.2.3 Relevant Previous Isotope Studies

The most relevant previous isotope work is the study of Heaman and Machado (1992), which described the timing and origin of the Coldwell magmas using the Sr, Nd, and Pb isotopic composition of the intrusive centers and U-Pb geochronology. Based on the U-Pb zircon/baddelyite age dating, from the different intrusive units, Heaman and Machado (1992) described a rapid cooling history when the magmas were intruded into cold Archean country rock. Heaman and Machado (1992) found a considerable degree of scatter in the Sr-Nd-Pb isotopic composition of the different intrusive units and attributed this to the presence of

magmas with different initial isotopic compositions. The study of Heaman and Machado (1992) found that the more evolved granitic and syenitic units had less radiogenic Pb isotope signatures than the gabbroic units. This was attributed to the interaction of these magmas with older granulite facies lower crust. In addition to the heterogeneity found between the different intrusive phases, Heaman and Machado (1992) noted that minerals from the same intrusive unit also had heterogeneous initial isotope ratios. The Sr and Nd isotopic composition of clinopyroxene and plagioclase from an unaltered sample of the TDL gabbro were found to be identical. Heaman and Machado (1992) suggested that the identical Sr and Nd isotopic compositions of plagioclase and clinopyroxene indicated that these minerals crystallized in a closed system. In contrast, apatite from the same sample had different Sr and Nd isotopic compositions. Based on textural evidence, the significantly lower Nd isotopic composition of apatite in the gabbro was attributed to an inherited signature. It is also possible that the anomalous Nd isotopic composition of apatite is due to a small amount of contamination from an Archean upper crustal source during the late stages of gabbro crystallization.

3.3 Experimental

3.3.1 Sampling

A suite of rocks has been collected from field sites and drill core to represent a section through the deposit from the Archean country rock to the Eastern Gabbro. Field samples were collected from unweathered rocks exposed by recent stripping during exploration activity. Drill core was sampled from well-preserved cores that have been stored in a covered building and therefore have not been subject to weathering. Rock samples were characterized by optical microscopy and SEM imaging. Mineral samples were analyzed in the form of polished 100 μm thick thin sections. Immediately prior to analysis the thin section surfaces were re-polished with high purity gamma alumina powder. The polished sections were then sonicated for 15 minutes in ethyl alcohol and for 15 minutes in ultra-pure milli-Q water.

Micro-sampling was conducted by laser-ablation as described below. Laser sampling traverses conducted under the conditions described produced craters in feldspars which were 430 μm in length, had a width of 45 μm , a depth of 21 μm , and sampled $4 \times 10^5 \mu\text{m}^3$ (0.01

µg) of feldspar. Traverses conducted on sulphide minerals were of similar dimensions and sampled 1.0µg of sulphide. Traverse locations were chosen using optical microscopy to select regions of mineral grains free of visible inclusions, fractures, and alteration products. Prior to laser ablation analysis

3.3.2 Pb Isotope Ratio Determination

Pb Isotope ratios were determined by LA-ICP-MS which allows for mineral-scale resolution, rapid analysis time, and minimal contamination from the laboratory environment and reagents. This method is described in detail in Crowe et al. (Chapter 2) and only a general description and modifications are presented here. The method is capable of producing high precision ($\leq 0.2\%$ RSE) Pb isotope ratios in sample materials with Pb concentrations as low as 2 ppm.

This work was conducted using a non-homogenized, high power (1.0 mJ pulse⁻¹), frequency quadrupled (266nm) Continuum[®] Surelite I Nd-YAG laser. The laser was operated in the Q-switched mode at a pulse rate of 17-20 Hz, a pulse width of 4 to 6 ns and an initial beam diameter of 5mm. The laser optics system has been purpose designed by BJB and the Metals Research Laboratory of the Great Lakes Institute (GLI), and the Department of Earth Sciences at University of Windsor.

The ablated sample material was delivered to the ICP-MS via 4mm i.d. plastic tubing and was introduced directly into the ICP torch. The transport gas consisted of a mixture of ultra-pure Ar gas and ultra-pure N₂ gas. ICP-MS analysis was conducted using a high-sensitivity (450 million cps ppm⁻¹ on U, using solution nebulization) Thermo Elemental[®] X-7 quadrupole instrument. The X-7 instrument, operated with ultra-high purity gases, has very low backgrounds of 15 cps for ²⁰⁸Pb and less than 1 cps for ²³⁸U and ²³²Th. The instrument was operated in rapid Peak Jumping Mode and data was acquired for the 206, 207, 208, 232 and 238 isotopes, with a dwell time of 10ms and an average settling time of 0.8 ms. The ICP-MS was tuned for flat response over a mass range from ¹¹⁵In to ²³⁸U. Under these tuning conditions laser ablation produced instrument signals that were greater than 10 000 cps ppm⁻¹ for Pb.

Data reduction was conducted manually using commercial spreadsheets. Instrumental mass discrimination corrections were accomplished using external calibration with NIST 612

glass. Laser induced elemental fractionation was minimized by conducting computer controlled constant velocity traverses (cf Christensen et al., 1997; Li et al., 2001). Individual experiments were conducted as a series of 28 measurements with measurements being conducted on the NIST glass standard in the 1st, 2nd, 3rd, 14th, 15th, 26th, 27th and 28th positions of the analysis sequence. To reduce the effects of NIST heterogeneity and measurement uncertainty on the calibration procedure, the mean was calculated for each group of analyses (ie 1-3, 14-15, and 26-28). Correction factors were calculated based on the difference in the isotope ratios obtained from these means and the accepted values. Short-term instrument drift was corrected for based on systematic differences between the three NIST glass means. Isotope ratios were obtained by calculating the mean count rate for 10 sweeps to separate the signal variability from instrumental noise. The mean integrated count rate for the entire traverse was calculated from the 10 sweep averages. The mean integrated count rates for given isotopes were normalized by dividing by the ²⁰⁷Pb isotope. The ²⁰⁷Pb isotope was used for normalization due poor counting statistics on the low abundance ²⁰⁴Pb isotope; the implications of this are discussed in section 5. Ratios were also calculated from the 10 sweep mean count rates. This allowed for outliers to be excluded from the integration by calculating mean ratios from the 10 sweep averages and removing regions more than 3 standard deviations from this mean. Sample (thin section) averages have been calculated by calculating the mean of multiple (n) traverses from multiple grains. The relative standard error (RSE) for 20 measurements of NIST 614 is 0.2 % (RSE) (Crowe et al. Chapter 2).

3.4 Results

3.4.1 Petrography

The petrology and petrography of the TDL has been recently described by Dahl et al. (2001), Barrie et al. (2002), and Watkinson et al. (2002) and only points of contention or observations specifically important to this study are described here.

The Basal Zone rocks described in this study are broadly equivalent to the lower sub-unit of Dahl et al. (2001). These rocks consist primarily of plagioclase altered to alkali-feldspar. The feldspars often occur together in a granophyric texture with quartz, and the mafic-mineralogy is variable and often pervasively altered. It includes augite, olivine, magnetite and variable amounts of orthopyroxene. These minerals are frequently altered to

biotite, hornblende, chlorite and serpentine. Basal Zone sulphide occurs as massive to net textured pyrrhotite containing pentlandite exsolution flames. Chalcopyrite occurs around the margins of the pyrrhotite and has rounded, equilibrium type grain boundaries with pyrrhotite (Figure 3c).

The Lower-Zone described in this work is equivalent to the Middle sub-unit of Dahl et al. (2001). In brief, several important petrographic observations have been made of the Lower Zone rocks. First, the mafic minerals in nonsulphide-bearing gabbroic rocks are unaltered. These rocks are fine-grained to pegmatitic, contain unaltered anhedral to subhedral grains of plagioclase, olivine, and clinopyroxene as the major phases and exhibit well developed ophitic to sub-ophitic textures. Accessory minerals in these samples include cumulus magnetite, and interstitial biotite and apatite of variable abundance. In contrast, sulphide-bearing samples in the Lower Zone exhibit similar textures but also contain clinopyroxenes that have been altered to hornblende and biotite, and plagioclase that is variably altered and has been partly replaced by muscovite. Second, in the sulphide bearing samples the chalcopyrite grains are intimately inter-grown with the products of pyroxene alteration (Figure 3d-h) (i.e. hornblende and biotite). These sulphide assemblages consist of irregular grains of chalcopyrite that often occur around cores of pyrrhotite (Figure 3b). The chalcopyrite is also present along cleavage planes in plagioclase and hornblende (Figure 3e-h). Hornblende, apatite and calcite are present as inclusions in chalcopyrite. Minor sulphide phases include pentlandite flames within the pyrrhotite and cubanite lamellae in chalcopyrite (Figure 3b). In addition, pentlandite occurs as euhedral grains at the contact of chalcopyrite and pyrrhotite. Importantly, these sulphide assemblages disrupt optically continuous grains of clinopyroxene that has been partially replaced by hornblende and biotite (Figure 3ef). In some cases, where this replacement is almost complete the sulphide assemblages appear to be interstitial to the primary plagioclase framework. In fact, in this case the sulphide assemblage pseudomorphs the preexisting interstitial clinopyroxene. This texture can be misleading in sections where most of the primary mineralogy is well preserved, and could easily be misinterpreted as the crystallized product of a primary interstitial sulphide melt. The interpretation of the sulphide textures are discussed in more detail in section 3.5 below.

The upper zone rocks are medium to fine-grained and have a primary mineralogy that is equivalent to the lower zone. Notably, these rocks are relatively unaltered in comparison to

the Lower-Zone rocks and contain laterally extensive reef like magnetite layers. Sulphides are absent with the exception of the magnetite layers where they replace the primary magnetite.

3.4.2 Pb Isotopes

Common lead isotope ratios have been determined in multiple grains of plagioclase from six samples (greater than 120 individual measurements) that represent the dominant textural and lithological variations in the gabbroic rocks of the Eastern Gabbro (Table 1). The $^{206}\text{Pb}/^{207}\text{Pb}$ ratios determined for samples of plagioclase range from 1.062 ± 0.003 (σ) to 1.081 ± 0.003 (σ). This is moderately more variability than the range previously observed in feldspars from the multiple intrusive centers of the Coldwell complex which is 1.063 ± 0.003 (σ) (error calculated from those reported in Heaman and Machado, 1992) (Nepheline Syneite) to 1.071 ± 0.004 (σ) (TDL Gabbro) (Heaman and Machado, 1992). Similarly, the $^{208}\text{Pb}/^{207}\text{Pb}$ ratios determined for these same samples range from 2.371 ± 0.006 (σ) to 2.386 ± 0.001 (σ) and are more variable than the range of $^{208}\text{Pb}/^{207}\text{Pb}$ ratios, 2.376 ± 0.004 (σ) to 2.379 ± 0.003 (σ), previously reported for the different intrusive centers (Heaman and Machado, 1992). Importantly, sample G10-3B, a medium- to coarse-grained nonsulphide bearing olivine gabbro, has Pb isotope ratios that are within analytical error of those reported for the lithologically equivalent sample, 86CL1, in the study of Heaman and Machado (1992). The reported ratios (Table 1) have not been corrected for the *in situ* decay of ^{238}U , ^{235}U , or ^{232}Th . The low abundance of these parent isotopes in the feldspar samples results in corrections that are less than the analytical uncertainty.

Pb isotope ratios have been determined for a variety of accessory minerals and alteration products from different stages of the paragenetic sequence (Table 1). The Pb isotope ratios in these minerals are highly variable and are not well correlated with the respective U/Pb and Th/Pb ratios. As some of these minerals contain significant concentrations of U and Th, radiogenic Pb has been subtracted to obtain age corrected initial Pb isotope ratios at 1108 Ma (Table 2). Corrections of ratios normalized to the ^{207}Pb isotope are not as straightforward as the age corrections made for ratios normalized to the ^{204}Pb isotope. This is due to the fact that both the numerator and denominator are subject to radiogenic Pb production. Equations that describe the evolution of radiogenic $^{206}\text{Pb}/^{207}\text{Pb}$ and

$^{208}\text{Pb}/^{207}\text{Pb}$ ratios have been derived in the study of Getty and DePaolo (1995). Age corrections can be made according to slightly modified versions of these equations as follows:

$$\left(\frac{^{206}\text{Pb}}{^{207}\text{Pb}}\right)_0 = \left(\frac{^{206}\text{Pb}}{^{207}\text{Pb}}\right)_t - \left(\frac{^{238}\text{U}}{^{207}\text{Pb}}\right)_t \left[e^{\lambda_{238}t} - 1 \right] - \left(\frac{^{206}\text{Pb}}{^{207}\text{Pb}}\right)_{0.it} \left(\frac{^{235}\text{U}}{^{238}\text{U}}\right)_t \left[e^{\lambda_{235}t} - 1 \right] \quad (1)$$

$$\left(\frac{^{208}\text{Pb}}{^{207}\text{Pb}}\right)_0 = \left(\frac{^{208}\text{Pb}}{^{207}\text{Pb}}\right)_t - \left(\frac{^{232}\text{Th}}{^{207}\text{Pb}}\right)_t \left[e^{\lambda_{232}t} - 1 \right] - \left(\frac{^{208}\text{Pb}}{^{207}\text{Pb}}\right)_{0.it} \left(\frac{^{235}\text{U}}{^{232}\text{Th}}\right)_t \left[e^{\lambda_{235}t} - 1 \right] \quad (2)$$

where $(^{206}\text{Pb}/^{207}\text{Pb})_0$, and $(^{208}\text{Pb}/^{207}\text{Pb})_0$ are the age corrected initial Pb isotope ratios, and $(^{206}\text{Pb}/^{207}\text{Pb})_t$ and $(^{208}\text{Pb}/^{207}\text{Pb})_t$ are the present day Pb isotope ratios. Similarly, $(^{238}\text{U}/^{207}\text{Pb})_t$, $(^{232}\text{Th}/^{207}\text{Pb})_t$, $(^{235}\text{U}/^{238}\text{U})_t$, and $(^{235}\text{U}/^{232}\text{Th})_t$ are the present day ratios of the parent isotopes for both numerator and denominator daughters. The decay constants used in the calculations ($\lambda_{23(2,5,8)}$) were those given in Faure (1986). The age of the rock (t) is 1108 Ma (Heaman and Machado, 1992). The ratios $(^{206}\text{Pb}/^{207}\text{Pb})_{it}$ and $(^{208}\text{Pb}/^{207}\text{Pb})_{it}$ are proxies for $(^{206}\text{Pb}/^{207}\text{Pb})_0$ and $(^{208}\text{Pb}/^{207}\text{Pb})_0$. As $(^{206}\text{Pb}/^{207}\text{Pb})_0$ and $(^{208}\text{Pb}/^{207}\text{Pb})_0$ cannot be known *a priori* the measured $^{206}\text{Pb}/^{207}\text{Pb}$ and $^{208}\text{Pb}/^{207}\text{Pb}$ values were substituted for $(^{206}\text{Pb}/^{207}\text{Pb})_0$ and $(^{208}\text{Pb}/^{207}\text{Pb})_0$, to obtain an approximation of the age corrected value. The correction was then iterated, substituting the approximated age corrected ratios $(^{206}\text{Pb}/^{207}\text{Pb})_{app}$ and $(^{208}\text{Pb}/^{207}\text{Pb})_{app}$ for $(^{206}\text{Pb}/^{207}\text{Pb})_0$ and $(^{208}\text{Pb}/^{207}\text{Pb})_0$, until the differences between successive iterations were less than the analytical error (for the analysed minerals, this was not more than once) to obtain $^{206}\text{Pb}/^{207}\text{Pb}_{it}$ and $^{208}\text{Pb}/^{207}\text{Pb}_{it}$. Uncertainties (1σ) for the age corrected ratios were calculated based on the limit of 20% accuracy for the $^{238}\text{U}/^{207}\text{Pb}$ and $^{232}\text{Th}/^{207}\text{Pb}$ ratios measured by LA-ICP-MS (Crowe et al. Chapter 2). This limit is due to laser induced elemental fractionation which is extremely sensitive to matrix composition. As a result U/Pb and Th/Pb ratios corrected externally for mass and elemental bias suffer from matrix effects due to differences in the physical and chemical properties of the NIST 612 glass standard and the mineral. However, given that U/Pb and Th/Pb ratios are low in comparison to $^{206}\text{Pb}/^{207}\text{Pb}$

and $^{208}\text{Pb}/^{207}\text{Pb}$ ratios, the uncertainty in the corrected values is dominantly a function of the analytical uncertainty for the Pb/Pb ratios.

Common Pb isotope ratios have been determined in chalcopyrite and pyrrhotite in a variety of textural settings including most importantly Basal Zone massive to net-textured sulphides, and Lower Zone chalcopyrite dominated pseudomorphic assemblages (Table 1). The $^{206}\text{Pb}/^{207}\text{Pb}$ ratios determined for samples of sulphide mineral assemblages range from 1.059 ± 0.002 (σ) to 1.079 ± 0.005 (σ). The $^{208}\text{Pb}/^{207}\text{Pb}$ ratios determined for these same samples range from 2.347 ± 0.002 (σ) to 2.342 ± 0.003 (σ). The Pb isotope ratios of chalcopyrite grains are more variable than those of pyrrhotite which has much lower Pb content. In addition, the range of Pb isotope ratios in sulphide minerals greatly exceeds that of the feldspars.

3.5 Discussion

3.5.1 Textural Relationships

The association of hydrous alteration minerals with PGE enriched sulphide assemblages has previously been interpreted in two ways. One way this association has been interpreted is that both the alteration minerals and the sulphide assemblage, including PGE bearing phases, precipitated from a hydrothermal fluid (e.g. Farrow and Watkinson 1992). The other way to interpret this feature is that, upon crystallization, magmatic sulphide liquid exsolved incompatible volatile components that altered pre-existing magmatic silicates (e.g. Li and Naldrett, 1993, Mungall and Brenan 2003). In the Marathon deposit the association of hydrous alteration minerals and sulphide assemblages is often manifested as pseudomorphs of interstitial and sub-ophitic clinopyroxene. It is evident, based on disequilibrium grain boundaries, that biotite and hornblende have replaced clinopyroxene. The presence of chalcopyrite along cleavage planes in hornblende and biotite and the existence of hornblende, biotite, calcite and apatite as inclusions in chalcopyrite indicate that these minerals crystallized before chalcopyrite. Furthermore, the generally irregular, disequilibrium type grain boundary between chalcopyrite and pyrrhotite indicates that the former replaces the latter. Although the textural relationship of pyrrhotite to clinopyroxene is ambiguous with respect to the crystallization sequence, the presence of flames of pentlandite in pyrrhotite is

characteristic of magmatic sulphide assemblages. A paragenetic sequence based on these observations is proposed in figure (Figure 4.).

From existing literature it is unclear that this paragenetic sequence is possible under magmatic conditions. The most difficult observation to explain in terms of magmatic processes is the disruption of optically continuous pyroxene fragments by sulphide and hydrous silicate assemblages. For this to occur requires that the clinopyroxene be entirely crystallized prior to the introduction of the putative sulphide melt. Although sulphides would still be liquid at temperatures below the clinopyroxene solidus, it seems unlikely that a sulphide liquid would preferentially erode clinopyroxene crystals without having a similar effect on the adjacent plagioclase framework, and that there would not have been some mechanical rotation of clinopyroxene fragments. Though it has been shown that sulphide liquids can be sufficiently mobile, at magmatic temperatures (1300° C) under oxidizing conditions, to produce segregated evolved sulphide melts (Rose and Brenan 2001) there is no evidence for sulphide mobility at lower (sub-solidus) conditions. Hornblende undergoes a dehydration reaction to produce clinopyroxene at temperatures between 720° and 770° C (Spear 1981). Given that hornblende had crystallized prior to chalcopyrite, most of the sulphide liquid would have had to crystallize below 770° C. A liquid with a composition required to produce the observed assemblage would have crystallized chalcopyrite at temperatures above 900° C (Ebel and Naldrett 1997). These observations are inconsistent with the replacement of clinopyroxene by a magmatic sulphide liquid. Conversely, given the above constraints, it is certainly possible to replace pyroxene with the hydrous mineral assemblage and deposit the sulphide minerals under sub-solidus conditions. The alteration of clinopyroxene to amphibole (uralitization) is well documented and commonly occurs in the late stage crystallization of basaltic magmas. Therefore these observations are most consistent with chalcopyrite mineralization that resulted from deuteric or post-magmatic hydrothermal events.

3.5.2. *Pb Isotope Systematics*

The ^{207}Pb isotope was selected for normalization for several reasons. Importantly, both the ^{206}Pb and ^{208}Pb isotopes have mass differences from the ^{207}Pb isotope of 1 amu, which minimizes the effects of ICP-MS mass bias. In addition, the ^{207}Pb isotope has been

found to be the most homogenous in feldspars (Ludwig and Silver 1977) and due to the relatively short half-life of ^{235}U , has had minimal radiogenic production (<4% in the last 2.5 billion years) since the Archean (Doe and Hart 1963). Thus, any differences in the $^{206}\text{Pb}/^{207}\text{Pb}$ and $^{208}\text{Pb}/^{207}\text{Pb}$ ratios between minerals should be the result of differences in the abundances of the ^{206}Pb and ^{208}Pb isotopes, with younger Pb having higher abundances of ^{206}Pb and ^{208}Pb relative to ^{207}Pb than older Pb, *sensu lato*.

The evolution of the $^{206}\text{Pb}/^{207}\text{Pb}$ and $^{208}\text{Pb}/^{207}\text{Pb}$ ratios over time is a function of both the decay rates of the ^{238}U , ^{235}U , and ^{232}Th radioactive isotopes and the present day $^{238}\text{U}/^{204}\text{Pb}$ (μ) and $^{232}\text{Th}/^{238}\text{U}$ (κ) ratios of the source material. The modeled evolution of these ratios over time, according to the two-stage model of Stacey and Kramers (1975), is plotted in figure 5 for various values of μ at a κ of 4.2 for the bulk Earth (Fig. 5a) and a κ of 2.4 for depleted mantle (Fig. 5b) (Gariépy and Dupré, 1991). The initial Pb isotope ratios for the modeling presented in figure 5 are those of Canyon Diablo Troilite. An increase in the μ value, at a constant κ and age, results in a decrease in the $^{208}\text{Pb}/^{207}\text{Pb}$ ratio and an increase in the $^{206}\text{Pb}/^{207}\text{Pb}$ ratio. An increase in the value of κ results in more rapid increase in the $^{208}\text{Pb}/^{207}\text{Pb}$ ratio over time (at a constant μ value).

For a given isotope ratio measurement the analytical uncertainty should be approximately equal to 1.5 times the counting statistics error (which is related to Pb concentration) (Fryer et al. 1993, Crowe et al. Chapter 2). Any additional uncertainty in the measurement can be attributed to heterogeneity of the isotope ratios within the sample. As shown in figure 6, the uncertainty associated with several measurements made on grains of plagioclase from sample G10-2 have isotope ratios for individual traverses that are less than 1.5 times the counting statistics error (Figure 6). The better precision obtained on these feldspar grains than expected from the study of Crowe et al. (Chapter 2) could be attributed to better ablation characteristics of the feldspar mineral sample than the glass standards used to evaluate the limit of precision (Crowe et al., Chapter 2). This is consistent with the relatively large difference between the theoretical counting statistics error and the observed precision (5 fold higher) for Pb isotope ratio measurements of calcite, a mineral with characteristically poor ablation behavior (Craig et al. 2000).

At the scale of a single sample there is heterogeneity between traverses on the same grain and between mineral grains in a single thin section (Figure 6). Notably, the magnitude

of this heterogeneity is approximately equivalent to the magnitude of the heterogeneity observed between samples from the different intrusive units (i.e. Centers 1,2 and 3) (Heaman and Machado, 1992). This heterogeneity occurs in portions of minerals with no petrographic evidence for alteration, fractures, melt or fluid inclusions or compositional differences. As minerals crystallizing from magma would exhibit uniform Pb isotope signatures multiple sources of Pb are required to produce the observed heterogeneity. It is possible that mixing of two isotopically distinct magmas could produce mineral overgrowths that have different isotope ratios than the cores of these minerals (Christensen et al. 1995). Clearly, there is abundant evidence including compositional zoning and mineral overgrowths on plagioclase (Good and Crocket, 1994) that supports disequilibrium conditions and magma mixing. There is also evidence for multiple, isotopically distinct magmatic events during the emplacement of the Coldwell complex (Heaman and Machado 1992). However, it has not yet been possible to relate the observed, mineral-scale, isotopic variation to petrographic evidence for zoning or chemical evidence for these magmatic events. This may be, in part, due to in the spatial resolution ($\sim 450\mu\text{m}$) of the LA-ICP-MS technique, however the close approximation of the observed analytical uncertainty to the theoretical counting statistics error indicates that the minerals are homogeneous at this scale. Alternatively, if the feldspars, a low Pb (~ 2 ppm) system, were subjected to hydrothermal fluids, which have potentially high Pb concentrations, it may be easy to alter the isotope signature of the feldspar by introducing small amounts of Pb along cleavage planes and in crystal defects. The study of Thompson and Malpas (2000) showed a random heterogeneous distribution of trace elements in individual mineral grains that was equivalent to the variation between samples. The trace element heterogeneity observed in the study of Thomson and Malpas (2000) had no corresponding petrographical or major element zoning and was attributed to crystallographic defects and mineralogical variations. Similarly, Sinha (1969) found that radiogenic Pb in Precambrian K-feldspars can be concentrated along grain boundaries and in distorted lattice sites. Ludwig and Silver (1977) recognized that two types of radiogenic Pb could be incorporated into feldspars. One type, "normal" radiogenic Pb, is produced by the *in situ* decay of U and Th that was incorporated during crystallization. This Pb would have an insignificant effect on the Pb isotope ratios of plagioclase due to the low concentrations of U and Th. A second type of radiogenic Pb, could have been derived from the long term

migration of U and Th daughters. This radiogenic Pb component would be indistinguishable from common Pb and thus could account for the observed isotope heterogeneity.

As traverse locations were selected to avoid visible alteration products, micro-fractures, and inclusions, the heterogeneity, in general, cannot be attributed to the sampling of multiple Pb populations. It is important to note that isotope heterogeneity has been observed near grain boundaries and near micro-fractures where the presence of U and Th has resulted in the production of radiogenic Pb since 1.1 Ga.

Pb isotope ratios of plagioclase and sulphide samples from the Eastern Gabbro are plotted in figure 7 along with modeled Pb evolution curves, isochrons derived from these modeled curves, calculated ideal reservoirs at 1.1 Ga and Pb isotope ratios from rocks of similar age also associated with the Midcontinent Rift System. The modeled growth curves for μ values of 7, 7.9, 8.2, and 9.27 and a κ of 3.88 have been calculated based on the two-stage model of Stacey and Kramers (1975). The μ value of 9.27 and the κ value of 3.88 have been calculated from the Pb isotope ratios of plagioclase in sample Ma 137 as follows:

$$\mu = \frac{Y_0 - \frac{^{206}\text{Pb}}{^{207}\text{Pb}} X_0}{\frac{^{207}\text{Pb}}{^{206}\text{Pb}} (e^{\lambda_{238}T_0} - e^{\lambda_{238}t}) - \frac{(e^{\lambda_{235}T_0} - e^{\lambda_{235}t})}{137.88}} \quad (3)$$

$$\kappa = \frac{\left(\frac{^{208}\text{Pb}}{^{206}\text{Pb}} (X_0 + \mu (e^{\lambda_{238}T_0} - e^{\lambda_{238}t})) \right) - Z_0}{\mu (e^{\lambda_{232}T_0} - e^{\lambda_{232}t})} \quad (4)$$

where X_0 , Y_0 , Z_0 are the $^{206}\text{Pb}/^{204}\text{Pb}$, $^{207}\text{Pb}/^{204}\text{Pb}$, and $^{208}\text{Pb}/^{204}\text{Pb}$ ratios at 3.70 Ga respectively (Faure, 1986). The ratios $^{207}\text{Pb}/^{206}\text{Pb}$, $^{208}\text{Pb}/^{206}\text{Pb}$ are the initial (determined) Pb isotope ratios of the sample mineral at 1.1 Ga. The constants λ_{232} , λ_{235} , λ_{238} , are the decay constants of ^{232}Th , ^{235}U , and ^{238}U from Faure (1986), and T_0 and t are 3.70 and 1.1 Ga respectively. Plagioclase from sample Ma 137 is thought to be the least affected by subsolidus events and therefore the closest approximation to the initial magmatic composition. The sample exhibits well developed cumulate layering and contains very pristine (unaltered) interstitial and phenocrystic plagioclase. The other igneous minerals in

sample Ma 137, including olivine and clinopyroxene, are well preserved. As the μ and κ ratios were calculated based on the Pb isotope ratios of plagioclase from sample Ma 137 the 1.1 Ga isochron is constrained to pass through this point. In relation to Ma 137 plagioclase, plagioclase samples from the TDL, including the TIMS ratio from the study of Heaman and Machado (1992), are displaced towards lower $^{206}\text{Pb}/^{207}\text{Pb}$ and higher $^{208}\text{Pb}/^{207}\text{Pb}$ values. A similar relationship was noted by Heaman and Machado (1992) when comparing plagioclase from the TDL to K-feldspar from the center 2 nepheline syenites. The study of Heaman and Machado (1992) suggested that the difference in Pb isotope ratios between the two centers could be attributed to the progressive contamination of a deep seated magma chamber with lower continental crustal material. Interestingly, there is a trend in plagioclase Pb isotope ratios, along the 1.1 Ga isochron, towards the calculated ideal Archean lower crustal ratios at 1.1 Ga. The K-feldspar ratios from Heaman and Machado plot within analytical error of the 1.1 Ga isochron between the Ma 137 point and Archean lower crust. Superimposed on this trend is a small displacement of the Pb Isotope ratios of feldspars towards the calculated values for the Archean upper crust at 1.1 Ga.

A possible explanation for these trends is that the large syenite dykes that cross-cut the TDL were injected into the TDL during emplacement of the center 2 magmas. Fluids derived from these relatively evolved melts that had been subjected to lower crustal contamination in a deep seated magma chamber would likely have higher Pb concentrations than the plagioclase in the TDL (Zartman and Haines 1988). It is possible that the dykes were emplaced while the TDL magmas were still relatively hot (ie. above plagioclase closure temperatures) and that plagioclase incorporated some Pb derived from these dykes resulting in an isotope signature intermediate to Ma 137 plagioclase and the center 2 syenite. Sample Ma 137 plagioclase would not have been affected by this event as it is spatially removed from the dykes and also was likely already completely crystallized (Walker et al. 1991, Dahl et al. 2001).

The shift in plagioclase isotope ratios towards the Archean Upper crust signature is not surprising. The TDL is, spatially, in close proximity to the Archean felsic metavolcanic country rocks and contains abundant mesoscopic and microscopic evidence for assimilation. This includes; abundant country rock xenoliths, granophyric textures developed both from partial melting and devolatilization of alkalic country rock inclusions (Dahl et al. 2001), and

the variable presence of orthopyroxene overgrowths on olivine and clinopyroxene which is indicative of a local increase in silica activity. Additionally, it has been suggested (Barrie et al. 2002) that the TDL crystal mush was fluxed with volatile rich fluids derived from the country rock late in the crystallization history. If this fluxing event occurred above the plagioclase closure temperature it could produce the observed isotopic shift.

The calculated μ (9.27) and κ (3.88) from the Ma 137 plagioclase are consistent with magma derivation from an enriched mantle plume source relative to bulk silicate earth (Zartman and Haines 1988, Gariépy and Dupré 1991). The μ (9.27) and κ (3.88) values for sample Ma 137 are higher than the μ (7.9) and κ (3.96) calculated from the data of Heaman and Machado (1992). This difference could be attributed to the progressive contamination of a deep crustal magma chamber with lower crustal material which has an ideal μ of 6.49 and κ of 6.05 (Zartman and Haines 1988).

The Pb isotope ratios in sulphide are more complicated than plagioclase. It would be expected, due to the typically much higher (~10 times) concentration of Pb in chalcopyrite, that it would be much less susceptible to post-crystallization disturbances in the isotope ratios than plagioclase. However, in contrast to the relatively narrow range of isotopic composition of plagioclase, grains of chalcopyrite are displaced up to two times this range from the 1.1 Ga isochron and the Ma 137 isotopic signature. This situation becomes increasingly complicated considering that these isotopic shifts occur at the scale of a thin section and even in the same grain.

In contrast, to plagioclase which exhibits moderate variation compared to analytical precision, chalcopyrite, having much better counting statistics, can be heterogeneous well in excess of analytical uncertainty. Furthermore, there is no apparent correlation between the Pb isotope composition of plagioclase and that of chalcopyrite in the same sample. These observations are strong evidence for isotope disequilibrium between these two minerals in the same thin section. As discussed above for feldspars, minerals crystallizing from magma would exhibit uniform common Pb isotope ratios, and multiple sources of Pb are required to produce the observed isotope heterogeneity. Again, although magma mixing processes could certainly provide multiple sources of isotopically different Pb, it is not clear how magma mixing could produce mineral specific Pb isotope variation, and is inconsistent with the textural relationships described above. Alternatively, the selective replacement of

clinopyroxene by a Pb bearing hydrothermal fluid could result in secondary alteration minerals, including chalcopyrite, with different Pb isotope ratios than the primary assemblage.

3.5.4 Constraints on Models

Several genetic models have been proposed to explain the metal enrichment in the Marathon deposit. Initially, Watkinson and Ohnenstetter (1992) proposed a hydrothermal model for Cu and PGE enrichment. They noted that the PGE enriched sulphide assemblages in the Marathon deposit occurred in the most Cu rich rocks and that the platinum group minerals (PGM) were associated with pyrrhotite poor assemblages of chalcopyrite, cubanite, and minor bornite, digenite and chalcocite. Importantly, Watkinson and Ohnenstetter (1992) noted that although the majority of TDL rocks are relatively unaltered, PGE and Cu-rich rocks were partly altered to an assemblage of amphibole, chlorite, epidote, muscovite and calcite, and that the highest PGE concentrations occur in coarse-grained gabbroic rocks. Texturally, the PGM are found; included or adjacent to postcumulus sulphides (chalcopyrite and cubanite), in chalcopyrite or cubanite along sulphide-oxide grain boundaries, in veinlets along the contact of chalcopyrite with other minerals, and in veins that cut magnetite and other primary minerals. Watkinson and Ohnenstetter (1992) noted that the PGM found in chalcopyrite are often spatially related to galena (PbS) and altaite (PbTe). The common occurrence of Pb bearing minerals with PGM led Watkinson and Ohnenstetter (1992) to postulate that the PGE enrichment was related to the interaction of a Pb bearing fluid, derived from the country rock, with magmatic minerals. This is supported by the ubiquitous association of PGE enriched sulphide assemblages with Pb bearing hydrous silicates (this study) and the association of the PGM with fluid inclusions in these hydrous silicates. Watkinson and Ohnenstetter (1992) argued that PGE and Cu-rich sulfide assemblages are uncharacteristic of classical magmatic assemblages. Furthermore, they noted similarities including the replacement of pyrrhotite and magnetite by the PGE and Cu-rich assemblage, and the occurrence of PGM in veinlets that cross-cut minerals, to other Cu-rich sulfide deposits such as the New Rambler mine (McCallum et al. 1979), the Salt-Chuck deposit (Watkinson and Melling, 1992) and the Messina mine (Mihálik et al. 1974).

Based on these considerations, Watkinson and Ohnenstetter (1992) presented a model whereby the enrichment of Cu and PGE in sulphide assemblages resulted from the interaction of fluid, derived from both the country rock and the intrusion, with magmatic sulphides, oxides and silicates. PGM precipitated from these fluids under reducing conditions when the chloride bearing solutions interacted with magnetite and pyrrhotite to produce chlorite, epidote, carbonates, chalcopyrite and cubanite. The model of Watkinson et al. (1992) suggests that the presence of these fluids resulted in the replacement of pyroxene by amphibole and plagioclase by chlorite, albite and epidote.

In contrast, Good and Crocket (1994) have proposed a modified version of the classical (cf. Campbell et al. 1983) magmatic model for the Marathon deposit. Good and Crocket have argued that the significant correlation between sulphur and chalcophile element concentrations is inconsistent with hydrothermal processes. Furthermore, Good and Crocket (1994) suggested that the coherent behavior of Ni and Ir, given that thermodynamic calculations indicate that Ni is an order of magnitude more volatile than Ir under most conditions, is inconsistent with hydrothermal transport. They also noted that the preservation of primary minerals is inconsistent with the interaction of the enriched rocks with a large volume of fluid that would be required for significant PGE transport under reducing conditions at 25-300°C. The absence of evidence for alkali metal mobility was given as additional support against a high fluid/rock ratio. Based on these observations Good and Crocket (1994) proposed the following magmatic model. The progressive devolatilization and assimilation of the surrounding country rock caused sulphur saturation and the formation of immiscible sulphide liquid droplets during the formation of a stratified, deep-seated magma chamber by the crystallization of olivine. The progressive sulphur addition and the stratified nature of the magma chamber resulted in the formation of sulphide droplets with variable metal concentrations depending on the amount of olvine crystallized at the time of liquation. Turbulent mixing of these layers occurred during injections of a sulphide droplet bearing, plagioclase crystal mush to the current upper crustal position. Plagioclase settled *in situ* and formed a framework for the crystallization of the sulphide bearing interstitial melt. Good and Crocket (1994) suggested that, following a rapid crystallization of the crystal mush, a small amount of volatile rich melt migrated toward the center of the intrusion, crystallized granophyre and released water into the surrounding gabbro causing pegmatitic

texture development. Good and Crocket (1994) argued that sub-solidus reactions with deuteric fluids caused the local migration of elements, and accounts for the replacement textures and deposition of PGM in association with hydrous silicates. Good and Crocket (1994) found no geochemical evidence for fluid migration beyond the hand sample scale.

Based on the textural observations discussed above it is clear that the bulk of the chalcopyrite mineralization occurred at sub-solidus temperatures. This is most strongly supported by the disruption of optically continuous magmatic clinopyroxene by chalcopyrite and by the replacement of secondary hydrous minerals by the sulphide assemblage. This observation suggests that most of the Cu enrichment is the result of post-magmatic hydrothermal processes. The difference in the Pb isotope ratios between chalcopyrite and plagioclase necessitates the addition of exotic Pb subsequent to plagioclase crystallization. This is also consistent with the deposition of chalcopyrite, and Cu enrichment by hydrothermal fluids. The textural association of the PGM with chalcopyrite and with Pb rich minerals and Pb bearing hydrous silicates suggests that the PGM enrichment process is related to the chalcopyrite mineralization event and Pb enrichment.

The magmatic model of Good and Crocket (1994) is inconsistent with the timing of the chalcopyrite mineralization in relation to clinopyroxene and hydrous silicate crystallization. Furthermore, the differences in the Pb isotope ratios observed in minerals from the same thin section necessitates the post-magmatic migration of elements (Pb) at a large scale. In contrast, these observations are largely consistent with the model proposed by Watkinson and Ohnenstetter (1992) which explicitly dictates that clinopyroxene was altered at sub-solidus conditions by an exotic Pb bearing hydrothermal fluid. However, the difference in the Pb isotope ratios between chlorite minerals and the rest of the alteration assemblage and chalcopyrite suggests that the chloritization event is not related to chalcopyrite mineralization, and is probably a much later retrograde reaction.

A possible mechanism (similar to Barrie et al. 2002) for the introduction of exotic Pb might involve the injection of hydrothermal fluids, generated during the subsequent intrusion of center 2 and 3 magmas, and possibly related to the intrusion of the large syenite dykes, along the intrusive contact of the gabbroic rocks with country rock. During transport the fluids would have interacted with the basal zone massive sulphide and the footwall Archean country rocks. During this interaction the fluids would accumulate metals, including Pb, from

both the basal zone sulphide and the country rock in addition to S and metalloids. These fluids may have then infiltrated the recently crystallized TDL gabbro and caused feldspathic alteration and selectively replacing the preexisting mineral assemblage with hydrous minerals and Cu rich sulphides and PGM. It is entirely possible that this fluid event could be responsible for the small scatter observed in the plagioclase data.

3.6 Summary

This study presents the first precise, mineral-scale Pb isotope ratio measurements of major primary magmatic phases, minor accessory minerals, and secondary sulphides using LA-ICP-MS. Even in the early stages of technique development mineral-scale Pb isotope ratios determined by LA-ICP-MS have proven a powerful tool for the delineation of multiple sources of Pb in minerals and rocks, and the mechanisms by which exotic Pb was introduced. The mineral-scale Pb isotope data in conjunction with petrographic evidence has been successfully used to test genetic models proposed for PGE and Cu enrichment in the Marathon PGE-Cu deposit. This study supports a model that involves the enrichment of igneous rocks by externally derived, Pb bearing, Cu and precious metals enriched fluids at sub-solidus temperatures.

Although generating a comprehensive database of Pb isotope ratios for the Coldwell Complex is beyond the scope of this study, the Pb isotope data presented here dictate that a more complete study would yield considerable insight into the genesis of PGE-Cu deposits, the differentiation of large layered intrusions, and the nature and evolution of intra-plate rift-systems. Specifically, in the Coldwell complex it would be useful to conduct a study on the Pb isotopes of the different intrusive phases, comparing mineral-scale isotope ratios with those of mineral separates and whole rock. In addition, it would be useful to investigate the relationship between mineral-scale Pb isotope systematics and those of another isotope system (e.g., Rb-Sr for plagioclase or Re-Os for sulphides).

Given the association between the replacement of pyroxene and mineralization, deposit-scale exploration might focus on rocks exhibiting this textural feature. In addition, the apparent correlation between Pb and PGM enrichment should be investigated as another possible exploration tool. Furthermore, the Pb isotope data obtained in this study suggest an enriched mantle plume source, similar to OIBs, for the Eastern Gabbro magmas. This is

consistent with previous isotope work on both the Coldwell complex and the Mid-continent rift system as a whole (Heaman and Machado 1992, Shirey and Nicholson 1990, Nicholson et al., 1997, Barrie et al. 2002). As the Coldwell complex was emplaced early in the rift-system development (Heaman and Machado, 1992), it is possible that the initial magmas generated by the plume source were enriched in PGE (Barnes et al. 1997). Thus, on a regional scale exploration efforts might focus on Midcontinent Rift system intrusive rocks that bear this isotope signature.

3.7 References

- Andrews, D.R.A., and Brenan, J.M. (2002) The solubility of ruthenium in sulfide liquid: implications for platinum group mineral stability and sulfide melt-silicate melt partitioning. *Chemical Geology*, **192**, 163-181
- Ballaus, C.G., and Stumpfl, F.F. (1986) Sulfide and Platinum mineralization in the Merensky reef; evidence from hydrous silicates and fluid inclusions. *Contributions to Mineralogy and Petrology*, **94**, 193-204
- Barnes, S.J., and Campbell, I.H. (1988) Role of late magmatic fluids in Merensky-type platinum deposits: A discussion. *Geology*, **16**, 488-491
- Barnes, S.J., Zientek, M.L., and Severson, M.J. (1997) Ni, Cu, Au, and platinum-group element contents of sulphides associated with intraplate magmatism: a synthesis. *Canadian Journal of Earth Sciences*, **34**, 337-351
- Barrie, C.T., MacTavish, A.D., Walford, P.C., Chataway, R., and Middaugh, R. (2002) Contact-type and Magnetite Reef-type Pd-Cu Mineralization in Ferroan Olivine Gabbros of the Coldwell Complex, Ontario. In *The Geology, Geochemistry, Mineralogy and Mineral Beneficiation of Platinum-Groups* (ed. L.J. Cabri), pp. 321-337. Canadian Institute of Mining, Metallurgy and Petroleum.
- Bell, K (1989) Carbonatites, pp. 360-384. Unwin Hyman, London, UK
- Boudreau, A.E., Mathez, E.A., and McCallum, I.S. (1986) The halogen geochemistry of the Stillwater and Bushveld Complexes: Evidence for the transport of the platinum-group elements by Cl-rich fluids. *Journal of Petrology*, **27**, 967-986
- Boudreau, A.E., Meurer, W.P., (1999) Chromatographic separation of the platinum-group elements, gold, base metals and sulfur during degassing of a compacting and solidifying igneous crystal pile. *Contributions to Mineralogy and Petrology*, **134**, 174-185
- Campbell, I.H., Naldrett, A.J., and Barnes, S.J. (1983) A model for the origin of the platinum-rich sulfide horizons in the Bushveld and Stillwater complexes. *Journal of Petrology*, **24**, 133-165
- Christensen, J.N., Halliday, A.N., Godfrey, L.V., Hein, J.R., Rea, D.K. (1997) Climate and Ocean Dynamics and the lead isotopic records in Pacific ferromanganese crusts. *Science*, **277**, 913-918
- Craig, C-A, Jarvis, K, and Clarke, L.J. (2000) Assessment of calibration strategies for the quantitative and semi-quantitative analysis of calcium carbonate matrices by laser ablation-inductively coupled plasma-mass spectrometry (LA-ICP-MS). *Journal of Analytical Atomic Spectrometry*, **15**, 1001-1008
- Crocket, J.H., Fleet, M.E., and Stone, W.E. (1997) Implications of composition for experimental partitioning of platinum-group elements and gold between sulfide liquid and basalt melt: The significance of nickel content. *Geochimica et Cosmochimica Acta*, **61**, 4139-4149
- Crowe, S.A., Fryer, B.J., Samson, I.M., and Gagnon, J.E. (submitted) Precise isotope ratio determination of common Pb using quadrupole LA-ICP-MS with optimized laser sampling conditions and a robust mixed-gas plasma. *Journal of Analytical Atomic Spectrometry*, submitted
- Dahl, R., Watkinson, D.H., Taylor, R.P. (2001) Geology of the Two Duck Lake Intrusion and the Marathon Cu PGE Deposit, Coldwell Complex, Northern Ontario. *Exploration and Mining Geology*, **10**, 51-65
- Doe, B.R., and Hart, S.R. (1963) The effect of contact metamorphism on Pb in potassium feldspars near the Eldora stock, Colorado, *Journal of Geophysical Research*, **70**, 3521-3530
- Ebel, D.S., and A.J. Naldrett (1997) Crystallization of sulfide liquids and the interpretation of ore composition. *Canadian Journal of Earth Sciences*, **34**, 352-365

- Faure, G. (1986) Principles of Isotope Geology, Second Edition, pp. 282-334. John Wiley and Sons, New York, USA
- Farrow, C.E.G., and Watkinson, D.H. (1992). Alteration and the role of fluid in Ni, Cu and platinum-group element deposit, Sudbury Igneous Complex contact, Onaping-Levack area, Ontario. *Mineralogy and Petrology*, **46**, 67-83
- Fleet, M.E., and Wu, T-W. (1995) Volatile transport of precious metals at 1000°C: speciation, fractionation, and the effect of base metal sulfide. *Geochimica et Cosmochimica Acta*, **59**, 487-495
- Fleet, M.E., Crocket, J.H., Liu, M., and Stone, W.E. (1999) Laboratory partitioning of platinum-group elements (PGE) and gold with application to magmatic sulfide-PGE deposits. *Lithos*, **47**, 127-142
- Fryer, B.J., Greenough, J.D. (1992) Evidence for mantle heterogeneity from platinum-group-element abundances in Indian Ocean basalts. *Canadian Journal of earth Sciences*, **29**, 2329-2340
- Fryer, B.J., Jackson, S.E., and Longerich, H.P. (1993) The application of laser ablation microprobe – inductively coupled plasma – mass spectrometry (LAM-ICP-MS) to in-situ (U)-Pb geochronology. *Chemical Geology*, **109**, 1-8
- Gammons, C.H. (1996) Experimental investigations of the hydrothermal geochemistry of platinum and palladium: V. Equilibria between platinum metal, Pt (II), and Pt (IV) chloride complexes at 25 to 300°C. *Geochimica et Cosmochimica Acta*, **60**, 1683-1694
- Getty, S.R., DEPaulo, D.J. (1995) Quaternary geochronology using the U-Th-Pb method. *Geochimica et Cosmochimica Acta*, **59**, 3267-3272
- Good D.J., and Crocket J.H. (1994) Genesis of the Marathon Cu-platinum-group element deposit, Port Coldwell Alkalic Complex, Ontario: A Midcontinent Rift-related magmatic sulfide deposit. *Economic Geology*, **89**, 131-149
- Greenough, J.D., Fryer, B.J and Owen, J.V. (1995) Mantle processes affecting the concentrations of Au, Pd, Pt, Rh, Ru and Ir in mafic magmas: Constraints from alkaline lamprophyres of Atlantic Canada. *Anais da Academia Brasileira de Ciencias*, **67**, 235-255.
- Harris, C., and Chaumba, J.B. (2001) Crustal Contamination and Fluid-Rock Interaction during the Formation of the Platreef, Northern Limb of the Bushveld Complex, South Africa. *Journal of Petrology*, **42**, 1321-1347
- Heaman, L.M., Machado, N (1992) Timing and origin of mid-continent rift alkaline magmatism, North America: evidence from the Coldwell Complex. *Contributions to Mineralogy and Petrology*, **110**, 289-303
- Li, C., and Naldrett, A.J. (1993) High chlorine alteration minerals and calcium-rich brines in fluid inclusions from the Strathcona Deep Copper Zone, Sudbury Ontario. *Economic Geology*, **88**, 1780-1796
- Li, X-H, Liang, X-R, Sun, M., Guan, H., Malpas, J.G. (2001) Precise $^{206}\text{Pb}/^{238}\text{U}$ age determination on zircons by laser ablation microprobe-inductively coupled plasma-mass spectrometry using continuous linear ablation. *Chemical Geology*, **175**, 209-219
- Ludwig, K.R., and Silver, L.T. (1977) Lead isotope inhomogeneity in Precambrian igneous K-feldspars. *Geochimica et Cosmochimica Acta*, **41**, 1457-1471
- MacDonald, A.J. (1987) The Platinum Group Element Deposits: Classification and Genesis. In *Ore deposit models* (ed. Roberts, R.G., and Sheahan, PA), pp. 117-131. Geological Association of Canada

- Mahnes, G., Allegre, C., Dupre, B., Hamelin, B. (1980) Lead isotope study of ultrabasic layered complexes: speculations about the age of the earth and primitive mantle characteristics. *Earth and Planetary Science Letters*, **47**, 370-382
- McCallum, M.E., Loucks, R.R., Carlson, R.R., Cooley, E.F., Doerge, T.A. (1976) Platinum metals associated with hydrothermal copper ores of the New Rambler Mine, Medicine Bow Mountains, Wyoming. *Economic Geology*, **71**, 1429-1450
- McCallum, I.S., Thurber, M.W., O'Brien, H.E., and Nelson, B.K. (1999) Lead isotopes in sulfides from the Stillwater Complex, Montana: evidence for subsolidus remobilization. *Contributions to Mineralogy and Petrology*, **137**, 206-219
- Mihálik, P., Hiemstra, S.A., DE Villiers, J.P.R. (1975) Rustenburgite and atokite, two new platinum-group minerals from the Merensky Reef, Bushveld Igneous complex. *Canadian Mineralogist*, **13**, 146-150
- Mountain, B.W., and Wood, S.A. (1988) Chemical Controls on the Solubility, Transport, and Deposition of Platinum and Palladium in Hydrothermal Solutions: A Thermodynamic Approach. *Economic Geology*, **83**, 492-510
- Mungall, J.E., and Brenan, J.M. (2003) Experimental evidence for the chalcophile behavior of the halogens. *The Canadian Mineralogist*, **41**, 207-220
- Nicholson, S.W., and Shirey S.B., (1990). Midcontinent Rift volcanism in the Lake Superior region: Sr, Nd, and Pb isotopic evidence for a mantle plume origin. *Journal of Geophysical Research*, **95**, 10851-10868
- Nicholson, S.W., Shirey, S.B., Schulz, K.J., and Green, J.C. (1997). Rift-wide correlation of 1.1 Ga Midcontinent rift system basalts: Implications for multiple mantle sources during rift development. *Canadian Journal of Earth Sciences*, **34**, 504-520
- Nyman, M.W., Sheets, R.W., and Bodnar, R.J. (1990) Fluid inclusion evidence for the physical and chemical conditions associated with intermediate temperature PGE mineralization at the New Rambler deposit, southwestern Wyoming. *Canadian Mineralogist*, **28**, 629-638
- Pasteris, J.D., Harris, T.N., and Sassani, D.C. (1995). Interactions of mixed volatile-brine fluids in rocks of the southwestern footwall of the Duluth Complex, Minnesota: evidence from fluid inclusions. *American Journal of Science*, **295**, 125-172
- Peach, C.L., Mathez, E.A., Keays, R.R., and Reeves, S.J. (1994). Experimentally determined sulfide melt silicate melt partition coefficients for iridium and palladium. *Chemical Geology*, **117**, 361-377
- Pearce, N.J.G., Perkins, W.T., Westgate, J.A., Gorton, M.P., Jackson, S.E., Neal, C.R., Chenery, S.P. (1997) A compilation of new and published major and trace element data for NIST SRM 610 and NIST SRM 612 glass reference materials. *Geostandards Newsletter*, **21**, 115-144
- Peck, D.C., Keays, R.R., James, R.S., Chubb, P.T., Reeves, S.J. (2001) Controls on the formation of contact type platinum-group element mineralization in the East Bull Lake Intrusion. *Economic Geology*, **96**, 559-581
- Ripley, E.M., and Al-Jassar, T.J. (1987) Sulfur and oxygen isotope studies of melt-country rock interaction, Babbitt Cu-Ni deposit, Duluth Complex, Minnesota. *Economic Geology*, **80**, 201-210
- Ripley, E.M., Lambert, D.D., Frick, L.R. (1999) Re-Os, Sm-Nd, and Pb isotopic constraints on mantle and crustal contributions to magmatic sulfide mineralization in the Duluth Complex. *Geochimica et Cosmochimica Acta*, **62**, 3349-3365
- Rose, L., and Brenan, J.M. (2001) Wetting properties of Fe-Ni-Co-Cu-O-S melts against olivine: Implications for sulfide melt mobility. *Economic Geology*, **96**, 145-157

- Sage, R.P. (1991) Alkalic rock, carbonatite and kimberlite complexes of Ontario, Superior Province. In *Geology of Ontario*. (Ed. Thurston, P.C., Williams, H.R., Sutcliffe, R.H., and Scott, G.M.), pp. 683-709. Ontario Geological Survey
- Shaw, C.S.J. (1997) The petrology of the layered gabbro intrusion, Eastern Gabbro, Coldwell Alkaline Complex, northwestern Ontario, Canada: Evidence for multiple phases of intrusion in a ring dyke. *Lithos*, **40**, 243-259
- Sinha, A.K. (1969) Removal of Radiogenic lead from potassium feldspars by volatilization. *Earth and Planetary Science Letters*, **7**, 109-115
- Smith, A.R., and Sutcliffe, R.H. (1987) Keweenawan intrusive rocks of the Thunder Bay area: *Ontario Geological Miscellaneous Paper*, **137**, 248-255
- Sutcliffe, R.H. (1991) Proterozoic geology of the Lake Superior area. *Ontario Geological Survey Special Volume 4*, 627-255
- Thériault, R.D., Barnes, S.-J. and Severson, M.J. (1997) The influence of country-rock assimilation and silicate to sulfide ratios (R factor) on the genesis of the Dunka Road Cu-Ni- platinum-group element deposit, Duluth Complex, Minnesota. *Canadian Journal of Earth Sciences*, **34**, 375-389
- Tosdal, R.M., Wooden, J.L., and Bouse R.M. (1999) Pb Isotopes, Ore Deposits, and Metallogenic Terranes. In *Application of Radiogenic Isotopes to Ore Deposit Research and Exploration* (Ed. Lambert, D.L., and Ruiz, R.). Society of Economic Geologists Inc., Boulder, CO, USA, pp. 1-25
- Walker, E.C., Sutcliffe, R.H., Shaw, C.S.J., and Shore, G.T. (1991) Geology of the Coldwell alkaline complex. *Ontario Geological Survey Miscellaneous Paper*, **157**, 107-116
- Watkinson, D.H., and Ohnenstetter, D. (1992) Hydrothermal Origin of platinum-group mineralization in the Two Duck Lake Intrusion, Coldwell Complex, northwestern Ontario. *Canadian Mineralogist*, **30**, 121-136
- Watkinson, D.H., and Melling, D.R. (1992) Hydrothermal origin of platinum-group mineralization in low temperature copper sulfide-rich assemblages, Salk Chuck intrusion, Alaska. *Economic Geology*, **87**, 175-184
- Watkinson, D.H., Lavigne, M.J., Fox, P.E. (2002) Magmatic-Hydrothermal Cu- and Pd-rich Deposits in Gabbroic Rocks from North America. In *The Geology, Geochemistry, Mineralogy and Mineral Beneficiation of Platinum-Groups* (ed. L.J. Cabri), pp. 321-337. Canadian Institute of Mining, Metallurgy and Petroleum.
- Wilkinson, S.J. (1983) Geology and sulfide mineralization of the marginal phases of the Coldwell Complex, Northwestern Ontario. M.Sc. thesis, Carleton University, Ottawa, 129p.
- Willmore, C.C., Boudreau, A.E., Kruger, F.J. (2000) The Halogen Geochemistry of the Bushveld Complex, Republic of South Africa: Implications for Chalcophile Element Distribution in the Lower and Critical Zones. *Journal of Petrology*, **41**, 1517-1539
- Wooden, J.L., Czmanske, G.K., Zientek, M.N. (1991) A lead isotope study of the Stillwater Complex, Montana: constraints on crustal contamination and source regions. *Contributions to Mineralogy and Petrology*, **107**, 80-93
- Zartman, R.E., Haines, S.M. (1998) The plumbotectonic model for Pb isotopic systematics among major terrestrial reservoirs- A case for bidirectional transport. *Geochimica et Cosmochimica Acta*, **52**, 1327-1339

3.8 Tables

Table 1. Mineral Pb Isotope Ratios (not corrected for *in situ* decay)
n is the number of traverses per measurement, * from Heaman and Machado (1992),

Sample	Mineral	Lithology	(n)	$^{206}\text{Pb}/^{207}\text{Pb}$	σ	$^{208}\text{Pb}/^{207}\text{Pb}$	σ	$^{232}\text{Th}/^{207}\text{Pb}$	$^{238}\text{U}/^{207}\text{Pb}$
Ma 137	Plagioclase	LG	17	1.081	0.003	2.371	0.006	0.085	0.015
G10-1	Plagioclase	FGOG	19	1.076	0.003	2.386	0.001	0.081	0.003
G10-3B	Plagioclase	MGOG	20	1.071	0.004	2.381	0.007	0.028	0.007
G10-2	Plagioclase	MCGG	20	1.064	0.003	2.378	0.007	0.073	0.009
G11-11I	Plagioclase	MCGG	20	1.065	0.001	2.377	0.004	0.010	0.001
G10-8I	Plagioclase	MCGG	16	1.062	0.003	2.385	0.005	0.120	0.016
86CL1*	Plagioclase	CGOG	-	1.072	0.004	2.379	0.003	-	-
Neph*	K-feldspar	NSY	-	1.063	0.003	2.376	0.004	-	-
G10-2	Chalcopryrite	MCGG	10	1.075	0.002	2.404	0.005	0.000	0.000
G10-2	Chalcopryrite	MCGG	20	1.062	0.002	2.375	0.003	0.000	0.000
G10-8I	Chalcopryrite	MCGG	5	1.072	0.003	2.414	0.003	0.000	0.000
G11-7I	Chalcopryrite	MCGG	4	1.071	0.004	2.391	0.005	0.000	0.000
G11-7I	Chalcopryrite	MCGG	6	1.076	0.002	2.394	0.002	0.000	0.000
F28-3	Chalcopryrite	MPGG	10	1.065	0.002	2.388	0.003	0.000	0.000
G11-11I	Chalcopryrite	MPGG	5	1.067	0.002	2.416	0.003	0.000	0.000
G10-8I	Chalcopryrite	MCGG	5	1.059	0.002	2.347	0.002	0.000	0.000
G10-8I	Chalcopryrite	MCGG	5	1.064	0.002	2.359	0.002	0.000	0.000
G11-1I	Chalcopryrite	MCGG	5	1.063	0.004	2.372	0.005	0.000	0.000
G11-16I	Chalcopryrite	MCGG	6	1.077	0.003	2.397	0.006	0.000	0.000
G10-8I	Pyrrhotite	MCGG	4	1.079	0.005	2.402	0.007	0.000	0.000
G10-7I	Pyrrhotite	MCGG	9	1.071	0.003	2.390	0.008	0.000	0.000
G11-11I	Pyrrhotite	MPGG	5	1.069	0.005	2.405	0.004	0.000	0.000
G11-1I	Pyrrhotite	MSFGG	5	1.067	0.005	2.387	0.008	0.000	0.000
G11-1I	Pyrrhotite	MSFGG	5	1.072	0.003	2.372	0.005	0.000	0.000
G11-1I	Pyrrhotite	MSFGG	5	1.065	0.005	2.368	0.006	0.000	0.000
G11-2	Feldspar core	MCGG	1	1.084	0.011	2.367	0.009	0.081	0.006
G11-2	Feldspar rim	MCGG	1	1.038	0.022	2.319	0.019	0.000	0.000
G11-2	Pb sulphate ?	MCGG	1	1.087	0.004	2.424	0.004	0.001	0.000
G11-2	Felspar	MCGG	1	1.050	0.011	2.342	0.010	0.048	0.003
G11-2	Green Biotite	MCGG	1	1.054	0.012	2.355	0.016	0.048	0.002
G11-2	Green Biotite	MCGG	1	1.076	0.013	2.365	0.012	0.116	0.020
G11-2	Green Biotite	MCGG	1	1.094	0.010	2.403	0.009	0.349	0.038
G11-2	Calcite	MCGG	1	1.096	0.008	2.378	0.009	0.036	0.022
G11-2	Calcite	MCGG	1	1.096	0.007	2.408	0.008	0.051	0.028
G11-2	Brown Biotite	MCGG	1	1.090	0.007	2.371	0.007	0.000	0.086
G11-2	Brown Biotite	MCGG	1	1.076	0.007	2.340	0.007	0.000	0.037
G11-2	Brown Biotite	MCGG	1	1.095	0.007	2.381	0.007	0.000	0.046
G11-2	Chlorite	MCGG	1	1.149	0.015	2.429	0.015	0.068	0.012
G10-2	Hornblende	MCGG	1	1.056	0.015	2.377	0.012	0.837	0.088
G10-2	Hornblende	MCGG	1	1.108	0.011	2.372	0.011	0.479	0.050
G10-2	Chlorite	MCGG	1	1.189	0.013	2.450	0.010	0.012	0.003
G10-2	Chlorite	MCGG	1	1.160	0.013	2.411	0.010	0.006	0.003
G10-2	Chlorite	MCGG	1	1.158	0.012	2.451	0.011	0.006	0.004
G10-2	Chlorite	MCGG	1	1.197	0.013	2.456	0.011	0.007	0.003
G10-2	Calcite	MCGG	1	1.066	0.011	2.371	0.012	0.069	0.026
G10-2	Calcite	MCGG	1	1.093	0.012	2.428	0.013	0.081	0.031
G10-2	Calcite	MCGG	1	1.092	0.015	2.371	0.014	0.077	0.026
G10-2	Calcite	MCGG	1	1.092	0.012	2.398	0.011	0.062	0.021
G10-2	Hornblende	MCGG	16	1.066	0.002	2.346	0.013	0.175	0.030
G10-9I	Hornblende	MCGG	19	1.054	0.007	2.329	0.022	0.532	0.125

LG=Layered Gabbro, F,M,CGOG= Fine,Mediumm,Coarse-Grained Olivine Gabbro, MC,PGG= Mineralised(sulphide bearing) Coarsc-Graincd,Pegmatitic Gabbro

Table 2. Age (1108 Ma) corrected Pb Isotope ratios

Sample	Mineral	$^{206}\text{Pb}/^{207}\text{Pbc}$	σ	$^{208}\text{Pb}/^{207}\text{Pbc}$	σ
G11-2	Green Biotite	1.054	0.012	2.352	0.010
G11-2	Green Biotite	1.073	0.013	2.359	0.012
G11-2	Green Biotite	1.088	0.010	2.385	0.010
G11-2	Calcite	1.092	0.008	2.377	0.009
G11-2	Calcite	1.091	0.007	2.406	0.008
G11-2	Brown Biotite	1.075	0.008	2.374	0.007
G11-2	Brown Biotite	1.070	0.007	2.341	0.007
G11-2	Brown Biotite	1.087	0.007	2.383	0.007
G11-2	Chlorite	1.147	0.015	2.426	0.015
G10-2	Hornblende	1.041	0.015	2.333	0.015
G10-2	Hornblende	1.099	0.011	2.347	0.012
G10-2	Chlorite	1.188	0.013	2.449	0.010
G10-2	Chlorite	1.159	0.013	2.411	0.010
G10-2	Chlorite	1.157	0.012	2.451	0.011
G10-2	Chlorite	1.196	0.013	2.456	0.011
G10-2	Calcite	1.062	0.011	2.368	0.012
G10-2	Calcite	1.088	0.012	2.425	0.013
G10-2	Calcite	1.088	0.015	2.368	0.014
G10-2	Calcite	1.088	0.012	2.395	0.011
G10-2	Hornblende	1.061	0.002	2.337	0.013
G10-9I	Hornblende	1.033	0.008	2.303	0.023

3.9 Figures

Figure 1. Geological Map of the Coldwell Complex (after Shaw, 1997)

Figure 2. Idealized stratigraphic-section of the Marathon deposit (after Barrie et al. 2002)

Figure 3. Photomicrographs of Marathon deposit textures, interference colors are atypical due to the thickness (100 μm) of the sections: a.) Transmitted, cross-polarized light image of two laser traverses (black lines) across unaltered interstitial plagioclase (PLAG) from sample Ma 137; b.) reflected light image of typical sulphide assemblage consisting mostly of chalcopyrite (CP) around a core of pyrrhotite (PO), pyrite (PY) occurs in veinlets that cut chalcopyrite and pentlandite (PN) occurs at the margins of the pyrrhotite; c) reflected light image of typical magmatic net-textured sulphide in clinopyroxene (CPX), chalcopyrite (CP) has smooth, equilibrium grain boundaries with pyrrhotite (PO); d.) transmitted, cross-polarized light image of typical alteration assemblage after clinopyroxene (CPX) and plagioclase (PLAG), clinopyroxene is replaced by amphibole (AMPH) which is in turn replaced by chlorite (CHL), calcite (CAL) occurs at the margin between plagioclase and chlorite; e.) Transmitted, cross-polarized light image of chalcopyrite (CP) disrupting optically continuous clinopyroxene (CPX), optically continuous fragments are indicated by white boxes; f.) reflected light image of e; g) reflected light image of an intergrowth of chalcopyrite and amphibole (AMPH) and apatite (AP) note that chalcopyrite replaces amphibole along cleavage planes; h) transmitted, cross-polarized light image of h.

Figure 4. Paragenetic Sequence, discontinuous lines indicate uncertainties in the order of crystallization.

Figure 5. Modeled Pb isotope ratios according to the two stage model of Stacey and Kramers (1975) where μ is the present day $^{238}\text{U}/^{204}\text{Pb}$ ratio and κ is the present day $^{232}\text{Th}/^{204}\text{Pb}$ ratio; a.) $\kappa = 2.4$ b.) $\kappa = 2.4$ $\kappa = 4.2$. Note that increasing κ results in steeper growth curves for $^{208}\text{Pb}/^{207}\text{Pb}$ relative to $^{206}\text{Pb}/^{207}\text{Pb}$

Figure 6. Plot showing the Pb isotope ratios measured by multiple traverses on multiple grains of plagioclase from sample G10-2. Inner error bars represent 1σ based on theoretical counting statistics and the outer error bars are the observed 1σ errors based on the standard deviation of the mean of "n" measurements or for $n=1$ the standard deviation of the mean of the ratios (~180-200) obtained from a single traverse. Note the close approximation of the theoretical to observed error.

Figure 7. Plot of Pb isotope ratio results. Open diamonds are plagioclase from the Marathon deposit, closed diamonds are sulphides from the Marathon deposit, open diamonds are K-feldspars from the Coldwell complex (Bell, 1989), closed squares are sulphides from the Duluth complex and open squares are plagioclase from the Duluth complex (Ripley et al. 1999). Dashed lines are growth curves at various μ values and a κ of 3.88. S/K BSE is the modeled composition of the bulk silicate earth based on the two stage model of Stacy and Kramers (1975). Stars represent idealized compositions of different reservoirs at 1.1 Ga; EM = e enriched mantle, AUC = Archean upper crust, ALC = Archean lower crust, and DM = depleted mantle (Zartman and Haines, 1988, Bell, 1989, Nicholson and Shirey, 1990).

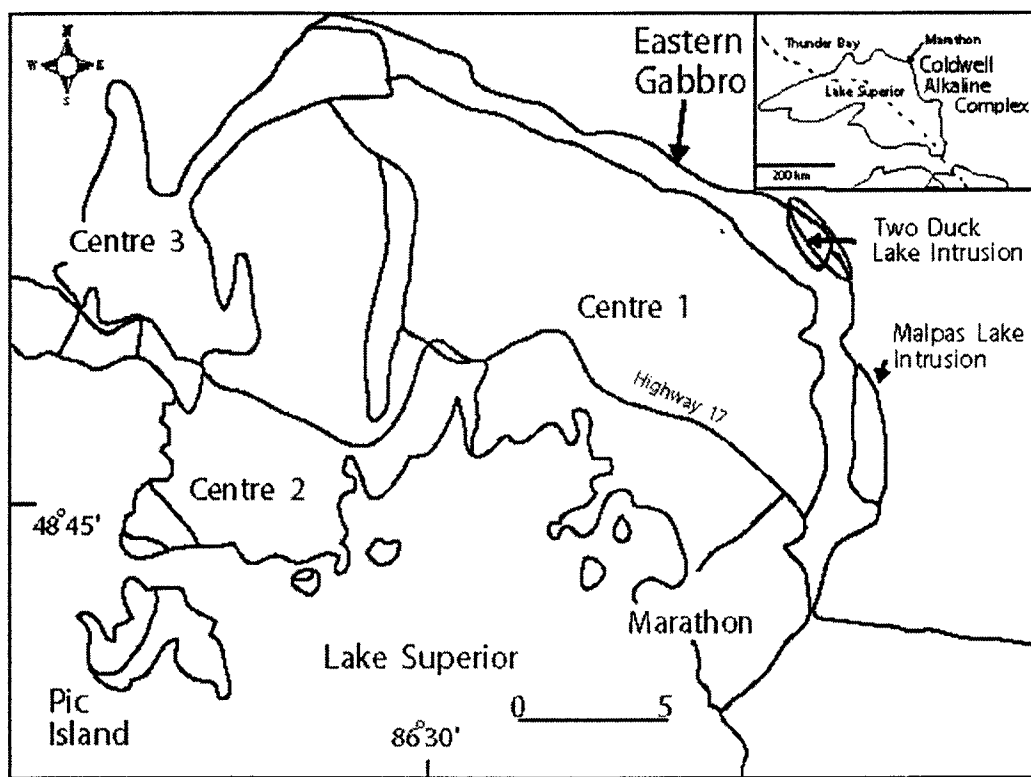


Figure 1.

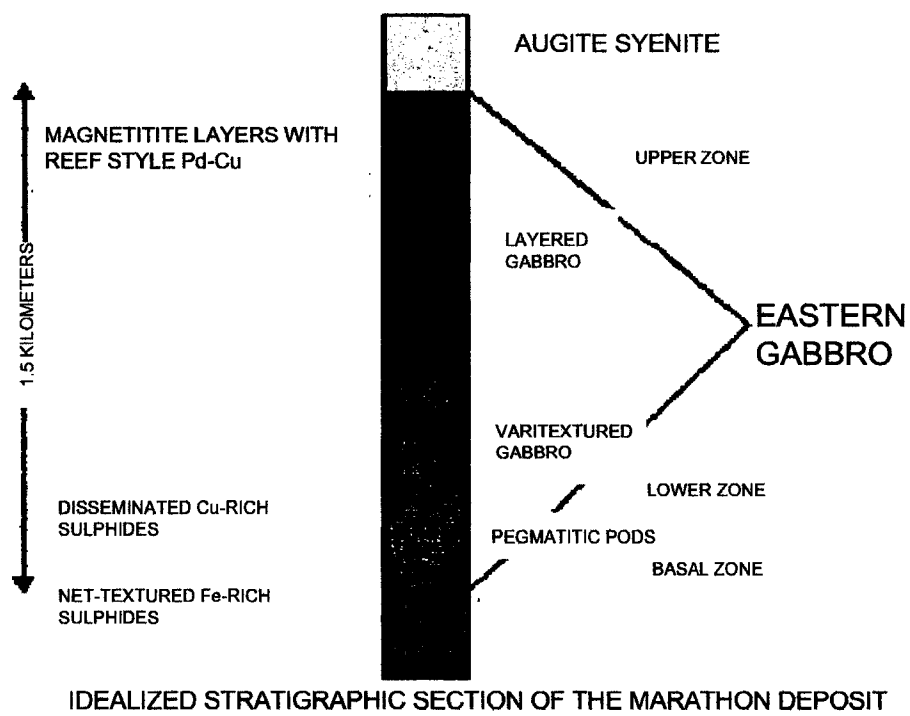


Figure 2.

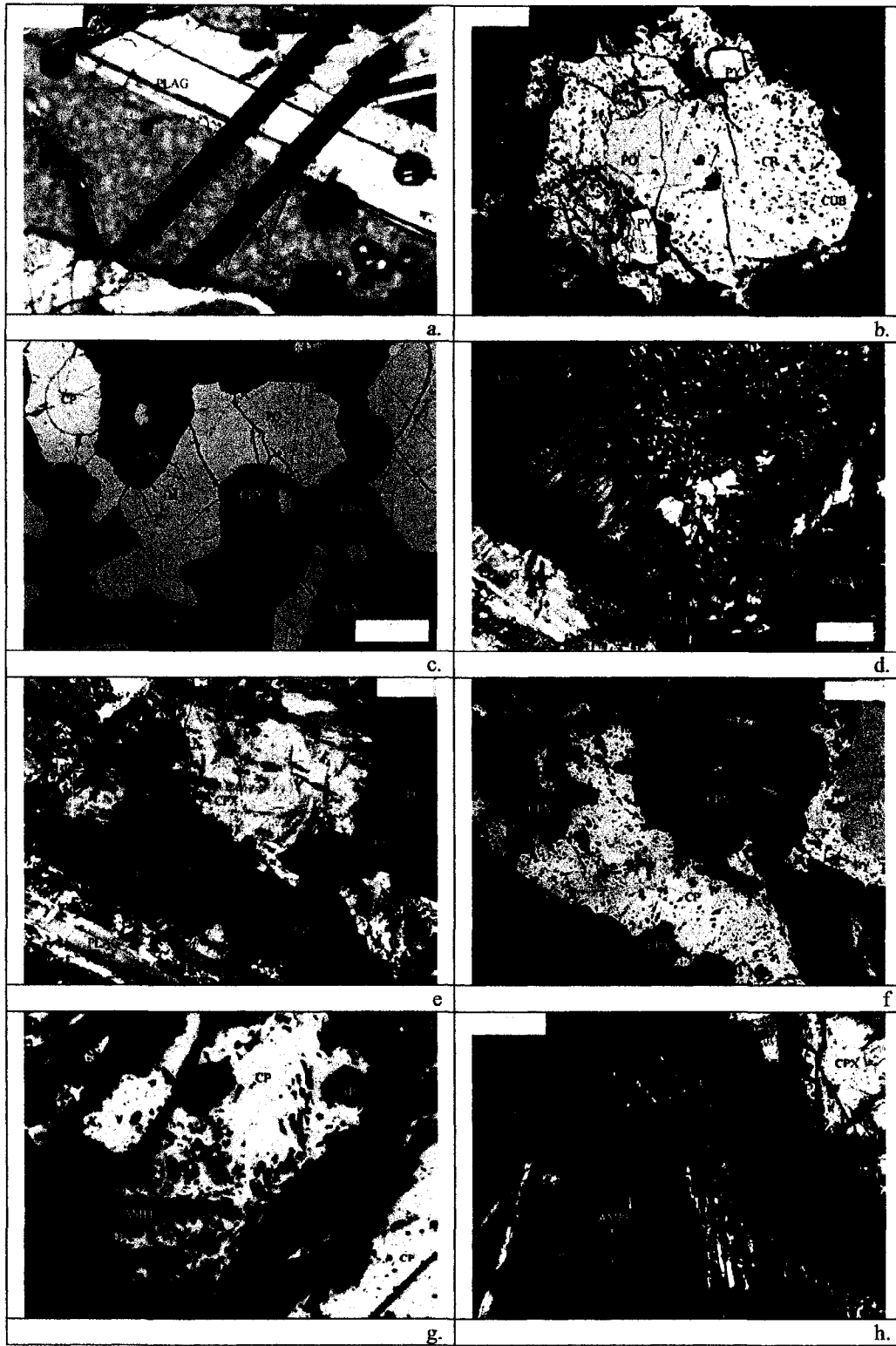


Figure 3.

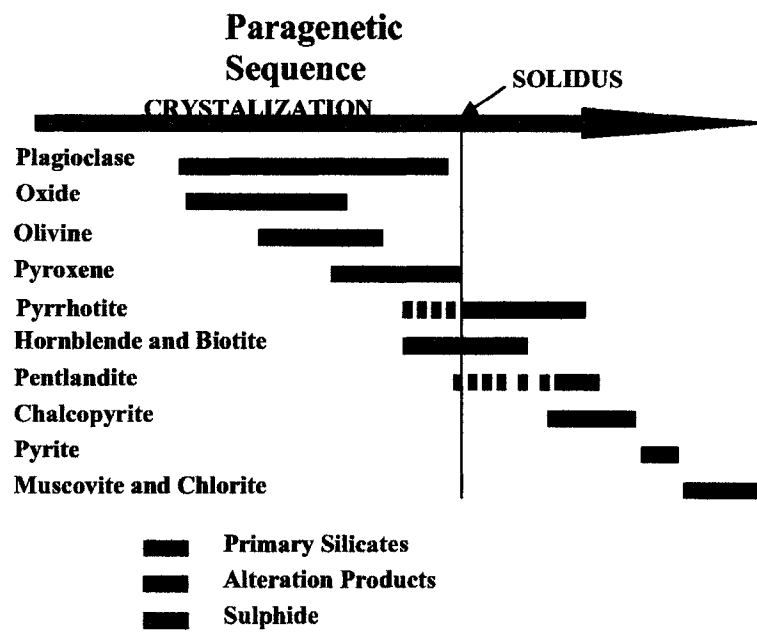


Figure 4.

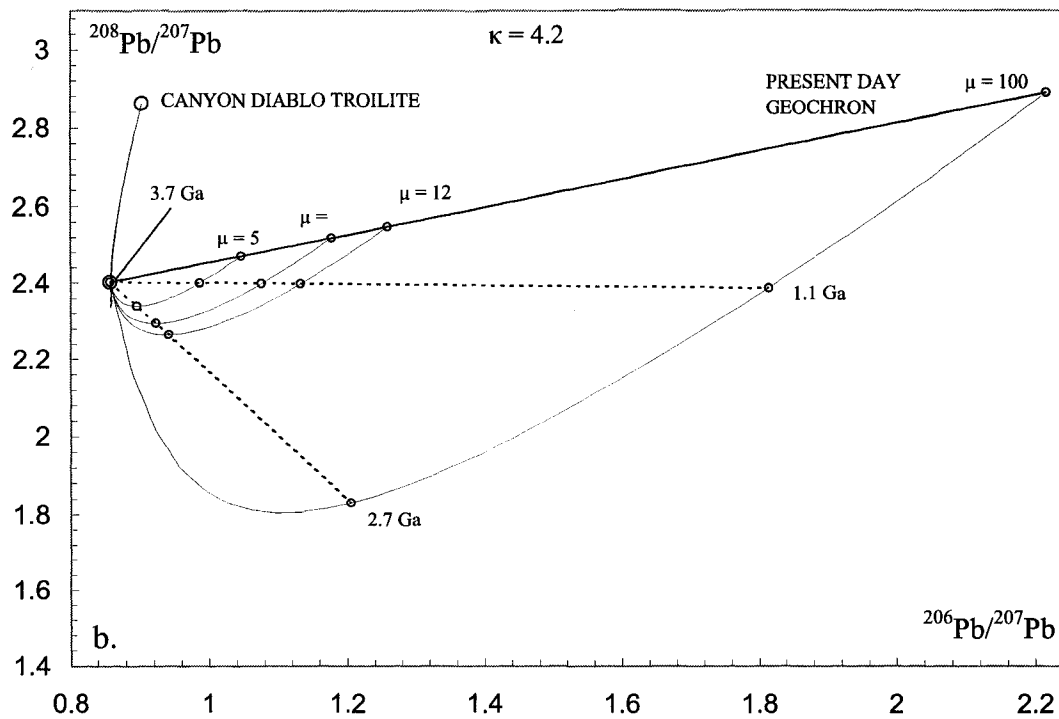
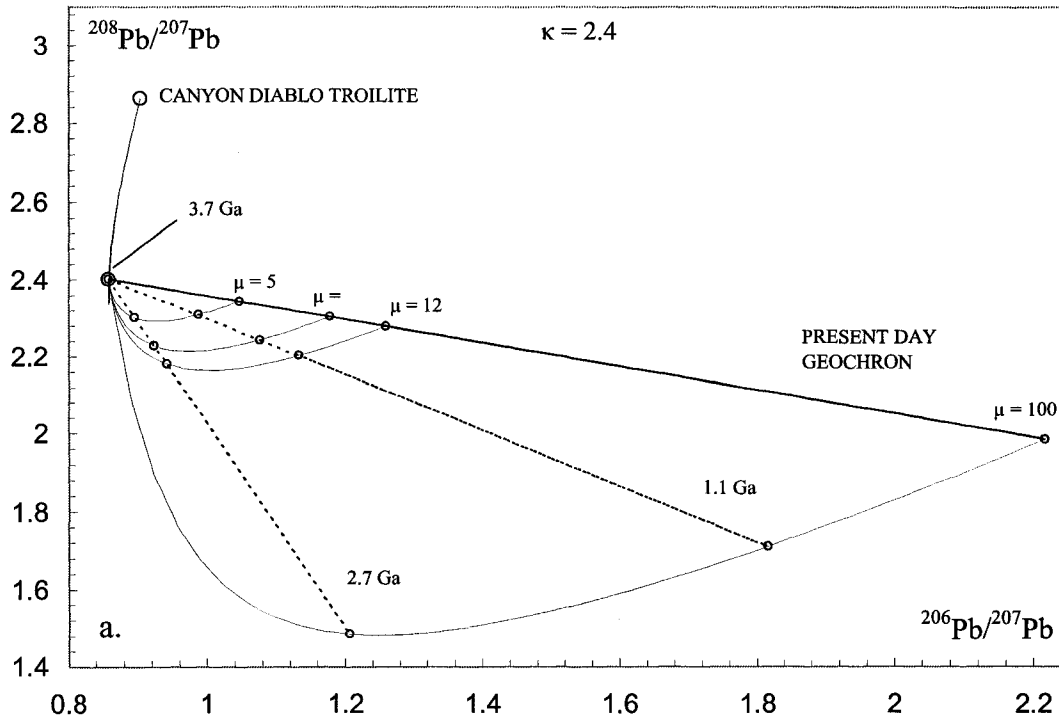


Figure 5.

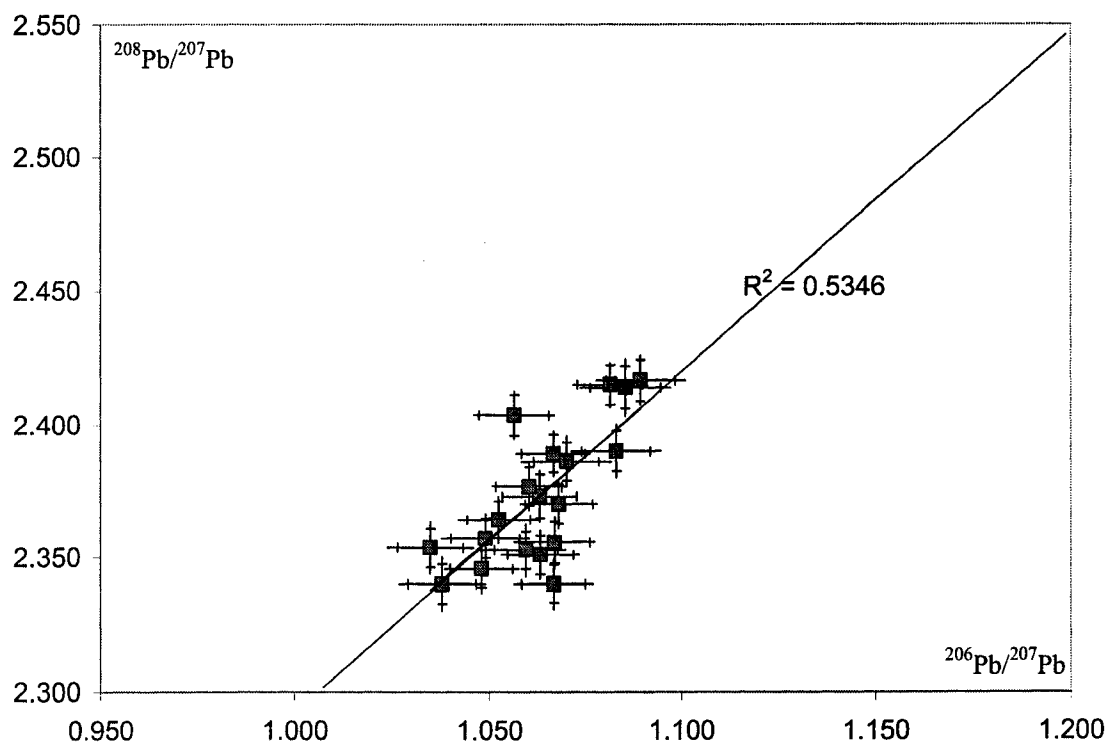


Figure 6.

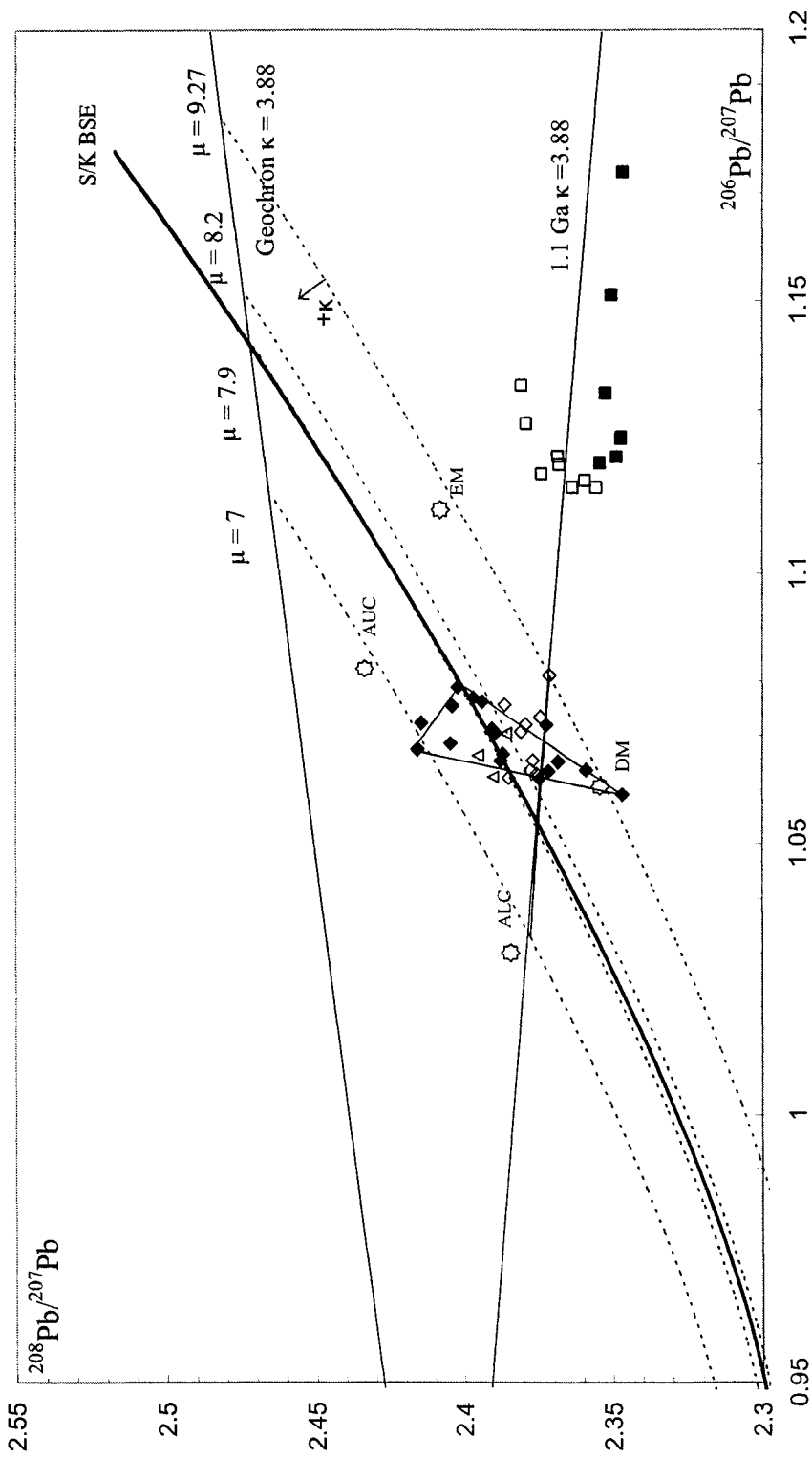


Figure 7.

CHAPTER 4

Preliminary investigation of Platinum-Group Element and trace element distribution and fractionation in the Marathon PGE-Cu deposit:

4.1 Introduction

The ubiquitous fractionation of the PGE in PGE ore deposits is one of the most difficult features to explain with classical magmatic models (Campbell et al. 1983). Due to the very high partition coefficients of all six PGE and Au from a silicate melt into a magmatic sulphide liquid ($D^{\text{sul/sil}}$ range from $\sim 10^3$ - 10^4 Fleet et al. 1999 to $>10^7$ Andrews and Brenan 2002), the segregation and mixing of an immiscible sulphide liquid would scavenge all of the noble metals from the silicate melt equally (*sensu lato*). As a result, more complex magmatic models involving magma mixing, sulphide fractional crystallization, and PGE partitioning into oxide and silicate phases have been proposed to account for the fractionation of the noble metals in PGE deposits (cf. Naldrett 1989). Alternatively, metal fractionation has been attributed to processes involving the interaction of the noble metals with volatile fluids and the variable complexation of the metals in these fluids under both magmatic and sub-solidus conditions (Farrow and Watkinson 1992, Boudreau and Meurer 1999).

Several opposing models have been proposed to describe the enrichment of Cu and PGE, and the accompanying precious metal fractionation, in the Marathon PGE-Cu deposit, Ontario (Watkinson and Ohnenstetter 1992, Good and Crocket 1994, Barrie et al. 2002). Watkinson and Ohnenstetter (1992) proposed a sub-solidus hydrothermal model and noted that the PGE-enriched sulphide assemblages in the Marathon deposit occurred in the most Cu-rich rocks, where the platinum group minerals (PGM) are associated with pyrrhotite-poor assemblages of chalcopyrite, cubanite and pyrite. Importantly, Watkinson and Ohnenstetter (1992) noted that, although the majority of the rocks in the deposit are relatively unaltered, the PGE and Cu-rich rocks are coarse-grained and are partly altered to an assemblage of hydrous minerals. The PGM observed by Watkinson and Ohnenstetter (1992) were often spatially related to galena (PbS) and altaite (PbTe). The common occurrence of Pb bearing minerals with PGM led Watkinson and Ohnenstetter (1992) to postulate that PGE enrichment was related to the interaction of magmatic minerals with an exotic fluid, containing Pb, partially derived from the Archean country rock. Watkinson and Ohnenstetter (1992) argued

that PGE- and Cu-rich sulfide assemblages are uncharacteristic of classical magmatic assemblages. They noted similarities, including the replacement of pyrrhotite and magnetite by the PGE and Cu-rich assemblages, to other Cu-rich sulfide deposits such as the New Rambler mine (McCallum, 1979), the Salt-Chuck deposit (Watkinson and Melling, 1992) and the Messina mine (Mihálik et al. 1974) that have been attributed to hydrothermal enrichment.

In contrast, Good and Crocket (1994) proposed a modified version of the classical magmatic model (cf. Campbell et al. 1983) for the Marathon deposit. Good and Crocket (1994) argued that the significant correlation between whole-rock sulphur and chalcophile element concentrations is inconsistent with hydrothermal processes. Furthermore, Good and Crocket (1994) suggested, based on thermodynamic considerations, that the coherent behavior of Ni and Ir is inconsistent with hydrothermal transport. They also noted that the good preservation of primary minerals is inconsistent with the interaction of the enriched rocks with a sufficiently large volume of fluid to transport the PGE under reducing conditions at 25-300°C. Based on these observations, Good and Crocket (1994) proposed that the progressive contamination of a deep-seated magma chamber by the surrounding country rock, caused sulphur saturation and the formation of immiscible sulphide liquid droplets that scavenged the PGE from the silicate melt. Turbulent mixing occurred during injection of the sulphide-droplet bearing plagioclase crystal mush into the current upper crustal position of the deposit. Good and Crocket (1994) argue that sub-solidus reactions with deuteritic fluids, which caused only the local migration of elements, account for the replacement textures and deposition of PGM in association with hydrous silicates. Importantly, Good and Crocket (1994) found no geochemical evidence for fluid migration beyond the hand sample scale.

Recently, Barrie et al. (2002) proposed that the concentration of PGE in assemblages of Cu-rich disseminated sulphides is due to fluid fluxing and constitutional zone refining. Barrie et al. (2002) suggested that a model involving the addition of sulphur by volatile fluxing and subsequent zone refining processes can account for the spatial distribution of chalcophile elements and sulphur, including their association with coarse-grained to pegmatitic textures. Barrie et al. (2002) suggest that the spatial association of the deposit with felsic metavolcanic country rocks is due to the low temperature melting points and relatively high volatile element and sulphur contents of these rocks. This makes the felsic metavolcanic

country rocks more conducive to deposit formation by volatile fluxing and zone refining than the granitic and mafic country rocks adjacent to non-mineralized gabbros. Although the fluid fluxing and zone refining mechanism is not described in detail by Barrie et al. (2002) a similar mechanism has been proposed by Brüggmann et al. (1989) to explain the PGE distribution in the Lac des Illes deposit.

In this study the noble metal abundances and distribution patterns of chalcophile elements have been used to test these models, based on the current understanding of the behavior of PGE in ore forming processes. Precious metal (Ru, Rh, Pd, Ir, Pt, and Au) concentrations have been determined in 17 rock samples that are representative of the various lithologies present in the Marathon deposit. This data set contains the first determination of Ru, an element important for using precious metals profiles to infer geological processes (e.g. Andrews and Brenan 2002, and references therein), in these rocks. This 17-sample data set has been supplemented by an extensive exploration geochemical database consisting of chalcophile element analyses for in excess of 1000 drill core samples.

4.2 Geological Setting

The Marathon deposit is hosted by the 1108 ± 1 Ma (U-Pb) (Heaman and Machado, 1992) Coldwell intrusive complex. The Coldwell magmas were emplaced into the Archean rocks of the Abitibi and Wawa sub-provinces, where continental rifting provided crustal dilation and associated structural features. The structural geology of the region has been described by Sage (1991), who determined that the emplacement of the mid-continent rift intrusive complexes occurred at inflections of major structural zones and sites of cross faulting. The intrusion of the Coldwell magmas was contemporaneous with the extrusion of voluminous amounts of Keweenaw, rift-related tholeiitic and transitional, tholeiitic-alkaline basalt (Sutcliffe 1991). The Keweenaw intrusive rocks and their associated economic deposits were described by Smith et al. (1987). The Geology of the Coldwell complex was most recently described in the study of Walker et al. (1993), which supported previous work, and subdivided the complex into three intrusive centers (Fig. 1). Center 1, the earliest intrusion, is composed of a gabbroic unit, the Eastern Gabbro, and ferroaugite syenite. This

was followed by the intrusion of the center 2 nepheline syenite magmas. Center 3, the youngest unit, is dominantly quartz-amphibole syenite.

4.3 Deposit Petrology and Mineralization

The Marathon deposit is hosted by the Two Duck Lake gabbro (TDL), a small intrusive phase of the Eastern Gabbro which has recently been described by Shaw (1997). The main intrusive phase of the Eastern Gabbro is the layered gabbro which constitutes 90% of the unit (Shaw, 1997). The layered gabbro is comprised of gabbro, olivine gabbro, troctolite, and anorthositic gabbro. The Eastern Gabbro contains two smaller units, the Two Duck Lake intrusion (TDL) and the Malpas Lake intrusion. The Malpas lake unit intrudes the layered gabbro, constitutes 5% of the Eastern Gabbro, and is comprised of amphibole-bearing olivine gabbro (Shaw 1997). The TDL intrusion constitutes 3% of the Eastern Gabbro and intrudes the Layered Gabbro at the contact with the meta-volcanic and meta-sedimentary Archean country rocks. This contact trends north-northeast and dips moderately to the west. The TDL intrusion is comprised of gabbro-norite, olivine gabbro-norite, olivine gabbro, and leucogabbro (Shaw 1997). Although the existence of a distinct TDL intrusive unit has been contested by Barrie et al. (2002) there is field evidence, including cross-cutting relationships and zones of igneous brecciation, that support a distinct intrusive phase.

The gabbroic rocks of the Marathon deposit have been subdivided into zones based on lithology and textural features (Good 1993, Barrie et al. 2002, Dahl et al. 2003). Although, the study of Barrie et al. has not considered the TDL unit as a separate intrusive phase the three-zone classification proposed in that work is most consistent with the observations of drill core and field relationships made in this study. Thus, a slightly modified zonal classification is presented here. The Basal Zone is characterized by massive, fine-grained, altered gabbro hosting abundant meta-volcanic xenoliths and containing variable amounts of Fe-rich massive to net-textured sulphides. The Basal Zone also contains sporadic, irregular pods of granophyre. The Lower Zone exhibits locally-developed cumulate layering defined by gradational changes in mineral abundance, irregular pegmatitic zones, and varies compositionally from biotite-hornblende gabbro to gabbroic anorthosite. The Lower Zone is host to the bulk of the PGE and Cu mineralization, which occurs in variably-textured,

commonly pegmatitic, hornblende gabbro that contains Cu-rich disseminated sulphide. The Cu-rich sulphide assemblages disrupt optically continuous pyroxenes and replace hornblende along cleavage planes (Crowe et al Chapter 3). The Lower Zone is broadly equivalent to the Lower zone of Good (1993) and the heterogeneous gabbro of Wilkinson (1983). Mineralized zones are located several tens of meters stratigraphically above the Basal Zone sulphide-rich rocks and often occur near the transition to the Upper Zone. The Upper Zone consists of olivine gabbro with well-developed rhythmic layering defined by changes in mineral morphology, grain size and modal abundance. Although PGE mineralization is dominantly contained by the Lower Zone the Upper Zone is host to laterally continuous Pd-Cu-bearing reef-type magnetite layers. A thin unit of leucogabbro has intruded between the contact of the TDL intrusion and the country rock (Good 1993). The TDL and Eastern Gabbro are cut by vertically dipping quartz syenite dikes that are approximately parallel to the TDL intrusive contact. The TDL intrudes the Eastern Gabbro at the contact with country rocks which trends north to northeast and dips moderately to the west. The TDL varies compositionally from olivine gabbro to gabbroic anorthosite

4.4 Experimental

4.4.1 Sampling

Rock samples were collected from drill core and unweathered field outcrops exposed by recent exploration activity. These samples were crushed and pulverized to -200 mesh by ALS Chemex. Sampling was conducted to obtain a suite of rocks representative of the various lithologies present in the deposit with emphasis on acquiring multiple mineralized samples with characteristic textures (i.e. massive to net-textured vs. disseminated sulphides).

4.4.2 Whole Rock PGE determination

The PGE including Ru, Rh, Pd, Ir, and Pt have been determined by ICP-MS after pre-concentration by nickel sulphide (NiS) fire assay (FA) and separation from base metals using a strongly acidic cation exchange resin. This technique is a slightly modified version of that described by Chen et al. (1996). Concentrated hydrochloric and nitric acids (American Chemical Society (ACS) standard reagent grade) were used as supplied. When required, these acids were diluted with ultra-pure (UP) milli-Q water. The ion exchange resin used,

DOWEX[®] 50WX8-200, was purchased from the Sigma[®] Chemical company. Both Ni (100 mesh, 99.99%) and S (100 mesh, sublimed) were purchased from the Aldrich[®] chemical company.

The NiS fire assay was performed as described in Jackson et al. (1990) except that a fusion temperature of 1100°C was used, and the fusion charge was for a nominal sample size of 15g. NiS buttons were weighed and crushed (1-5 mm fragments) in a stainless steel mortar and pestle. Between samples, the mortar and pestle were cleaned with SiO₂ powder and rinsed with ethyl alcohol. After crushing, 20 mg sub-samples were powdered in an agate mortar, which was cleaned twice between samples with SiO₂ powder and rinsed with ethyl alcohol. The 20 mg samples were dissolved at 100°C using 2 ml of concentrated (3:1) *aqua regia* in acid washed (15% *aqua regia*) Teflon[®] PTFE[®] beakers. Once dissolved, the solution was evaporated to dryness and reconstituted at room temperature in 1 M HCl. This solution was transferred directly to the ion-exchange column. Prior to use, the cation exchange resin was conditioned (transformed to chloride form) by soaking in 6 M HCl for 1 week. Subsequently, 3 ml of the resin slurry was added to acid washed (15% *aqua regia*) borosilicate columns and rinsed with 20 ml of 6 M HCl and 15 ml of 1 M HCl. The PGEs were eluted from the column with 17 ml of 1 M HCl. The eluate was collected in plastic vials containing 5 ml of a three element (Be, In, Tl) internal standard in 1% HNO₃ and analyzed directly on a Thermo Elemental X7 ICP-MS. Analytical ions and corrected interferences are presented in table 1. This preliminary data set has been supplemented by extensive exploration geochemical analyses by ALS Chemex. The Chemex exploration package (MEMS41) uses *aqua regia digestion* with determination using ICP-AES and ICP-MS. This data set includes the analysis of several chalcophile elements including Cu, Ni, Co, Pb, S, Sb, and As.

4.4.3 Mineral Pb Chemistry

The relative abundances of Pb have been determined in “co-existing” chalcopyrite-pyrrotite mineral grains in different textural settings by LA-ICP-MS. The sulphide Pb concentrations have been approximated by normalizing to the sensitivity obtained on an analysis of NIST 612 glass (38.96 ppm Pb, Pearce et al. 1997). Although there is a considerable difference in the ablation characteristics between sulphide minerals and the

glass standards, which results in a matrix-dependent response factor (Fryer et al. 1995), the data obtained in this way are useful for comparing the relative abundances of Pb between sulphides in different textural settings.

4.5 Results

4.5.1 Evaluation of the Ion exchange method

Preliminary investigations attempted to reproduce the method of Chen et al. (1996) using the DOWEX[®] 50WX8-200 cation exchange resin instead of the Amberlite CG-120 resin used by Chen et al. (1996). It was found that applying the procedure of Chen et al. (1996), which used 18 g of 0.1 M HCl eluent, that the recoveries of some precious metals were consistently low (Figure 2). Elution experiments were performed to select the appropriate strength and volume of HCl required to obtain better recoveries for standard solutions (Figure 3). It was found that 20 ml of 1.0 M HCl resulted in 100% recovery of all precious metals except Au. However, base metals, which cause severe polyatomic interferences during ICP-MS determination (Table 1), began to elute at 18 ml and so 16 ml eluent, which resulted in greater than 90% recovery for all metals, was selected.

The quality of data obtained by the NiS FA cation ion exchange method was evaluated by analyzing two certified standard reference materials (CRMs), namely WMG 1 and SARM 7 (Table 1). WMG 1 is a powdered sample of sulphide bearing gabbro from the Wellgreen intrusion and is likely fairly close in composition to many of the Marathon deposit samples. SARM 7 is a PGE bearing ultra-mafic rock powder from the Bushveld complex. Recoveries, calculated by dividing the mean measured concentration by the certified concentration, are in excess of 80 % for all elements except Au. These recoveries are well within the $\pm 25\%$ uncertainty, due to sample heterogeneity, commonly accepted for the analysis of the PGE in rock samples. The low recovery of Au can be attributed to poor collection by the NiS liquid during the FA pre-concentration and heterogeneous distribution in the resultant NiS button (Chen et al. 1996). The solid limits of detection (SLD), calculated as 3 times the standard deviation of four replicate blanks, are all below 2 ppb except for Au.

One problem found during the analysis of the PGE by ICP-MS is that the pure element standards (nominally 10 ppb), prepared from a 1 ppm stock standard solution (SPEX), are unstable. This problem is currently being investigated, however, as the instability

of these standards can result in erroneous results, all precious metals analyses have been normalized to a certified standard reference material (WGM 1).

4.5.2 Precious Metals content of Marathon Samples

The concentrations of precious metals in 17 samples of gabbroic rock from the Marathon deposit are presented in table 3. With the exception of one sample of pegmatitic gabbro and the samples of felsic meta-volcanic rocks, all Marathon samples contain PGE above the method detection limits. For the gabbroic samples, Pt and Pd concentrations determined in this study are within 25% of those determined by *aqua regia* digestion (ALS Chemex, data not shown). Table 2 also contains the concentrations of chalcophile elements determined by *aqua regia* digestion by ALS Chemex.

The concentration of Ru varies from 2.39 ppb in pegmatitic gabbro to 24.9 ppb in basal zone massive to net-textured sulphide samples. Sulphide-free rocks contain approximately 11 ppb Ru and Lower Zone Cu-rich disseminated sulphide-bearing rocks contain approximately 13 ppb Ru. In comparison, the Basal Zone Fe-rich massive to net-textured sulphide-bearing rocks contain 24.9 ppb Ru. The enrichment of Ru in Basal Zone Fe-rich massive to net-textured sulphides, relative to Lower Zone Cu-rich disseminated sulphides, is exactly opposite to the distribution of Pt and Pd which are enriched in the Cu-rich disseminated sulphides relative to the massive to net-textured sulphides. Although more variable than Ru, Ir and Rh exhibit similar behavior and are enriched in Basal Zone Fe-rich samples relative to Lower Zone Cu-rich samples.

4.5.3 Pb distribution in Marathon Sulphides

The Pb distribution in coexisting sulphides is shown in table 4. Clearly, Basal Zone Fe-rich sulphides have lower Pb concentrations than the Lower Zone Cu-rich, disseminated sulphides. Furthermore, Lower Zone chalcopyrite is enriched in Pb relative to pyrrhotite ($D^{CP/PO} \sim 8-10$) in comparison to the Basal Zone chalcopyrite ($D^{CP/PO} \sim 2$). Interestingly, the enrichment of Pb in chalcopyrite generally correlates well with the increase in whole rock Pd and Pt concentrations.

4.6 Discussion

4.6.1 Determination of the PGE using the NiS FA, cation exchange ICP-MS technique

Aside from the inaccuracy of the ICP-MS determination due to problems with the pure element standards, the NiS FA, cation exchange separation method yields suitably low detection limits for the precious metals (excluding Au and Os) analysis of the intrusive lithologies of the Marathon deposit. The method is particularly appealing because it uses small volumes of reagents, is relatively rapid, and even using small (20 mg) sub-samples of the NiS bead is very reproducible (<5 % RSD) which is comparable to the 4-14% observed in methods using the entire NiS button (Jackson et al. 1990). The low volumes of acid reagents required could facilitate the use of expensive ultra-pure reagents (e.g. Seastar[®]) when ultra-trace level measurements are required (e.g. depleted rocks in ore deposits or the analysis of MORBs). Furthermore, as the method uses only small sub-samples of the original bead, the remaining NiS chips can be easily stored for future reference. This could be particularly attractive for exploration programs, as an alternative to storing bulk rock powders, when preserving samples for future reference is important.

4.6.2 Precious metals content of Marathon Deposit

Mantle-normalized plots of the precious metals profiles are presented in Figure 3. Based on the mantle-normalized PGE patterns, the rocks of the Marathon deposit can be classified into four groups. Non-mineralized samples have mantle-normalized values of between 0.1 and 5 for all precious metals and have relatively flat metal patterns. Pegmatitic samples are enriched in Pt, Pd, Au and Cu relative to primitive mantle (PM), are depleted in Ni and Ir relative to PM and have approximately equivalent Ru and Rh concentrations to PM. Relative to PM, massive to net-textured Fe-rich sulphide bearing rocks are enriched in Ru, Rh, Pt, Pd, Au, and Cu, are depleted in Ni, and have approximately equivalent Ir concentrations to PM. Lower Zone Cu-rich, disseminated sulphide bearing rocks are highly enriched in Rh, Pt, Pd, Au, and Cu, relative to PM. A comparison of the metal concentrations of the Lower Zone Cu-rich samples to the Basal Zone Fe-rich samples shows a relative enrichment of Pt, Pd, Au, and Cu, and a relative depletion in Ni, Ir, Ru, and Rh in Lower Zone rocks.

This data is broadly consistent with metal fractionation due to the fractional crystallization of a magmatic sulphide liquid as described by Barnes et al. (1997). Barnes et al. proposed that the fractional crystallization of a magmatic sulphide liquid could produce Fe-rich cumulate rocks that are enriched in Os, Ir, Ru, and Rh relative to the initial sulphide liquid. The crystallization of monosulphide solid solution (mss) to form the Fe-rich cumulate results in the formation of a Cu-rich residual liquid enriched in Cu, Pt, Pd, and Au. The spatial separation of this Cu-rich residual melt from the Fe-rich cumulate has the potential to produce zoned sulphide deposits (i.e. an Fe-rich Zone and a Cu-rich Zone) such as the Basal and Lower Zones of the Marathon deposit.

Good and Crocket (1994) have suggested that the metal fractionation observed in the Marathon deposit is due to the formation of compositionally different sulphides from the progressive addition of S to a magma chamber undergoing fractional crystallization. Good and Crocket (1994) have suggested that the fractional crystallization of olivine, pyroxene and spinel, which incorporated PGE, resulted in the formation of a stratified magma chamber and that the segregation of sulphide droplets with variable metal (PGE) concentrations depended on the amount of olivine, pyroxene and spinel that had crystallized at the time of liquation. This is consistent with the recent experimental work of Andrews and Brenan (2002) who have found that Ru (and by inference Ir and Os) can be sequestered by spinel phases that crystallize prior to sulfide liquation. The role of olivine and pyroxene in sequestering PGE remains uncertain. Good and Crocket (1994) have dismissed the fractional crystallization of mss as a mechanism to produce the observed metal fractionation as it was inconsistent with the experimental work of Fleet and Stone (1991). Fleet and Stone (1991) found that both Ir and Ni were preferentially partitioned into the residual sulphide liquid during mss crystallization. Thus, Good and Crocket suggested that sulphide liquid fractional crystallization could not account for the observed metal fractionation in the Marathon deposit. However, as described above, the more recent experimental data of Barnes et al. (1997) found that under geologically reasonable conditions Ir is compatible in mss. Thus, based on current experimental data, the observed metal fractionation is consistent with the segregation of mss from a sulphide liquid.

However, the simple fractional crystallization of a sulphide liquid cannot produce compositionally zoned sulphide deposits. The formation of compositionally different zones

requires the subsequent segregation of the residual sulphide liquid from the crystallized mass. Although experimental studies have demonstrated the mobility of a sulphide liquid under late magmatic conditions, this mobility has been restricted to high temperature environments (Rose and Brennan, 2001) and would certainly not apply under sub-solidus (i.e. below ~900°C) conditions. This is difficult to reconcile with the textural observations of Crowe et al. (Chapter 3), which strongly suggest that the Cu-rich sulphide-mineralizing event occurred under sub-solidus conditions.

Given that Pb is enriched in Lower Zone Cu-rich sulphides compared to the Basal Zone Fe-rich sulphides, and that this correlates with the PGE content of the rocks, it is reasonable to suspect that the process responsible for the enrichment of Pd, Pt and Cu in the Lower Zone rocks also enriched these rocks in other chalcophile elements. Based on the fact that the distribution of Pb between coexisting chalcopyrite and pyrrhotite is different between the two zones suggests that these sulphide assemblages crystallized under different conditions. In conjunction with the textural relationships, which suggest that chalcopyrite in Lower Zone samples is replacing pyrrhotite, the difference in Pb distribution between chalcopyrite and pyrrhotite is strong evidence for disequilibrium conditions.

4.7 Summary

This preliminary work has shown that the NiS FA, cation-exchange separation ICP-MS technique is well-suited to the determination of the whole rock precious metal concentrations of mineralized and non-mineralized samples in the Marathon deposit. The current standardization problems can likely be resolved by preparing the standard solutions in more different (more concentrated) acid reagents and by preparing them immediately prior to analysis. The preliminary precious metal concentrations determined for the Marathon rock samples are broadly consistent with the fractional crystallization of a magmatic sulphide liquid however, this is difficult to reconcile with the textural observations of Crowe et al. (Chapter 3) which suggest Lower Zone mineralization event occurred under sub-solidus conditions. The trace element (Pb) enrichment of the Lower Zone sulphides, in comparison to Basal Zone sulphides, is generally consistent with both the fluid fluxing and zone-refining model of Barrie et al. (2002) and the hydrothermal model of Watkinson and Ohnenstetter

(1992). However, again, the textural observations of Crowe et al. (Chapter 3) are more consistent with the sub-solidus hydrothermal model. More data are required to rigorously evaluate these models and to characterize the relationship between PGE enrichment and fractionation and the behavior and distribution of other trace elements. Most importantly, a more complete whole rock PGE data set, that is representative of a complete stratigraphic section through the deposit (work in progress), is required to identify the possible chromatographic separation of elements that would be expected from zone-refining processes. In addition, the distribution of elements, for example In and Se, which are likely not easily fractionated by crystal chemical effects, will be key in identifying trace-element enrichment of pre-existing sulphides by hydrothermal fluids as described by Watkinson and Ohnenstetter (1992). More specifically, it would be expected that if Lower Zone chalcopyrite and pyrrohtite crystallized from a sulphide melt, these minerals would have approximately the same In or Se concentrations. Furthermore, if the Lower Zone sulphide crystallized from a residual sulphide liquid, derived from mss crystallization and the formation of the Basal Zone Fe-rich sulphides, the In concentrations should be the same in sulphides from both zones. Based on the fact that there is a difference in Pb concentrations between the two zones it is reasonable to expect differences in other trace elements.

4.8 References

- Andrews, D., and Brenan, J.M. (2002) The solubility of ruthenium in sulfide liquid: implications for platinum group mineral stability and sulfide melt-silicate melt partitioning. *Chemical Geology*, **192**, 163-191
- Barrie, C.T., MacTavish, A.D., Walford, P.C., Chataway, R., and Middaugh, R. (2002) Contact-type and Magnetite Reef-type Pd-Cu Mineralization in Ferroan Olivine Gabbros of the Coldwell Complex, Ontario. In *The Geology, Geochemistry, Mineralogy and Mineral Benefication of Platinum-Groups* (ed. L.J. Cabri), pp. 321-337. Canadian Institute of Mining, Metallurgy and Petroleum.
- Barnes, S-J, Makovicky, E., Makovicky, M., Rose-Hansen, J., and Karup-Moller, S. (1997) Partition coefficients for Ni, Cu, Pd, Pt, Rh, and Ir between monosulfide solid solution and sulfide liquid and the formation of compositionally zoned Ni-Cu sulfide bodies by fractional crystallization of sulfide liquid. *Canadian Journal of Earth Sciences*, **34**, 366-374
- Boudreau, A.E., Meurer, W.P., (1999) Chromatographic separation of the platinum-group elements, gold, base metals and sulfur during degassing of a compacting and solidifying igneous crystal pile. *Contributions to Mineralogy and Petrology*, **134**, 174-185
- Brüggemann, G.E., Naldrett, A.J., MacDonald, A.J. (1989) Magma mixing and constitutional zone refining in the Lac des Iles Complex, Ontario: Genesis of platinum-group element mineralization. *Economic Geology*, **84**, 1557-1573
- Crowe, S.A., Samson, I.M., Fryer, B.J. (Chapter 3) Micrometre scale Pb isotope composition of major magmatic phases and alteration products from the Marathon PGE-Cu deposit: Constraints on magmatic hydrothermal evolution (in prep)- for submission to *Geochimica et Cosmochimica Acta*
- Campbell, I.H., Naldrett, A.J., and Barnes, S.J. (1983) A model for the origin of the platinum-rich sulfide horizons in the Bushveld and Stillwater complexes. *Journal of Petrology*, **24**, 133-165
- Chen, Z., Fryer, B.J., Longerich, H.P., and Jackson, S.E. (1996) Determination of Precious Metals in Milligram Samples of Sulfides and Oxides Using Inductively coupled Plasma Mass Spectrometry After Ion Exchange Preconcentration. *Journal of Analytical Atomic Spectrometry*, **11**, 805-809
- Farrow, C.E.G., and Watkinson, D.H. (1992). Alteration and the role of fluid in Ni, Cu and platinum-group element deposit, Sudbury Igneous Complex contact, Onaping-Levack area, Ontario. *Mineralogy and Petrology*, **46**, 67-83
- Fleet, M.E., Crocket, J.H., Liu, M., and Stone, W.E. (1999) Laboratory Partitioning of platinum-group elements (PGE) and gold with application to magmatic sulfide-PGE deposits. *Lithos*, **47**, 127-142
- Fleet, M.E., and Stone, W.E. (1991) Partitioning of platinum-group elements in the Fe Ni-S system and their fractionation in nature. *Geochimica et Cosmochimica Acta*, **55**, 245-253
- Fryer, B.J., Jackson, S.E., and Longerich, H.P. (1995) The design, operation and role of the laser-ablation microprobe coupled with an inductively coupled plasma-mass spectrometer (LAM-ICP-MS) in earth sciences. *Canadian Mineralogist*, 303-312
- Good D.J., and Crocket J.H. (1994) Genesis of the Marathon Cu-platinum-group element deposit, Port Coldwell Alkalic Complex, Ontario: A Midcontinent Rift-related magmatic sulfide deposit. *Economic Geology*, **89**, 131-149
- Heaman, L.M., Machado, N (1992) Timing and origin of mid-continent rift alkaline magmatism, North America: evidence from the Coldwell Complex. *Contributions to Mineralogy and Petrology*, **110**, 289-303

- Jackson, S.E., Fryer, B.J., Gosse, W., Healey, D.C., Longerich, H.P., and Strong, D.F. (1995) Determination of precious metals in geological materials by inductively coupled plasma-mass spectrometry (ICP-MS) with nickel sulphide fire-assay collection and tellurium coprecipitation. *Chemical Geology*, **83**, 119-132
- McCallum, M.E., Loucks, R.R., Carlson, R.R., Cooley, E.F., Doerge, T.A. (1976) Platinum metals associated with hydrothermal copper ores of the New Rambler Mine, Medicine Bow Mountains, Wyoming. *Economic Geology*, **71**, 1429-1450
- Mihálik, P., Hiemstra, S.A., DE Villiers, J.P.R. (1975) Rustenburgite and atokite, two new platinum-group minerals from the Merensky Reef, Bushveld Igneous complex. *Canadian Mineralogist*, **13**, 146-150
- Naldrett, A.J. (1989) Magmatic Sulfide Deposits. Oxford Monographs on Geology and Geophysics No 14. Clarendon Press, New York, 186 pp.
- Oguri, K., Shimoda, G., Tatsumi Y. (1999) Quantitative determination of gold and the platinum group elements in geological samples using improved NiS fire-assay and tellurium coprecipitation with inductively coupled plasma mass spectrometry (ICP-MS). *Chemical Geology*, **157**, 189-197
- Rose, L., and Brenan, J.M. (2001) Wetting properties of Fe-Ni-Co-Cu-O-S melts against olivine: Implications for sulfide melt mobility. *Economic Geology*, **96**, 145-157
- Sage, R.P. (1991) Alkalic rock, carbonatite and kimberlite complexes of Ontario, Superior Province. In *Geology of Ontario*. (Ed. Thurston, P.C., Williams, H.R., Sutcliffe, R.H., and Scott, G.M.), pp. 683-709. Ontario Geological Survey
- Smith, A.R., and Sutcliffe, R.H. (1987) Keweenawan intrusive rocks of the Thunder Bay area: *Ontario Geological Miscellaneous Paper*, **137**, 248-255
- Sutcliffe, R.H. (1991) Proterozoic geology of the Lake Superior area. *Ontario Geological Survey Special Volume 4*, 627-255
- Walker, E.C., Sutcliffe, R.H., Shaw, C.S.J., and Shore, G.T. (1991) Geology of the Coldwell alkaline complex. *Ontario Geological Survey Miscellaneous Paper*, **157**, 107-116
- Watkinson, D.H., and Melling, D.R. (1992) Hydrothermal origin of platinum-group mineralization in low-temperature copper sulfide-rich assemblages, Salk Chuck intrusion, Alaska. *Economic Geology*, **87**, 175-184
- Watkinson, D.H., and Ohnenstetter, D. (1992) Hydrothermal Origin of platinum-group mineralization in the Two Duck Lake Intrusion, Coldwell Complex, northwestern Ontario. *Canadian Mineralogist*, **30**, 121-136

4.9 Tables

Table 1. Analytical ions and corrected interferences

Analytical Ion	Dwell time (ms)	Isotopic Abundance	Corrected Interference
$^{61}\text{Ni}^+$	10	1.16	
$^{65}\text{Cu}^+$	10	30.9	
$^{99}\text{Ru}^+$	10	12.7	
$^{101}\text{Ru}^+$	10	17.1	$^{61}\text{Ni}^{40}\text{Ar}$, $^{64}\text{Ni}^{37}\text{Cl}$
$^{103}\text{Rh}^+$	10	100	$^{63}\text{Cu}^{40}\text{Ar}$
$^{105}\text{Pd}^+$	10	22.2	$^{65}\text{Cu}^{40}\text{Ar}$
^{106}Pd	10	27.3	
$^{107}\text{Ag}^+$	10	51.8	
$^{115}\text{In}^+$	10	95.7	
$^{193}\text{Ir}^+$	10	62.6	
$^{194}\text{Pt}^+$	10	32.9	
$^{195}\text{Pt}^+$	10	33.8	
$^{205}\text{Tl}^+$	10	70.5	

Table 2. Analysis of certified standard reference materials. Concentrations are in ppb, solid limit of detection (SLD) is 3 times the standard deviation of the blank

	CRM	Ru	Rh	Pd	Ir	Pt	Au
1	WMG 1	35	25	372	65	759	15
2	WMG 1	38	27	411	62	768	25
3	WMG 1	39	27	413	61	787	39
4	WMG 1	35	24	380	51	715	93
WMG 1	Mean	37	26	394	60	757	43
	RSD	6%	6%	5%	10%	4%	81%
	Literature [†]	30.8	26.9	394.8	51.6	735.5	108.7
	Certified	35	26	382	46	731	110
	Recovery	105%	99%	103%	130%	104%	39%
5	SARM 7	489	189	1260	106	3401	84
6	SARM 7	524	205	1387	95	3287	63
7	SARM 7	493	191	1287	105	3315	76
8	SARM 7	490	190	1280	102	3378	69
SARM 7	Mean	499	194	1304	102	3345	73
	RSD	3%	4%	4%	5%	2%	12%
	Literature [‡]	430	244	1464	84	3297	179
	Certified	430	240	1530	74	3740	310
	Recovery	116%	81%	85%	138%	89%	23%
SLD (ppb)		1.21	0.07	1.51	0.11	0.61	2.02

[†] (Oguri et al. 1999), [‡] (Chen et al. 1996)

Table 3. PGE and chalcophile element concentrations of Marathon samples (PGE are in ppb, S is wt. %, all other elements are ppm):

Sample	DH	Type	Co	Ni	Ir	Ru	Rh	Pt	Pd	Au	Cu	S	Pb	As	Sb	Bi
1	G10	LZDS	55	239	0.77	13.9	10.4	155	514	52	711	0.09	2	<2	<2	<2
2	G10	NMFG	51	279	0.86	11.4	0.43	11.6	14.3	<2	17	<0.01	2	<2	<2	<2
3	G10	LZDS	62	540	2.90	14.6	52.1	588	2150	178	7510	0.96	14	6	<2	<2
4	G10	FSVC	15	41	<0.11	6.85	<0.07	2.34	5.29	2	80	0.3	<2	<2	2	2
5	G10	FSVC	14	37	<0.11	10.0	<0.07	1.75	1.52	8	61	0.29	2	<2	2	2
6	G10	FSVC	14	40	<0.11	7.32	<0.07	0.68	1.31	51	<2	0.11	<2	<2	<2	<2
7	G10	BZMS	108	831	7.39	24.9	125	139	693	12	1855	2.9	8	<2	<2	<2
8	G11	NMCG	38	61	0.28	10.1	0.84	13.3	29.2	4	151	0.1	<2	<2	<2	<2
9	G11	LZDS	57	393	1.64	13.0	0.61	17.4	10.8	28	1615	.23	2	<2	2	<2
10	G11	LZDS	50	337	3.45	14.0	70.0	625	2800	230	6600	0.71	10	<2	<2	<2
11	G11	FSVC	32	129	<0.11	11.5	0.21	10.2	24.2	8	345	.59	<2	8	2	<2
12	G6	FSVC	25	102	<0.11	1.93	<0.07	0.96	35.8	8	54	0.31	4	2	<2	<2
13	G6	FSVC	31	160	0.38	3.41	0.41	14.7	16.3	4	207	0.03	<2	<2	6	<2
14	G6	LZDS	57	278	7.43	12.7	114	1370	4370	254	2730	0.34	4	<2	<2	<2
15	G6	PGGB	29	85	0.12	2.44	3.05	47.5	93	2	246	0.06	2	2	<2	<2
16	G6	PGGB	40	137	0.44	2.10	6.82	130	366	62	1775	.27	6	<2	6	<2
17	G6	PGGB	34	59	<0.11	2.39	0.56	11.9	50.8	48	423	.09	6	2	2	2

DH = drill hole number, LZDS = Lower Zone Disseminated Sulphide, NMFG = nonmineralized fine-grained gabbro, FSVC = felsic volcanics, BZMS = Basal Zone Massive to net-textured sulphide, PGGB = pegmatitic gabbro, NMCG= nonmineralized coarse-grained gabbro.

Table 4. Pb distribution in “co-existing” sulphides

Sample	Description	Whole Rock Pb (ppm)	Pyrrhotite Pb (ppm)	Chalcopyrite Pb (ppm)	$\sim D^{CP/PO}$	Pd+Pt (ppb)
G11-1I	BZMS	2	1.250	2.499	2	276
G10-1I	BZMS	8	1.692	-	-	783
G11-1II	LZDS	2	2.665	20.28	8	2690
G10-8I	LZDS	14	9.106	87.06	9	1970
G10-2	LZDS	2	2.391	19.86	8	3385

4.10 Figures

Figure 1. Map of the Coldwell Complex (from Shaw, 1997)

Figure 2. PGE elution curves. Plot is the cumulative percentage of metals recovered using 4, 5ml aliquots of; 0.2 M HCl (solid line), 0.6M HCL (dashed line), and 1.0 M HCL (dotted line)

Figure 3. Mantle normalized plot of Marathon PGE concentrations. Blue lines are Lower Zone Cu-rich samples, green lines are Basal-Zone Fe-rich samples, red lines are pegmatitic samples, and black lines are non-sulphide bearing samples.

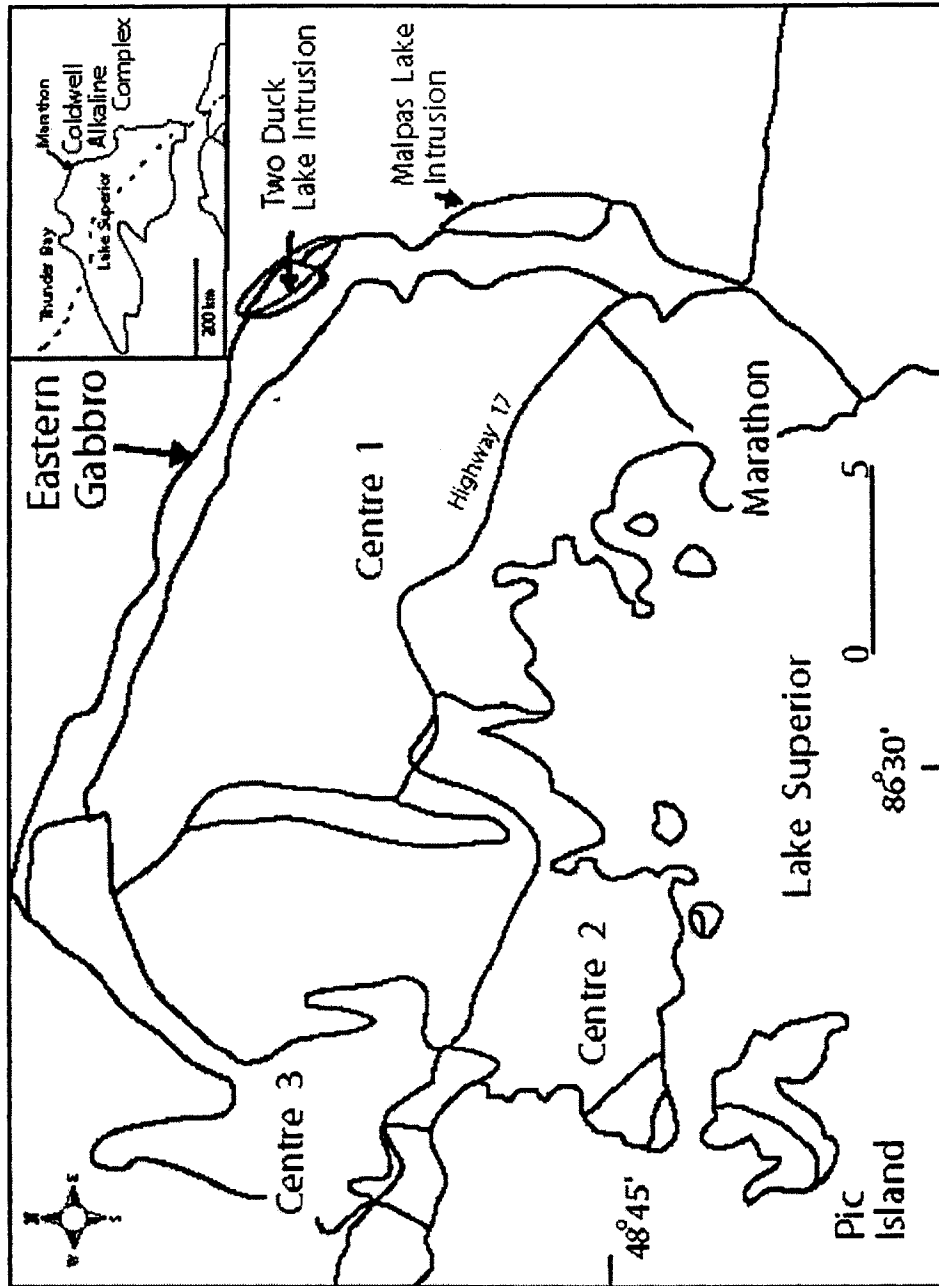


Figure 1.

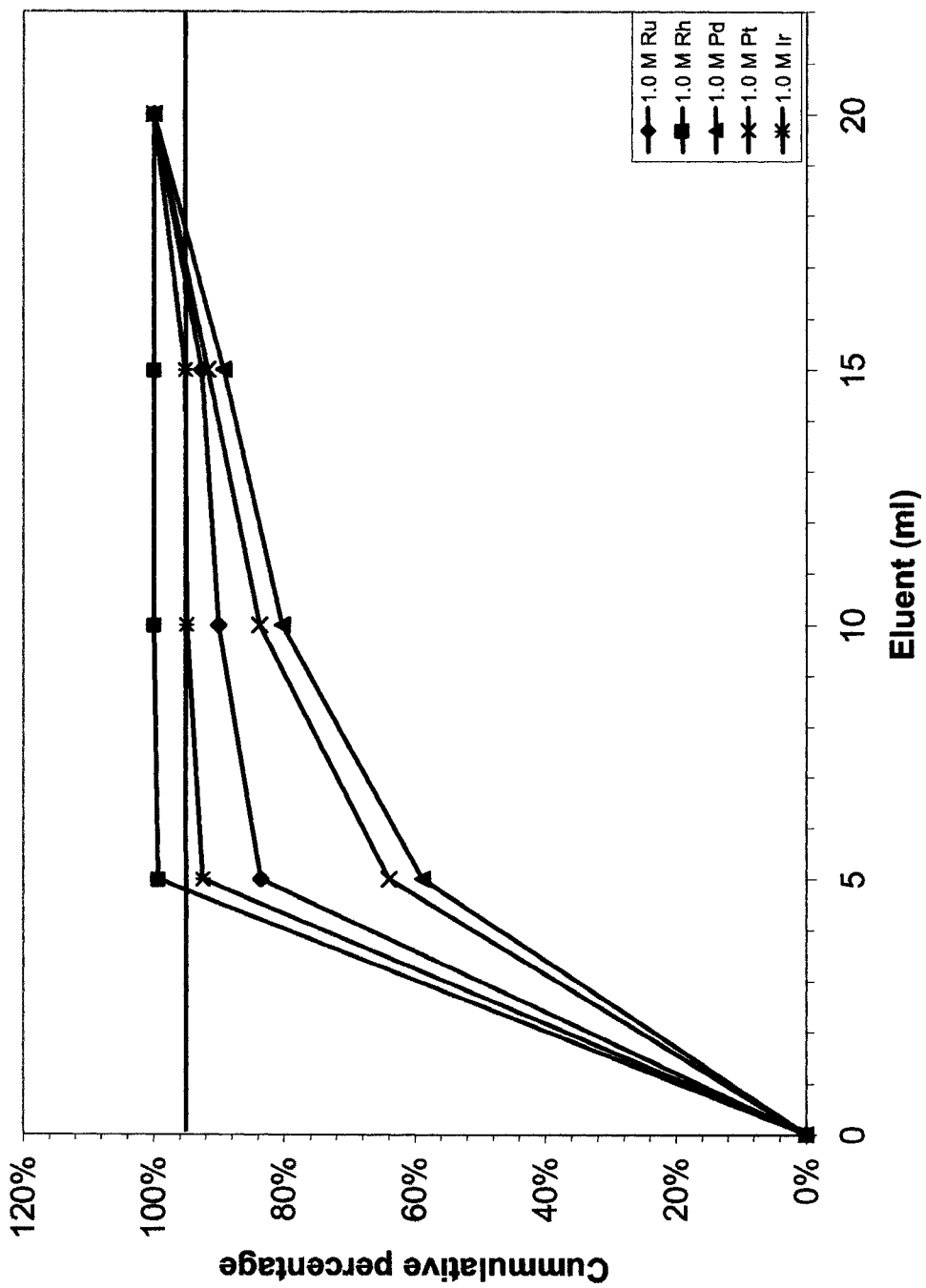


Figure 2.

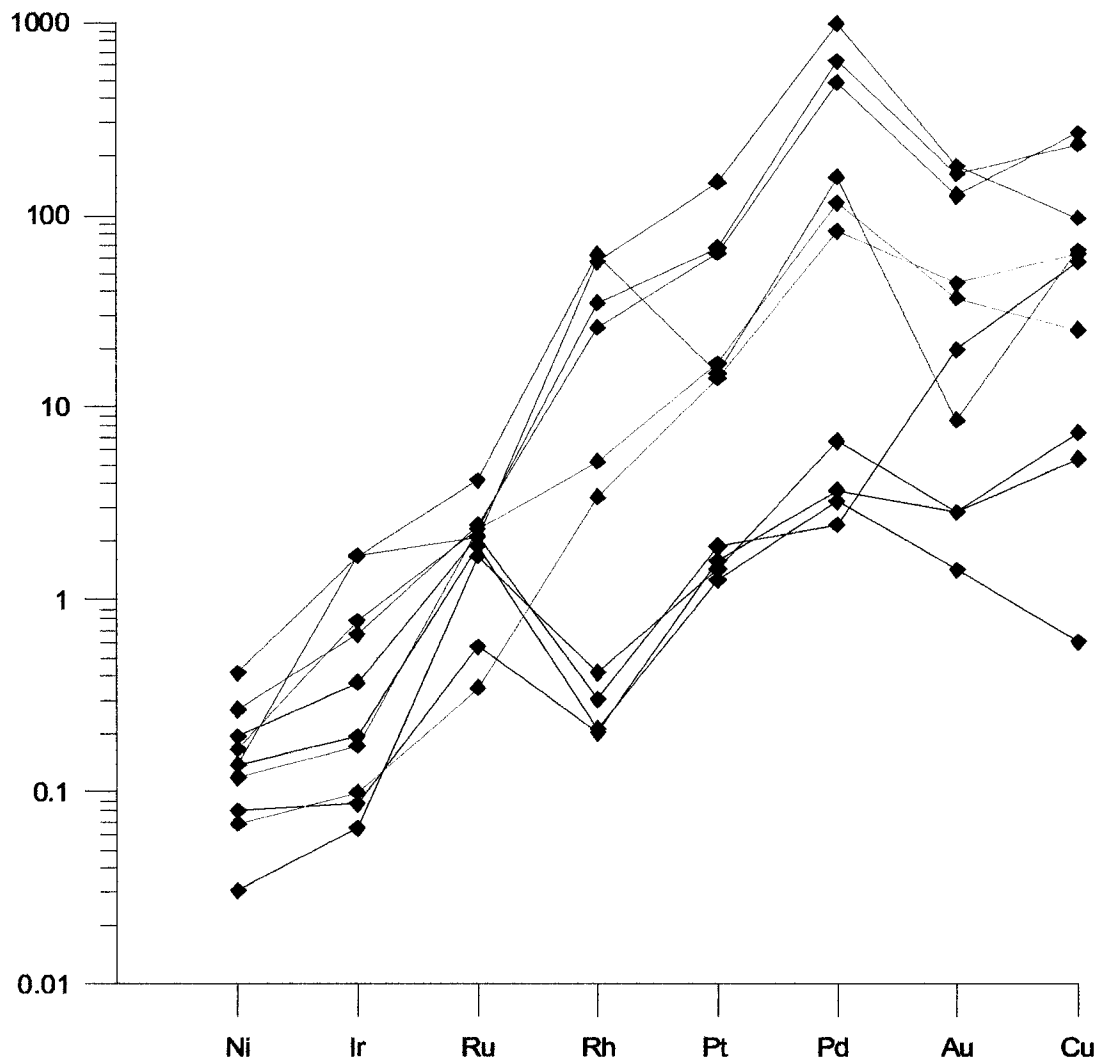


Figure 3.

CHAPTER 5

Summary

5.1 Summary and work progress

In summary, the work conducted in this thesis project has resulted in the development of a method for the determination of Pb isotope ratios in minerals using quadrupole LA-ICP-MS. The advantages of this method are several, including; micrometer-scale spatial resolution, rapid analysis time, and low risk of contamination during sample preparation. Importantly, in samples with low Pb concentrations (~2 ppm), the quadrupole instrument, with N₂ added to the nebulizer gas, can yield Pb isotope ratio measurements with a precision (0.2% RSE) that is comparable to LA-MC-ICP-MS.

Using the LA-ICP-MS method for Pb isotope ratio determination, Pb isotope ratios were measured in minerals from the Marathon deposit. With this Pb isotope data, it was possible to identify a significant difference between the Pb Isotope ratios in plagioclase and chalcopyrite (within the same thin section) from the PGE- and Cu-rich gabbroic rocks. With this information, in conjunction with textural constraints, most importantly the disruption of optically continuous clinopyroxene and the replacement of hornblende by chalcopyrite, it was possible to test opposing genetic models for the deposit.

The Pb isotope ratios, in conjunction with textural constraints, were found to be most consistent with a sub-solidus hydrothermal model. The fact that hornblende dehydrates to clinopyroxene at 750°C, and the melting point of chalcopyrite is above 900°C, requires that the chalcopyrite (which is the dominant Cu-rich phase in the deposit) must have been introduced by hydrothermal fluids under sub-solidus conditions. The presence of external Pb (likely from an Archean upper crustal source) in chalcopyrite suggests that these hydrothermal fluids were derived from, or at least interacted with, the local country rock. Watkinson and Ohnenstetter (1992) have proposed that a Pb-rich hydrothermal fluid, partially derived from the Archean country rock, enriched pre-existing magmatic minerals with Cu, Pb, PGE, and other chalcophile and volatile elements. Thus, for Cu enrichment (i.e. chalcopyrite mineralization) the work presented in this thesis is generally consistent with the model of Watkinson and Ohnenstetter (1992). However, as the PGE enrichment process maybe different from chalcopyrite mineralization, the origin of the PGE enrichment remains uncertain. However, it is reasonable to suspect that the PGE enrichment is related to

chalcopyrite mineralization as there is a strong association between PGMs and chalcopyrite, and also, good correlation between Cu, Pt, and Pd concentrations. More clearly defining this relationship is the subject of ongoing research that is investigating the distribution and fractionation of the PGE within the Marathon deposit and is also looking at the relationship of the PGE to other trace elements. A NiS fire assay, ion-exchange separation, ICP-MS method is being used to determine PGE concentrations in rock pulps. In addition synthetic, metal-doped, NiS buttons are being investigated for use as standards for the analysis of trace elements in sulphide minerals using LA-ICP-MS. Preliminary Pb analyses of sulphides by LA-ICP-MS, using NIST 610 glass standards, suggest that the trace element concentrations in Basal Zone Fe-rich sulphides are less than the Lower Zone Cu-rich sulphides. In addition, preliminary NiS fire assays suggest that the Lower Zone Cu-rich sulphides are depleted in Ni, Ir, and Rh and are enriched in Pd, Pt, and Cu relative to Basal Zone Fe-rich sulphides.

Future work might involve a fluid inclusion study to determine the chemical composition, and temperature of hydrothermal fluids that have interacted with the sulphide and silicate assemblages at various stages. The information gained from fluid inclusion studies would provide further constraints on models, and also enhance our understanding of the behavior of the PGE in hydrothermal fluids (e.g. Ballhaus and Stumpfl 1986, Farrow et al. 1994, Pasteris et al. 1995). In addition to fluid inclusion studies Re-Os isotopic work would also be useful in evaluating the role of fluids and possible sources for the precious metals in the deposit and would further constrain genetic models.

5.2 Reference

Watkinson, D.H., and Ohnenstetter, D. (1992) Hydrothermal Origin of platinum-group mineralization in the Two Duck Lake Intrusion, Coldwell Complex, northwestern Ontario. *Canadian Mineralogist*, **30**, 121-136

VITA AUCTORIS

Sean Andrew Crowe

Born

October 28, 1977
Edmonton, Alberta, Canada

Education

Bachelor of Science (2002): Okanagan University College, Kelowna, BC

(Chemistry and Earth and Environmental Science) Research Projects/Directed Studies: Geochemistry and Precious Metal Content of a Thick Section of Chilcotin Basalt (EESc), and Determination of Platinum Group Elements (PGE): A Review of Selected Methods (Chem.)

References

Crowe, S.A., Fryer, B.J., Samson, I.M., and Linnen R.L. (2003) The Genetic Implications of Platinum-Group Element, Cu and Ni Fractionation in the Marathon PGE-Cu deposit. GAC-MAC Abstracts and Program

Crowe, S.A., Fryer, B.J., Gagnon, J.E. (2003) The application of Nd:YAG (266nm) LA-ICP-MS to environmental geoscience with special reference to the problem of elemental fractionation. ESRC/CRSE programs and abstracts, p. 17

Crowe, S.A., Fryer, B.J., Samson, I.M., Walford, P.C., and Barrie, C.T. (2002). Crustal contamination and the role of volatile fluxing in the genesis of the Marathon Pd-Cu Deposit: Preliminary results from a Pb isotope study of sulphides and feldspars by LAM-ICP-MS. GAC-MAC Abstracts and Program, vol. 27, p. 24

Crowe, S.A., Samson, I.M., and Fryer, B.J. (2002). The role of crustal contamination in the genesis of the Marathon PGE-Cu deposit, Superior Province, Canada: Constraints based on LAM-ICP-MS trace element and Pb isotope studies of sulphides and silicates. IMA abstracts

McIlwraith, I, Linnen, R.L., Fryer, B.J., Samson, I.M., Gagnon, J., and **Crowe, S. (2002).** Sulphide Melt Inclusions at the Marathon PGE deposit, Coldwell Complex, Ontario, Canada. PACROFI VIII Program with Abstracts, p. 66